



저작자표시-비영리-변경금지 2.0 대한민국

이용자는 아래의 조건을 따르는 경우에 한하여 자유롭게

- 이 저작물을 복제, 배포, 전송, 전시, 공연 및 방송할 수 있습니다.

다음과 같은 조건을 따라야 합니다:



저작자표시. 귀하는 원저작자를 표시하여야 합니다.



비영리. 귀하는 이 저작물을 영리 목적으로 이용할 수 없습니다.



변경금지. 귀하는 이 저작물을 개작, 변형 또는 가공할 수 없습니다.

- 귀하는, 이 저작물의 재이용이나 배포의 경우, 이 저작물에 적용된 이용허락조건을 명확하게 나타내어야 합니다.
- 저작권자로부터 별도의 허가를 받으면 이러한 조건들은 적용되지 않습니다.

저작권법에 따른 이용자의 권리는 위의 내용에 의하여 영향을 받지 않습니다.

이것은 [이용허락규약\(Legal Code\)](#)을 이해하기 쉽게 요약한 것입니다.

[Disclaimer](#)

**이학박사학위논문**

Characterization of Chlorinated Ethenes  
Contamination Using Quantitative and  
Qualitative Evaluation Methods  
in a Complex Groundwater System

**복합적 규모 지하수계에서  
정량적 및 정성적 평가 방법을 이용한  
염화유기용제 오염 특성화 연구**

2016년 8월

**서울대학교 대학원**  
**지구환경과학부**  
**이 성 순**

**Characterization of Chlorinated Ethenes  
Contamination Using Quantitative and Qualitative  
Evaluation Methods in a Complex Groundwater System**

指導教授 李 岡 根

이 論文을 理學博士 學位論文으로 提出함

2016 年 07 月

서울大學敎 大學院

地球環境科學部

李 性 淳

李性淳의 理學博士 學位論文을 認准함

2016 年 07 月

委 員 長 : \_\_\_\_\_ (인)

副委員長 : \_\_\_\_\_ (인)

委 員 : \_\_\_\_\_ (인)

委 員 : \_\_\_\_\_ (인)

委 員 : \_\_\_\_\_ (인)

**Characterization of Chlorinated Ethenes  
Contamination Using Quantitative and Qualitative  
Evaluation Methods in a Complex Groundwater System**

**LEE, SEONG SUN**

**A dissertation submitted in partial fulfillment of the  
requirements for the degree of Doctor of Philosophy  
in Earth and Environmental Sciences**

**August 2016**

**School of Earth and Environmental Sciences**

**Seoul National University**

# ABSTRACT

Characteristics of contamination before and after the remedial action in a complex groundwater system contaminated with chlorinated ethenes such as trichloroethylene (TCE) were identified using quantitative and qualitative evaluation methods. The study site is located at an industrial complex of Wonju city, Korea, adjacent to a stream. Contamination by trichloroethylene (TCE) was detected in 1990's and had been investigated for contaminant identification and remediation. The precise information for initial mass and concentration of TCE spilled at the source zone was unknown. For this reason, it was hard to characterize sources that caused pollution and to find appropriate remediation strategies.

Analytical solutions which can assess and quantify the impacts of partial mass reduction on groundwater are used to estimate the unknown residual TCE source mass and dissolved concentration as time passed using long-term monitoring data. Initial spilled TCE mass (1,000 kg) and dissolved concentration (150,000  $\mu\text{g/L}$ ) were assessed with analytical solutions. The results of this study supports that an analytical solution can be applied to give the quantitative information for initial residual source mass and dissolved concentration at contaminated sites even when there are no document on the

source history such as spilled amount and concentration.

In scale of a locally heterogeneous stream watershed, if contaminated groundwater discharges to a stream, stream water pollution near the contamination source also can cause stream contamination problem. In this respect, the fate and transport of chlorinated ethenes around a stream in an industrial complex were evaluated using the concentration of each component, and hydrogeochemical, microbial, and compound-specific carbon isotope data. Groundwater geochemical data indicate that aerobic conditions prevail in the upgradient area of the studied aquifer, whereas conditions become anaerobic in the downgradient. An increasing trend in the molar fraction of *cis*-1, 2-dichloroethene (*cis*-DCE) and vinyl chloride (VC) was observed in the downgradient zone of the study area. The enriched  $\delta^{13}\text{C}$  values of TCE and depleted values of *cis*-DCE in the stream zone, compared to those of the source zone, also suggest biodegradation of volatile organic compounds (VOCs). Microbial community structures in monitoring wells adjacent to the stream zone were analyzed using 16S rRNA gene-based pyrosequencing to identify the microorganisms responsible for biodegradation. The multilateral approaches used in this study indicate that contaminants around the stream were naturally attenuated by active anaerobic biotransformation processes.

At the main source zone of this study site, remediation technologies

such as soil vapor extraction, soil flushing, biostimulation, and pump-and-treatment have been applied to eliminate the contaminant sources of TCE and to prevent the migration of TCE plume from remediation target zones. At each remediation target zone, the aqueous concentrations of TCE plume present at and around the main source areas decreased significantly as a result of remedial action. Variations in the contaminant flux across three transect lines and statistical trend in variation of TCE concentration using Sen's slope estimator were analyzed to identify the effect of remediation during the long period after the remedial action. After the remediation, the effect of remediation took place clearly at each transect line located at the main source zone and industrial complex and also was represented on results of Sen's slope estimator. By tracing a time-series of plume evolution, a greater variation in the TCE concentrations was detected at the plumes near the source zones compared to the relatively stable plumes in the downstream. The difference in the temporal trend of TCE concentrations between the plumes in the source zone and those in the downstream could have resulted from intensive remedial actions taken at the main source zones.

The efficiency of the intensive remediation actions performed was demonstrated using quantitative evaluation methods such as analytical solutions with a long-term monitoring data set. From results of quantitative evaluation

using analytical solutions, it is evaluated that the intensive remedial action had effectively been performed with the removal efficiency of 70 % for the residual source mass during the remediation period. The evaluation methods mentioned in this study will be helpful in assessing the long-term performance of remediation technologies at contaminated sites by chlorinated ethenes.

**Key words:** trichloroethylene (TCE), analytical solution, stream watershed, biodegradation, remedial action, mass discharge

**Student Number:** 2008 - 30114

## **TABLE OF CONTENTS**

<b>ABSTRACT .....</b>	<b>i</b>
<b>TABLE OF CONTENTS.....</b>	<b>v</b>
<b>LIST OF FIGURES .....</b>	<b>x</b>
<b>LIST OF TABLES .....</b>	<b>xvii</b>
<b>CHAPTER 1. INTRODUCTION .....</b>	<b>1</b>
1.1 Background theory.....	2
1.2 Objectives of this study.....	6
<b>CHAPTER 2. SITE DESCRIPTION AND CONTAMINANT HISTORY.....</b>	<b>9</b>

2.1 Study area .....	10
2.2 Hydrogeological condition .....	11
2.3 Contamination history .....	20
2.4 Remedial action .....	24

**CHAPTER 3. ESTIMATION OF THE UNKNOWN DNAPL  
RESIDUAL SOURCE MASS AND DISSOLVED  
CONCENTRATION 27**

- Based on analytical solution considering the partial source depletion

Abstract .....	28
3.1 Introduction .....	29
3.2 Study area and data description .....	32
3.2.1 Study site and contamination history .....	32
3.3.2 Groundwater sampling and data descriptions .....	33
3.3 Methods .....	36
3.3.1 Relationship between the contaminant source mass and source	

mass flux .....	36
3.3.2 Analytical solutions for the source mass and dissolved concentration .....	38
3.3.3 Effect of partial source reduction on source mass flux .....	40
3.4 Results and discussions .....	42
3.4.1 Determination of input parameters for analytical solution .....	42
3.4.2 Estimation of the initial source mass and dissolved concentration .....	47
3.5 Conclusions .....	54

**CHAPTER 4. EVALUATION OF THE FATE AND  
TRANSPORT OF CHLORINATED ETHENES IN A  
COMPLEX GROUNDWATER SYSTEM .....55**

Abstract .....	56
4.1 Introductions .....	57
4.2 Study site .....	61

4.3 Methods.....	66
4.3.1 Water sampling and water quality analysis .....	66
4.3.2 Microbial community analysis.....	68
4.4 Results and discussions .....	69
4.4.1 Spatial distributions of contaminants .....	69
4.4.2 Hydrogeochemistry .....	74
4.4.3 Compound-specific carbon stable isotope analysis .....	79
4.4.4 Microbial community structures and distribution of potential dechlorinatorsHydrogeochemistry .....	83
4.5 Conclusions .....	97

**CHAPTER 5. EVIDENCES OF IN SITU REMEDIATION  
FROM LONG-TERM MONITORING DATA.....99**

Abstract .....	100
5.1 Introductions.....	102
5.2 Materials and methods .....	105

5.2.1 Site description and history.....	105
5.2.2 Groundwater sampling and water quality analysis .....	109
5.2.3 Mass discharge.....	110
5.2.4 Statistical trend analysis .....	111
5.3 Results and discussions .....	114
5.3.1 Variations in TCE concentration and its mass discharge .....	114
5.3.2 Comparison of TCE contaminant plumes .....	120
5.3.3 TCE concentration monitoring at each remediation target.....	122
5.3.4 Evaluating the efficiency of intensive remedial action .....	125
5.3.5 Analyzing the trend in variation of contaminant concentration	136
5.4 Summary and conclusions.....	148
<b>CONCLUDING REMARKS.....</b>	<b>150</b>
<b>REFERENCES .....</b>	<b>154</b>
<b>ABSTRACT IN KOREAN .....</b>	<b>179</b>

## LIST OF FIGURES

### CHAPTER 1.

**Figure 1-1** Objectives of the study .....8

### CHAPTER 2.

**Figure 2-1** Location of the study site and distribution of groundwater sampling wells.....15

**Figure 2-2** The composition materials of aquifer system along the geological cross-section of A-B line, and also showing the groundwater levels (blue line) and the monitoring well intervals.....16

**Figure 2-3** Depth-discrete results (at 3 m, 5 m and 7 m) of flowmeter test performed at representative monitoring wells (MW-1, WS-3 and WS-7) around

the stream.....	17
<b>Figure 2-4</b> Average annual precipitations at the study site from January 2007 to November 2015. ....	18
<b>Figure 2-5</b> Locations of potential source zones identified using chemical fingerprinting and hydrological response analysis (from Yang et al., 2012).22	
<b>Figure 2-6</b> Contamination history of this study site .....	23
<b>Figure 2-7</b> Remediation target zone and remediation methods applied at each target zone.....	26

### **CHAPTER 3.**

<b>Figure 3-1</b> Relationship between source zone DNAPL mass and source zone dissolved concentration data. ....	45
<b>Figure 3-2</b> Field concentration data obtained from 2010 to 2015 for TCE plot on semi-log scale .....	49
<b>Figure 3-3</b> Match estimated data of each initial residual source mass (500, 1000, 1500 kg) data to field concentration data until before the remedial action.	

(Assumption: initial TCE concentration is 150,000  $\mu\text{g/L}$ ) .....50

**Figure 3-4** Figure 3-4. Match estimated data of each initial dissolved TCE source concentration (100, 150, 200 ppm) data to field concentration data until before the remedial action. (Assumption: initial TCE mass is 1,000 kg)..53

## **CHAPTER 4.**

**Figure 4-1** Location of the study site and layout of groundwater sampling wells

(a). Blue lines indicate the contour lines of the measured groundwater level (in meters) conducted in February 2013. The location of wells installed at (b) the Road Administrative Office (RAO); and (c) around the stream. Green open circles represent the monitoring wells used in this study.....65

**Figure 4-2** Spatial distribution of TCE in groundwater samples obtained at February 2012 and 2013, and molar fraction (%) of each contaminant ....72

**Figure 4-3** Seasonal variations of DO (Dissolved Oxygen, mg/L),  $\text{NO}_3^-$  (mg/L),  $\text{Fe}^{2+}$  (mg/L),  $\text{Mn}^{2+}$  (mg/L) concentrations and ORP (Oxidation Reduction Potential, mV) in groundwater samples, measured in November 2011, February,

May, August, and November 2012, and February 2013 .....	77
<b>Figure 4-4</b> (a) $\delta^{13}\text{C}$ value (‰) of TCE, and (b) <i>cis</i> -DCE with distance (m) from the main source zone. ....	82
<b>Figure 4-5</b> Hierarchical clustering of clone libraries from eight samples .....	91
<b>Figure 4-6</b> Phylogenetic classification and distribution of the dominant bacterial sequences at the order level .....	95
<b>Figure 4-7</b> Comparison of bacterial community structures at each monitoring well. DNA-derived 16S rRNA gene reads were classified at the genus level. The heat map shows the relative abundance (>5%) of the most prominent taxonomic groups of the most abundant phyla. ....	96

## CHAPTER 5.

<b>Figure 5-1</b> Location of study area showing main source area, monitoring wells, and groundwater level measured in August 2013. ....	108
<b>Figure 5-2</b> Seasonal concentration changes of multiple-DNAPL contaminants at selected wells along a groundwater flow path.....	117

**Figure 5-3** Study site showing the transect lines for mass discharge (a) and temporal mass discharge of TCE and cis-DCE plume at each transect (b).118

**Figure 5-4** Variation of TCE (a) and cis-DCE (b) mass discharge from 2010 to 2015 ..... 119

**Figure 5-5** Comparison of TCE plumes observed from November 2011 to November 2015 ..... 121

**Figure 5-6** Results of TCE concentration monitoring observed at each remediation target zone..... 124

**Figure 5-7** Match data estimated with initial TCE source mass (1,000 kg) considering the source mass depletion to field concentration data. (Assumption: fraction (X) is 0.5)..... 128

**Figure 5-8** Match data estimated with initial TCE source mass (1,000 kg) considering the source mass depletion to field concentration data. (Assumption: fraction (X) is 0.6)..... 129

**Figure 5-9** Match data estimated with initial TCE source mass (1,000 kg) considering the source mass depletion to field concentration data. (Assumption:

fraction (X) is 0.7) .....	130
<b>Figure 5-10</b> Match data estimated with initial dissolved TCE source concentration (150,000 $\mu\text{g/L}$ ) data considering the source mass depletion to field concentration data. (Assumption: fraction (X) is 0.5) .....	131
<b>Figure 5-11</b> Match data estimated with initial dissolved TCE source concentration (150,000 $\mu\text{g/L}$ ) data considering the source mass depletion to field concentration data. (Assumption: fraction (X) is 0.6) .....	132
<b>Figure 5-12</b> Match concentration data estimated with initial dissolved TCE source concentration (150,000 $\mu\text{g/L}$ ) data considering the source mass depletion to field concentration data. (Assumption: fraction (X) is 0.7) .....	133
<b>Figure 5-13</b> Results estimated with initial dissolved TCE source concentration (150,000 $\mu\text{g/L}$ ) and source mass (1,000 kg) considering the partial source mass depletion. (Assumption: fraction (X) is 0.7) .....	134
<b>Figure 5-14</b> Spatial distribution of variation trend of TCE concentration with Sens's trend analysis at the industrial complex [Plume zone 1] and around the stream [Plume zone 2] until the pre-remedial action [from 2009 to 2012] (a) and	

whole study period involving the post-remedial action [from 2009 to 2015] (b).

.....141

**Figure 5-15** Spatial distribution of variation trend of TCE concentration with Sens's trend analysis at ROA [the main source zone] until the pre-remedial action [from 2009 to 2012] (a) and whole study period involving the post-remedial action [from 2009 to 2015] (b). ....142

**Figure 5-16** Temporal variations of TCE concentration at monitoring well conducted the intensive remedial action until the pre-remediation (a) and the post-remediation (b). ....143

**Figure 5-17** Distribution of the number of monitoring wells involving each significant trend until (a) the pre-remedial action and (b) the post-remedial action at the main source zone .....144

**Figure 5-18** Zonal distribution of the number of monitoring wells involving each significant trend at (a) the pre-remedial action and (b) the post-remedial action.....145

## **LIST OF TABLES**

### **CHAPTER 2.**

<b>Table 2-1</b> Table 2-1. Average annual rainfall and temperature for 7 years (January 2007 – November 2015).....	19
---	----

### **CHAPTER 3.**

<b>Table 3-1</b> TCE concentration ( $\mu\text{g/L}$ ) in the main source area during the monitoring period from September 2010 to November 2015.....	35
<b>Table 3-2</b> Parameters used in analytical solution for estimating the initial source mass and dissolved concentration..	46

### **CHAPTER 4.**

<b>Table 4-1</b> Concentrations ( $\mu\text{g/L}$ ) of TCE, cis-DCE and VC in groundwater obtained at study site (February 2013; August 2013; September 2013)....	73
---	----

<b>Table 4-2</b> Concentrations ( $\mu\text{g/L}$ ) and carbon isotope ( $\delta^{13}\text{C}$ ) values ( $\text{‰}$ ) of TCE and cis-DCE in groundwater obtained at study site (February 2013). .....	78
<b>Table 4-3</b> Observed and estimated bacterial diversity in groundwater samples. ....	92
<b>Table 4-4</b> . Most active microbial community structures with groups A, B, C, as determined by ratios of relative abundance of DNA reads at phylum, class, and order levels. ....	93

## **CHAPTER 5.**

<b>Table 5-1</b> Estimated dissolved TCE concentration ( $\mu\text{g/L}$ ) and residual NAPL mass before and after remedial action. ....	135
<b>Table 5-2</b> Number of monitoring well data for this study.....	146
<b>Table 5-3</b> Results of Sen’s slope trend analysis for TCE concentration in main source zone and whole study area.....	147

**CHAPTER 1.**  
**INTRODUCTION**

# **CHAPTER 1. INTRODUCTION**

## **1.1 Background theory**

Trichloroethylene (TCE) is a chlorinated solvent that has been broadly used as cleaning and degreasing agent in various commercial applications. Due to its relatively low solubility in water and a low tendency to sorb, it continuously dissolved into groundwater, which results in long-term groundwater contamination. In Korea, chlorinated solvents are also among the most frequently detected contaminants in groundwater at industrial complexes and groundwater contaminated by dense non-aqueous phase liquid (DNAPL) is often associated with nitrate contamination (KMOE, 2010). The sites contaminated with DNAPL compounds such as TCE were characterized and remediated with various investigation and efforts for the past two decades (Marley et al., 1992; Schnarr et al., 1998; Stroo et al., 2003; Falta et al., 2005a, Chapman et al., 2007; Hunkeler et al., 2011; Lee et al., 2013; Kaown et al., 2014 a and b). Few studies including the above research have been carried out for the evaluation of contaminated sites with the known DNAPL source mass and concentration at the initial stage when DNAPL was spilled. However, in most contaminated sites, there is no information about the spilled histories such

as the initial DNAPL mass and dissolved concentration. Hence, the existence of unknown source can make the groundwater quality worse and more difficult to remediate.

Analytical solutions were used to assess the impact of partial source depletion (Parker and Park, 2004; Falta et al., 2005a; Fure et al., 2006). If field concentration monitoring data showed a simple exponential reduction pattern during a monitoring period, analytical solutions can be used in tracing the initial residual source mass and concentration at the spilled stage. This tracing method was performed through best-fit data matching which conducts an iterative process until finding the estimated data curve obtained from analytical solutions well matched with observed field data. Also, the residual contaminant mass and dissolved concentration as time passed can be predicted using the above analytical solutions which considered the impacts of source mass reduction.

Generally, DNAPL contaminated sites are divided into two zones, the source zone and the plume zone (Falta et al., 2005a; Xie et al., 2016). In a DNAPL source zone, dissolved contaminants originated from the source discharge to sustain a much larger groundwater plume along the groundwater flow path and then eventually reach to groundwater discharge area such as stream. Dissolved plume mass and volume may be increasing, constant, or decreasing, responding to the fluctuation of the source mass discharge relative

to the degradation rate in the plume (Falta et al., 2005a). In case of NAPL contaminated sites involving the groundwater discharge area such as stream and river, dissolved plume originated from the source zone may hold significant potential to discharge to stream water where they may pose threats to peripheral ecosystems and human health (Conant et al., 2004; McGuire et al., 2004; Moran et al., 2007; Freitas et al., 2015; Lee et al., 2015). Therefore, the fate and transport of contaminants in a stream watershed generally confronted with the border of plume zone should be investigated and evaluated in terms of stream water quality management (Lee et al., 2015).

The remediation methods for decontamination of chlorinated ethenes on a field scale include soil vapor extraction (SVE), soil flushing, pump-and-treat, and injection of nanoscale zero valent iron (nZVI) (Gordon, 1998; Mackay et al., 2000; Rivett et al., 2006; Wei et al., 2010; McCray et al., 2011). Long-term monitoring data have been used to evaluate the occurrence of natural attenuation or the site suitability and efficiency of remediation techniques (McGuire et al., 2004; McGuire et al., 2006; Phillips et al., 2010). Previous studies have assessed the efficiency of remediation based on the monitoring data, most of which were obtained from near-source zones (Hannesin and Gillham, 1998; Benner et al., 2000; Soga et al., 2004). Also, the temporal and spatial evaluation of contaminant removal efficiency before and after the

remedial action using data obtained for a long monitoring period are rarely investigated on catchment scale from the source zone to groundwater discharge area (Wilkin et al., 2002; Lee et al., 2013). For the better management of groundwater resources, the intensive monitoring of water systems on a catchment scale (from a contaminant source to the groundwater discharge area) is required for the groundwater quality management (Conant et al., 2004; Chapman et al., 2007; Peritta et al., 2013). Moreover, mass flux approaches (monitoring the concentration of contaminants in aqueous phase due to mass transfer between source zone DNAPL and flowing groundwater) have been used to evaluate the source zone remediation efficiency (Soga et al., 2004; Brusseau et al., 2013) and to understand the natural attenuation mechanisms (Chapman et al., 2007; Basu et al., 2009) as a primary tool of quantitative evaluation methods. The spatial and temporal variations of mass fluxes at contaminated sites before and after the remedial actions can provide an effective tool for assessing the efficiency of remediation and for envisioning the temporal evolution of contaminant plumes (Einarson and Mackay, 2001).

Statistical analyses for the detection and assessment of noteworthy trends in contaminant concentration monitoring data associated with contaminant remediation can be classified as parametric and non-parametric methods (Yue and Wang, 2002; Lee et al., 2006; Choi et al., 2009). Parametric

trend tests require data to be independent and normally distributed, while non-parametric trend tests such as Sen's trend test (Sen, 1968) require only the data to be independent. The results of Sen's slope estimator obtained at the contaminated site generally indicate the variation rate in contaminant concentration as time passes.

## **1.2 Objectives of this study**

The main objectives of this study were to identify the characteristics of chlorinated ethenes contamination in a complex groundwater system discharging to a stream (Figure 1-1), and to evaluate the efficiency of remedial actions performed at the main source zone using various quantitative and qualitative evaluation methods.

The first objective of this study is to identify the unknown residual TCE source mass and dissolved concentration at the initial spilled stage. This study site has no document on the history of spilled TCE. Therefore, in order to acquire the source information of the initial spilled stage, analytical solutions are used as a quantitative evaluation method.

The second and third objectives of this study performed in a locally heterogeneous stream watershed are as follows: 1) to evaluate the fate of

chlorinated ethenes associated with biodegradation in groundwater around the stream through an understanding of the spatial relationship between hydrogeochemical conditions and the composition and distribution of microbial communities, including dechlorinating bacteria; and 2) to investigate transport of the contaminant plume that could influence the quality of stream water. In this study, versatile approaches are used in combination with carbon isotope, hydrogeochemical, and microbial community analyses to gain an insight into the fate of the contaminant and its transport around the stream.

Finally, the fourth objective is to assess the effect of the remedial actions applied in the main source zone using various evaluation methods such as statistical trend analysis, mass discharge analysis, and analytical solutions based on the long-term monitoring data representing the variation of TCE concentration for the whole study area from the main source zone to a stream.

The research will improve our approach about selection and application of a reasonable evaluation method for characteristics of contamination at heterogeneous contaminated sites with lack of information about contaminant source mass. These efforts enable to plan the long-term plume management and to support in efficiently performing our decision-making for an optimized remediation strategy.

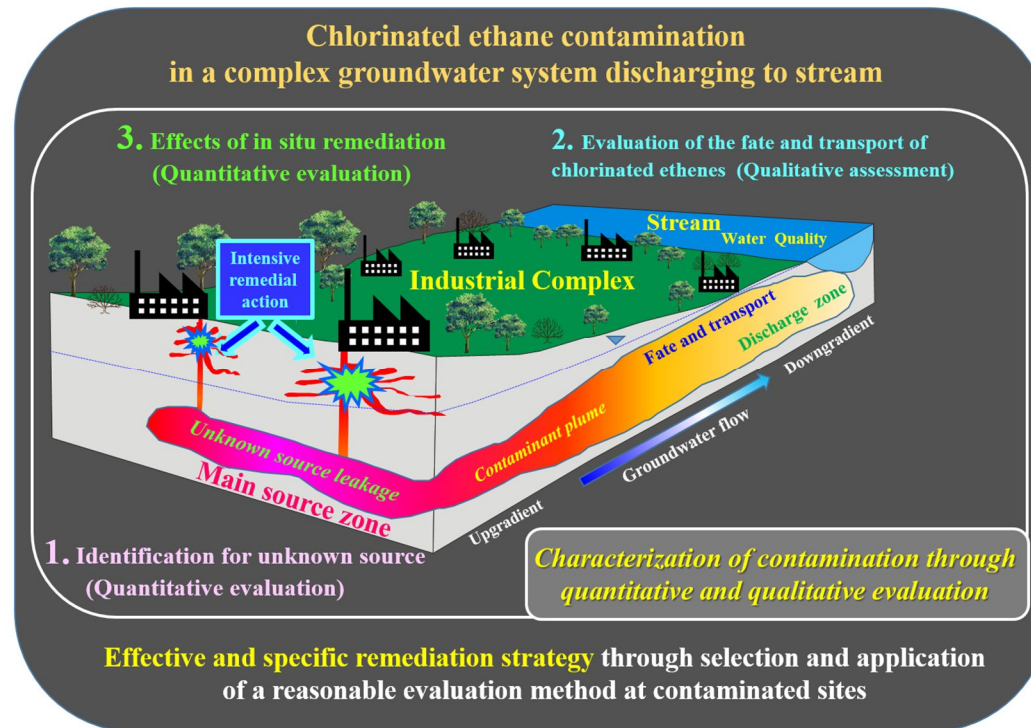


**Figure 1-1** Objectives of the study.

**CHAPTER 2.**

**SITE DESCRIPTION AND**

**CONTAMINANT HISTORY**

## **CHAPTER 2. SITE DESCRIPTION AND CONTAMINANT HISTORY**

### **2.1 Study area**

The study site is located approximately 120 km east of Seoul, Korea. As shown in Figure 2-1, the Wonju stream flows from southeast to northwest at the eastern area of the site, and is an important source of irrigation water for a paddy field. The Road Administrative Office (RAO) of Gangwon Province is situated within this site, together with the Woosan Industrial Complex (WIC). The RAO is located at the western area of the study site on a low hill surrounded by small mountains and forests. A large industrial company is based at the industrial complex, together with approximately 60 public, commercial, and residential buildings. There is an unpaved region in the downgradient area (not related to the stream zone) where groundwater recharge can actively occur during precipitation events, and this is the only area where groundwater can permeate the subsurface to recharge the aquifer. Most area of WIC is paved (91% of the area) and located at the downhill of the RAO with relatively low altitude (118 m, mean sea level; msl). Only a small amount of rainfall can be recharged

into the subsurface over the study area (Yang et al., 2011; Kaown et al., 2014a). Previous reports show that the aquifer at the study site has strong hydrogeological heterogeneity which means areal heterogeneity; the top soil layer is covered by impermeable paving material at several locations, and with weathered rocks to the biotite granite at the bottom (KMOE, 2010; Yang et al., 2011; Yang et al., 2012; Kaown et al., 2014a). A water treatment facility was previously installed near the Wonju stream to enable stream water treatment at a depth of 3-4 m below the ground surface. However, that facility ceased operation since 2010. The dominant groundwater flow direction is from the RAO to the Wonju stream.

## **2.2 Hydrogeological condition**

Boring log data show that the aquifer at the study site consists of weathered and highly fractured Jurassic biotite granite, with soil and alluvial deposits overlying weathered rocks (Baek and Lee 2001; Yu et al., 2006) shown in Figure 2-2. The thickness of the aquifer in the industrial complex is 10 to 15 m, and the alluvial deposits thinned near the stream zone, where they measure 3 to 4 m. During the summer, the depth of the water table has been measured as approximately 8 to 10 m below surface level (bsl) at RAO in the upgradient

area, and 1 to 3 m bsl in the downgradient area. The observed water table levels during the winter ranges from 11 to 13 m bsl in RAO, and approximately 2 to 3 m bsl in the downgradient area. Therefore, the water table in groundwater wells at the RAO shows high seasonal variations, with a range of approximately 3 m throughout the year. Hydraulic gradients around the main source area of RAO have been measured as between 0.013 and 0.023, but are much lower in the industrial complex area and the area around the stream, with a narrower range of between 0.008 and 0.011. These differences in hydraulic gradients can result from topographic and hydrogeological conditions at the study site. The much more pronounced hydraulic gradients and wider hydraulic ranges observed at the main source area are due to the site's hilltop location and the heterogeneity of the aquifer. The porosity has been measured as between 0.29 and 0.31 at the main source area and the industrial complex, and from 0.30 to 0.35 around a stream. Kaown et al. (2014b) previously estimated groundwater flow velocities at the study site by means of  $^3\text{H}$ - $^3\text{He}$  analysis. The groundwater flow velocities ( $1.9 \times 10^{-6}$  to  $2.1 \times 10^{-5}$  m/s) estimated around a stream were about ten times slower than those for the main source area ( $9.8 \times 10^{-6}$  to  $1.2 \times 10^{-4}$  m/s). The degradation rate ( $k$ : 0.015 to 0.08  $\text{yr}^{-1}$ ) was calculated using groundwater residence time and isotopic enrichment factor associated with TCE to *cis*-DCE dechlorination by Kaown et al. (2011). According to the results from pumping

and slug tests conducted in this study, the hydraulic conductivity values range between  $2.0 \times 10^{-4}$  cm/s and  $2.4 \times 10^{-3}$  cm/s and values in the area around the stream range between  $6.5 \times 10^{-4}$  cm/s and  $4.2 \times 10^{-3}$  cm/s. The direction of groundwater flow for the whole study site is from RAO located at the North West to Wonju stream located at the South East. Especially, around the stream was observed by depth-discrete flowmeter test performed at 3 different depths (3 m, 5 m and 7 m) using colloidal type flowmeter (AquaVision Colloidal Borescope, GEOTECH) (Figure 2-3). Results of MW-5 well showed that groundwater flows toward the Wonju stream which is applicable to groundwater discharge area. Especially, WS-7 well installed near the stream showed mixed flow pattern affected by groundwater-stream water interaction. At WS-3 well, flow direction of shallow depth (3 m) was similar with stream flow direction flowing from the North East to the South West. However, results observed at 7 m depth showed the reverse pattern of stream flow direction.

Precipitation data were obtained for the last 9 year period beginning from January 2007 from November 2015 at the Wonju meteorological station (Figure 2-4). For the last 9 years, 1352 mm of the average annual rainfall was observed, 72 % of which was concentrated in the rainy season (June to September) as shown in Figure 2-4. Elevated groundwater levels likely resulted in the contact of the residual DNAPL sources above the water table with

groundwater along with increased hydraulic gradients. Thus, rainfall would facilitate the dissolution of the residual DNAPLs and its migration in the downward.

The average annual temperature during the study period ranged over 11.7-14.6°C. High average monthly temperatures were observed mainly in August (24.5-27.1°C), while low average monthly temperatures were observed in January (-7.7-1.0°C), with about 20 degrees temperature difference between hot and cold seasons. Table 2-1 shows the rainfall and temperature data.

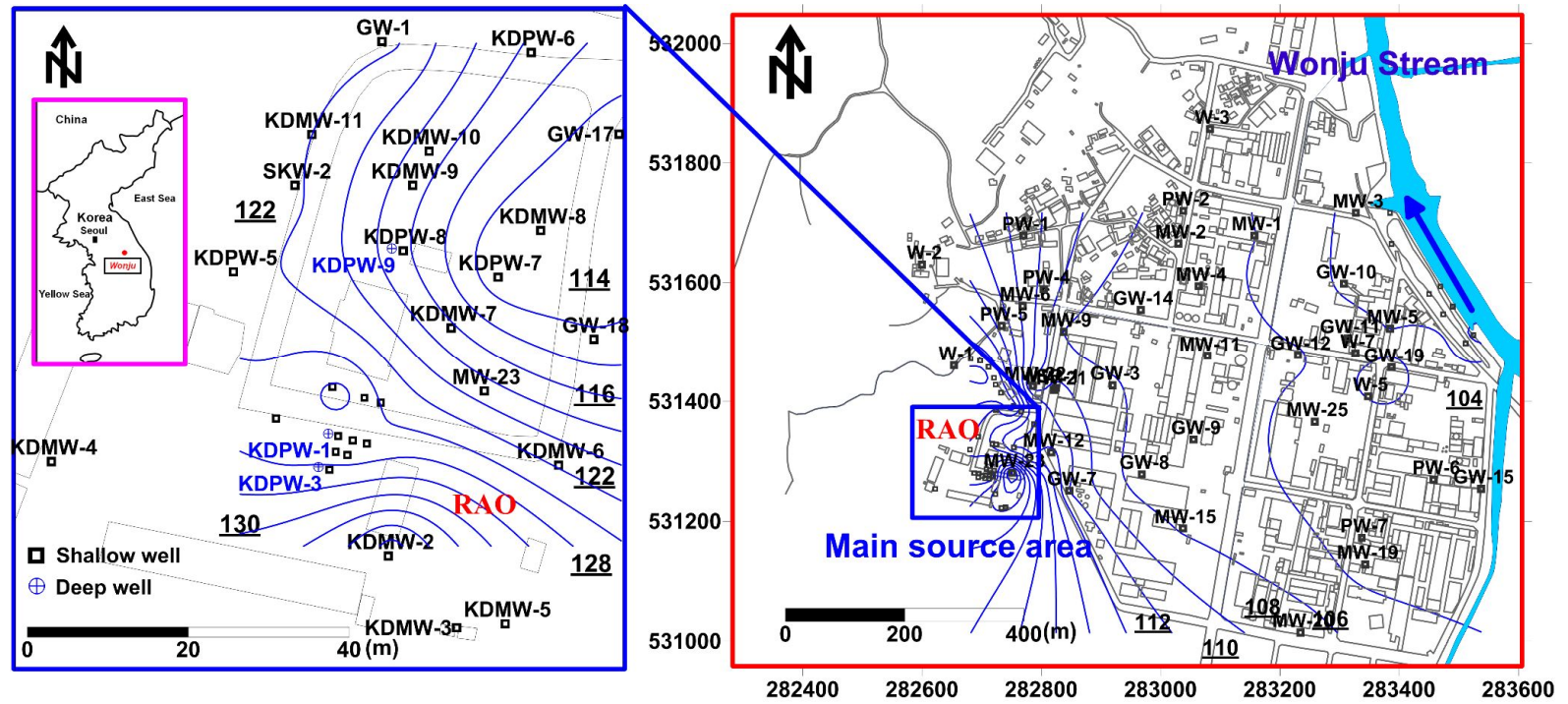
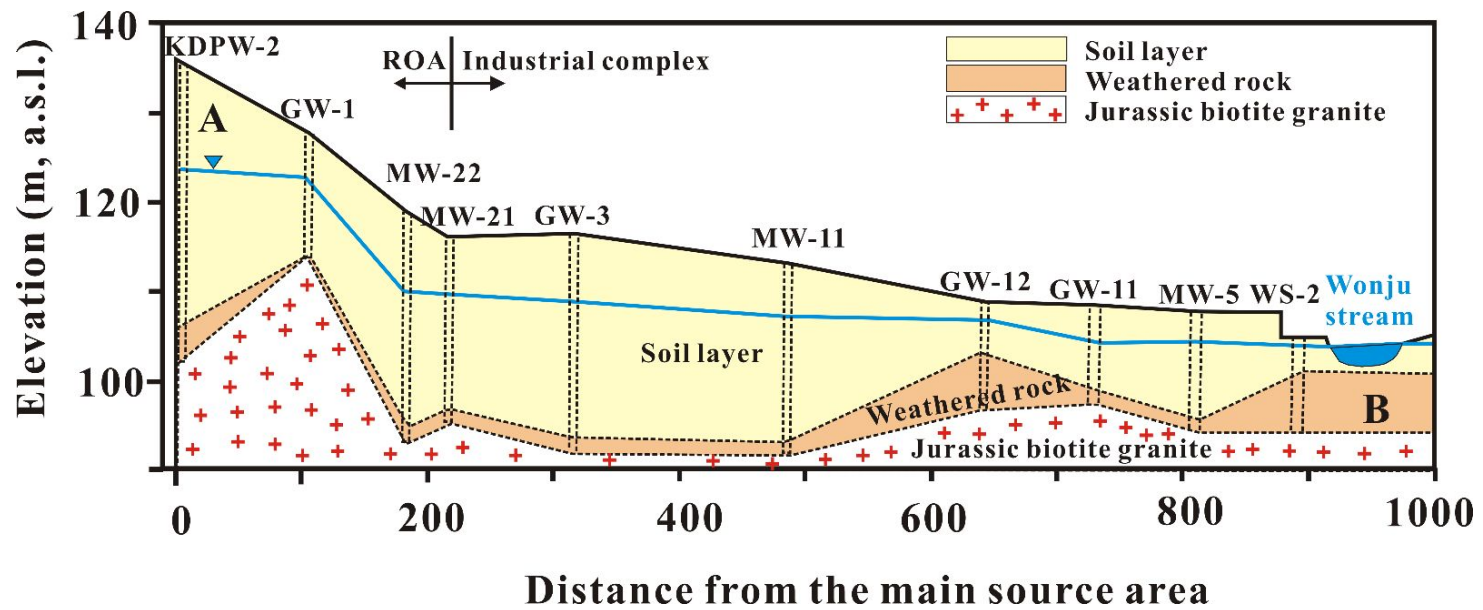
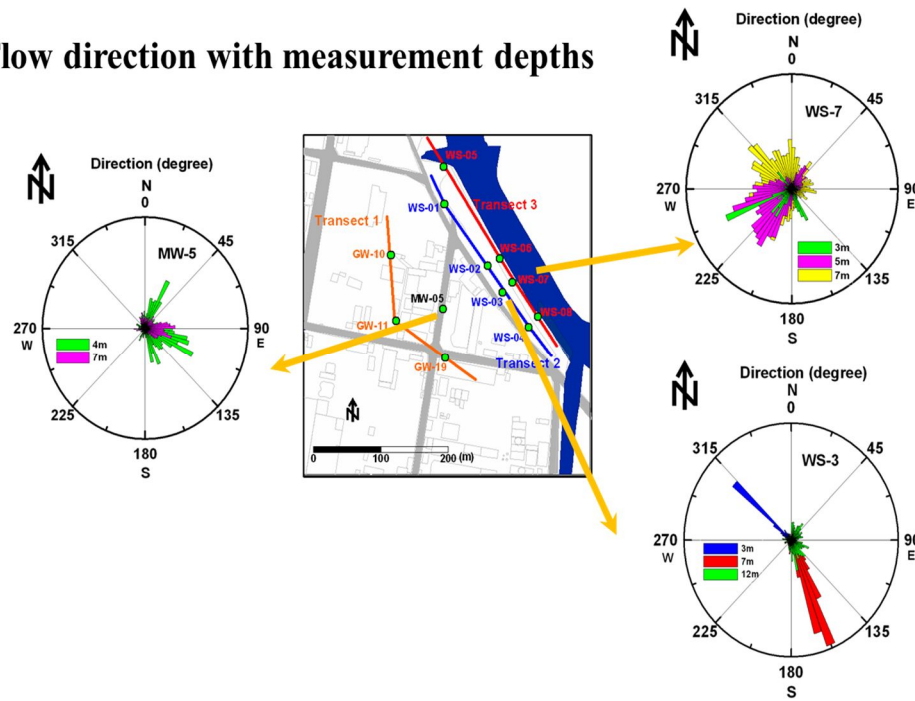


Figure 2-1. Location of the study site and distribution of groundwater sampling wells .



**Figure 2-2.** The composition materials of aquifer system along the geological cross-section of A-B line, also showing the groundwater levels (blue line) and the monitoring well intervals.

### Flow direction with measurement depths



**Figure 2-3.** Depth-discrete results (at 3 m, 5 m and 7 m) of flowmeter test performed at representative monitoring wells (MW-1, WS-3 and WS-7) around the stream.

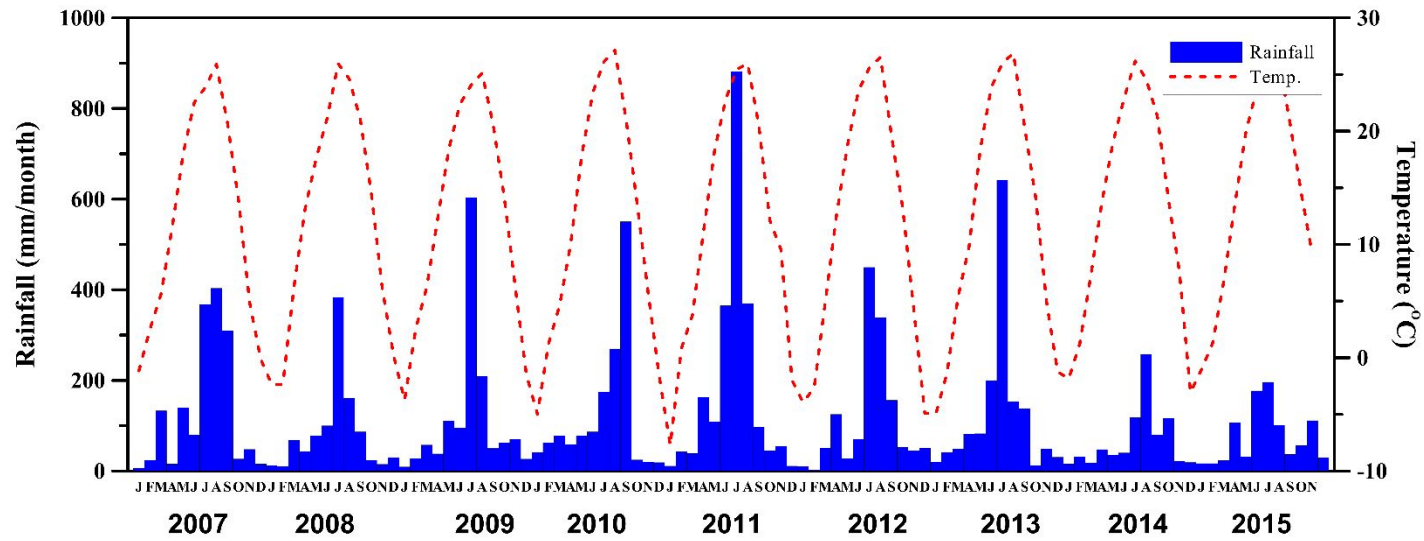


Figure 2-4. Average annual precipitations at the study site from January 2007 to November 2015.

**Table 2-1.** Average annual rainfall and temperature for 7 years (January 2007 – November 2015).

	<b>Jan</b>	<b>Feb</b>	<b>Mar</b>	<b>Apr</b>	<b>May</b>	<b>Jun</b>	<b>Jul</b>	<b>Aug</b>	<b>Sep</b>	<b>Oct</b>	<b>Nov</b>	<b>Dec</b>	<b>Ave</b>
<b>Average rainfall (mm/month)</b>	15.93	28.87	57.38	75.46	77.04	134.81	424.02	251.52	167.03	46.76	48.16	25.63	<b>112.72</b>
<b>Average temperature (°C)</b>	-4.03	0.44	5.54	11.85	18.64	23.23	25.65	26.06	20.60	13.73	6.77	-2.38	<b>12.18</b>
<b>Average high temperature (°C)</b>	-1.02	2.53	7.29	13.76	19.92	23.86	26.18	27.14	21.34	14.57	9.55	-1.24	<b>13.66</b>
<b>Average low temperature (°C)</b>	-7.73	-2.66	3.75	9.83	17.85	22.38	24.05	24.57	19.53	12.11	4.27	-4.29	<b>10.25</b>

## **2.3 Contamination history**

In this study site, it had been reported that groundwater was contaminated with several chlorinated solvents such as trichloroethylene (TCE) and carbon tetrachloride (CT) (Figure 2-5). The cause of contamination occurrence was revealed that the workers of the RAO laboratory were used various solvents for the asphalt quality test for about 16 years since 1982 and replaced it with TCE due to the restriction of the Korea Ministry of Environment (KMOE) (Yang and Lee, 2012; Kaown et al, 2014). Especially, TCE was spilled on a surface as inappropriate management from 1982 to 1997, which has aggravated groundwater quality until the present day (Figure 2-6). However, the precise information for initial mass and concentration of the spilled TCE was unknown (Baek and Lee, 2011; Yang and Lee, 2012; Kaown et al., 2014a). Also, previous research has reported that the groundwater at this site is contaminated by multiple DNAPL components, such as TCE, chloroform (CF), and CT (Baek and Lee, 2011; Yang and Lee, 2012). The main source of contaminants is located inside the RAO. Local TCE sources of groundwater contaminants exist near GW-10, GW-11, and GW-19 wells, which are located in the downgradient area. Site monitoring and investigation was performed intensively from 2009 to 2013 as part of a research program for KMOE. Yang

and Lee (2014) revealed that the study site was contaminated with multiple chlorinated contaminants; in particular, small contaminant sources were identified through a seasonal hydraulic impact analysis, historical approach, and chemical fingerprinting. Therefore, based on detection of multiple contaminants, a new set of monitoring wells for an organized investigation of the main source zone of RAO and the entire industrial area that was designed to monitor the contaminant the contamination plume and identify the causes and the local sources of the TCE contamination problem.

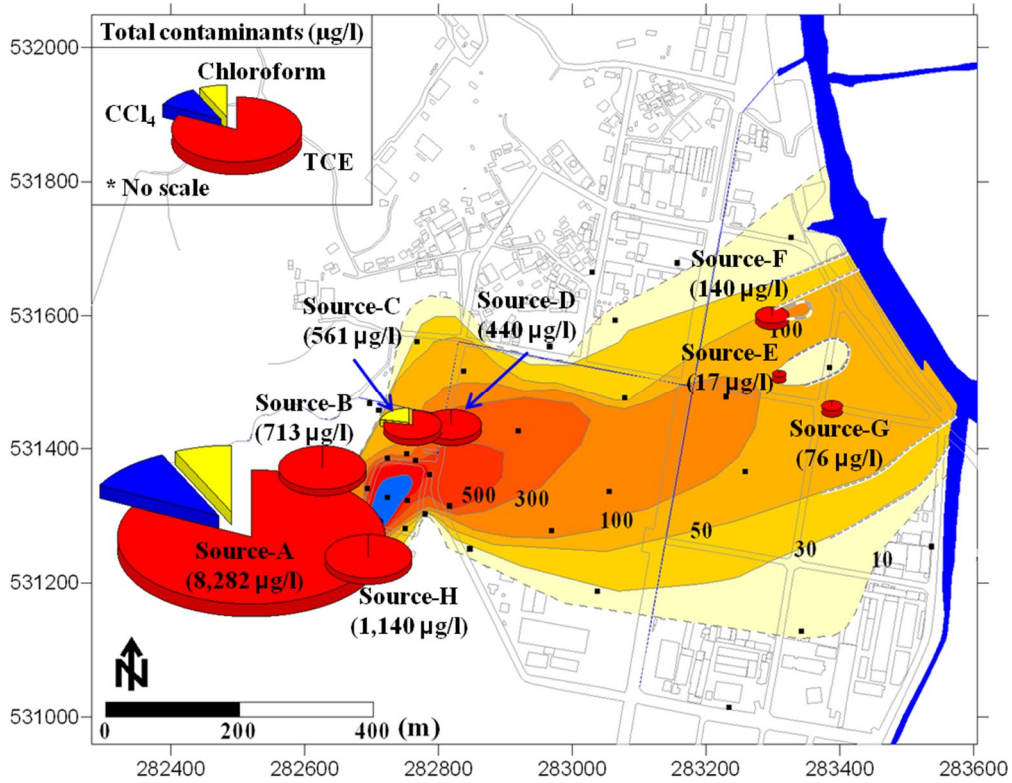


**Figure 2-5.** Locations of potential source zones identified using chemical fingerprinting and hydrological response analysis (from Yang and Lee, 2012).

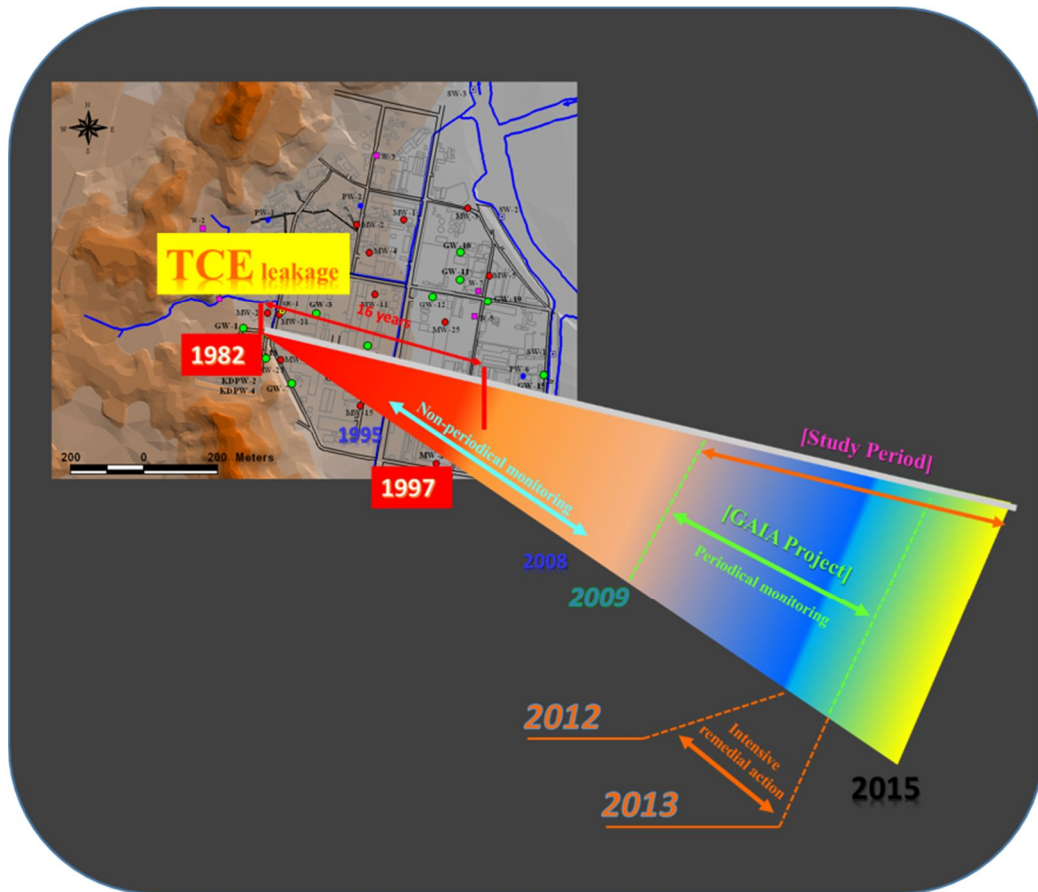


Figure 2-6. Contamination history of this study site.

## **2.4 Remedial action**

The TCE contamination of groundwater was first detected in 1995. Thereafter, the temporal monitoring of TCE concentrations were carried out by other institutions. In the middle of monitoring term, the low-thermal desorption method was applied to remediate the contaminant at the main spillage RAO area for the topsoil of up to 4 m depth. Meanwhile, WIC is considered as a typical example of an intensely monitored site, which has drawn considerable attention from KMOE as well as the public media (Yang and Lee, 2012). With the financial support from KMOE, a project team called ‘Smart-Environment friendly-Energy effective-DNAPL remediation-System (SEEDS) groundwater research team’ has initiated a GAIA (Geo-Advanced Innovative Action) project on the development of remediation technologies to restore contaminated groundwater at WIC from 2009 to 2013 (Figure 2-6).

For the first 2 years of the GAIA project period (years 2009–2010), 8 potential source locations responsible for various plumes were identified by Yang and Lee (2012) (Figure 2-6), and they also reported that some DNAPL sources existed above the groundwater table, which sporadically affects the groundwater quality by recharge. Therefore, several remediation technologies had been employed to eliminate the contamination sources at the main source

zone from 2010 to 2013. For the remediation of the main source area (A zone), soil vapor extraction and soil flushing techniques were performed to remediate the residual DNAPL existing at the unsaturated zone, and biostimulation technique were applied for the remediation of contaminant dissolved in the saturated zone at the hot source zone which shows high contaminant concentrations. Also, nZVI was injected to eliminate the TCE concentration near another local source area (B zone) around the main source zone. In the C zone located at the downgradient area of the main source zone, pump-and-treat method was implemented to prevent the migration of TCE plumes from the RAO to WIC and to reduce dissolved TCE concentration (Figure 2-7). To evaluate the effectiveness of the remedial actions, the concentrations of TCE, CT and CF dissolved in groundwater have been monitored for 6 years from 2010 to 2015 before and after implementing the remediation actions.

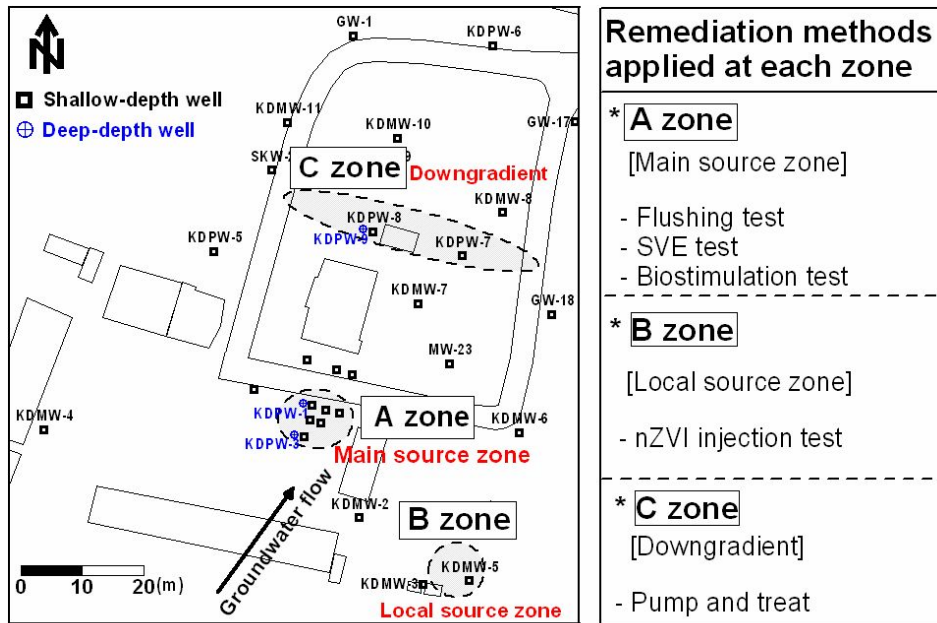


Figure 2-7. Remediation target zone and remediation methods applied at each target zone.

**CHAPTER 3. ESTIMATION OF THE  
UNKNOWN DNAPL RESIDUAL SOURCE  
MASS AND DISSOLVED CONCENTRATION**

**Based on analytical solutions  
considering the partial source depletion**

# **CHAPTER 3. ESTIMATION OF THE UNKNOWN DNAPL RESIDUAL SOURCE MASS AND DISSOLVED CONCENTRATION:**

**Based on analytical solutions considering the partial source depletion**

## **Abstract**

In this study site, previous studies have reported that trichloroethylene (TCE) was spilled on a surface as inappropriate management from 1982 to 1997, which has aggravated groundwater quality until the present day. However, the precise information for initial mass and concentration of the spilled TCE was unknown. For this reason, it was hard to characterize sources that caused pollution and to find appropriate remediation strategies. Prior to the delineation of remediation strategy, the quantitative evaluation such as identifying the initial source mass and dissolved concentration for contaminant sources should be conducted with the various evaluation methods. In this chapter, analytical solutions which can assess and quantify the impacts of partial mass reduction is used to estimate the unknown dense non-aqueous phase liquid (DNAPL) source mass and dissolved concentration using long-term monitoring data. Analytical

solutions can also evaluate the efficiency of the intensive remedial action, and predict a residual source mass and dissolved concentration as time passed before and after the remedial action. Parts associated with source mass reduction and prediction of residual mass and concentration as time passed will be discussed in Chapter 5.

Initial spilled TCE mass (1,000 kg) and dissolved concentration (150,000  $\mu\text{g/L}$ ) were estimated using analytical solutions. The results of this study indicated that analytical solutions can be applied to give the quantitative information for contaminant source such as initial source mass and dissolved concentration at contaminated sites even when there is no document on source history such as spilled amount and concentration.

### **3.1 Introduction**

Generally, DNAPL contaminated sites are divided into two zones, the source zone and the plume zone (Falta et al., 2005a; Xie et al., 2016). In a DNAPL source zone, dissolved contaminants originated from the source releases to sustain a much larger groundwater plume along the groundwater flow path. Dissolved plume mass and volume may be increasing, constant, or decreasing, depending on the fluctuation of the source mass discharge relative

to the degradation rate in the plume (Falta et al., 2005a).

At the source zone, a problem generally confronted with remediation is the identification of contaminant source locations and the spilled histories of contaminants using a set of long-term monitoring data (Aral et al., 2001). Most contaminated sites including this study site were contaminated for a long period. However, there are no accurate reports and data on the spilled locations and amounts of the solvents. Therefore, if studies identifying source locations and releasing histories such as types of contaminants, spilled volume and period, initial source mass and dissolved concentration are performed at contamination sites, the fate and transport of contaminant plumes can be assessed, and also strategy for remedial action and risk assessment may be accomplished. Hence, various studies for the contaminant source identification have been performed with various methodological approaches such as a linear optimization model (Gorelick et al., 1983), genetic algorithms (Aral and Guan, 1996), artificial neural networks (Singh et al., 2004). Also, quantitative or qualitative approach for source identification such as seasonal hydrological response analysis (Yang and Lee, 2012) and compound-specific isotope analysis (CSIA) (Hunkeler et al., 1999; Song et al., 2002; Chapman et al., 2007; Imfeld et al., 2008; Kaown et al., 2014; Lee et al., 2015) has been used. With regard to quantitative approach, Falta et al. (2005a and 2005b) developed analytical solutions for approximating

the time-dependent contaminant discharge from DNAPL source zones considering the relationship between DNAPL mass and source strength. They reported that the relationship between source mass and mass flux is a function of the DNAPL heterogeneity, the DNAPL distribution, and the correlation between them (Rao et al., 2001; Rao and Jawitz, 2003; Falta et al., 2005 a,b; Fure et al., 2006). Therefore, the temporal reduction of mass discharging at the source zone can be explained by a simple power- or exponential-type empirical functions of the mass reduction (Parker and Park, 2004; Zhu and Sykes, 2004; Falta et al., 2005a,b; Jawitz et al., 2005; Fure et al., 2006; Basu et al., 2008; Henri et al., 2016). Various researches for the relationship between the depletion of DNAPL source mass and the reduction of the contaminant mass flux have been carried out in detail through theoretical analyses and limited field monitoring data (Rao et al., 2001; Enfield et al., 2002, 2005; Rao and Jawitz, 2003; Falta et al., 2005 a and b; Chapman et al., 2007; Basu et al., 2008; Henri et al., 2016). Few studies including the above research have been carried out for the evaluation for contaminated sites with information for DNAPL source mass and concentration at the initial stage when DNAPL was spilled. However, in most contaminated sites, there are no information of the spilled histories such as the initial DNAPL mass and dissolved concentration. Hence, the existence of unknown source can make the groundwater quality worse and

more difficult to remediate.

Based on the previous studies dealing with analytical solutions, it is proposed that concentration monitoring data showing a simple exponential reduction pattern during a certain period can be used in tracing the initial source mass and concentration at the spilled stage through best-fit data matching which performs an iterative process until finding the estimated data curve well matched with observed field data. The residual contaminant mass and dissolved concentration as time passed can also be predicted through the analytical solution mentioned above.

The purpose of this study is to estimate the unknown TCE source mass and dissolved concentration at the initial spilled stage and to predict a residual source mass and dissolved concentration as time passed with analytical solutions.

## **3.2 Study area and data descriptions**

### **3.2.1 Study site and contamination history**

The Woosan Industrial Complex (WIC), which has an area of 355,235 m<sup>2</sup>, is located in Wonju city, Korea. The WIC was formed in 1970, and

accommodated 31 large and small companies in 2004 (Baek and Lee, 2011). The flow direction of regional groundwater is from the North West to the South East. The Road Administrative Office (RAO) of Gangwon Province, located in the uppermost area of the industrial complex, had used trichloroethylene (TCE) and carbon tetrachloride (CT) for asphalt test during 16 years from 1982 to 1997 and the estimated annual consumption of TCE is close to 500 L (Kaown et al., 2014a). However, the exact records of the solvent usage were not available at this site (Yang and Lee, 2012; Kaown et al., 2014a). The previous researches revealed that the groundwater at this site is contaminated by multiple DNAPL components, such as TCE, chloroform (CF), and CT (Baek and Lee, 2011; Yang and Lee, 2012). The main source of the contaminants is located inside the RAO. Local TCE sources of groundwater contaminants exist in the downgradient area of industrial complex (see Figure 2-5 in Chapter 2).

### **3.2.2 Groundwater sampling and data descriptions**

Monitoring works for water quality which initiated in 1995, have been performed non-periodically until 2008. In 2009, with the financial support from Korea Ministry of Environment (KMOE), a project team called 'SEEDS groundwater research team' has initiated the GAIA (Geo-Advanced Innovative

Action) project. GAIA research team had been regularly monitored from 2009 to 2013. Additionally, the continuous monitoring for this study was performed until 2015 after the GAIA project.

During the study period, nineteen rounds of groundwater sampling were taken at approximately 100 monitoring wells from May 2009 to November 2015. In this study, harmonic mean values of total 16 TCE concentration data collected at each representative monitoring well (KDPW-2, SKW -1, -3, -4, -6, -7, and MLW-1) which showed the continuous high level of TCE during 6 years from August 2010 to November 2015 were used (Table 3-1.).

**Table 3-1.** TCE concentration ( $\mu\text{g/L}$ ) in the main source area during the monitoring period from September 2010 to November 2015.

Well name /	2010 Aug.	2010 Nov.	2011 Feb.	2011 May	2011 Aug.	2011 Nov.	2012 Feb.	2012 May	2012 Aug.	2012 Nov.	2013 Feb.	2013 May	2013 Aug.	2013 Nov.	2014 Feb.	2015 Nov.
<b>Sampling date</b>																
KDPW-2	6,842	3,413	3,813	2,567	3,112	2,705	3,110	3,622	2,004	2,267	552	516	567	783	633	399
SKW-1	N.O.	13,148	1,555	550	6,786	1,246	602	540	385	1,409	177	377	890	66	754	704
SKW-3	N.O.	8770	9,427	1,621	6,553	11,282	4,294	1,060	224	1,058	130	161	326	353	74	69
SKW-4	10,444	5,995	4,136	2,932	1,458	1,348	1,220	1,462	1,933	1,299	1,608	1,304	751	180	1,345	830
SKW-6	N.O.	806	7,007	6,977	3,118	3,037	3,210	3,245	2,650	3,297	2,017	1,485	763	1,251	1,031	813
SKW-7	N.O.	3,184	1,474	1,419	363	926	741	864	637	691	577	397	192	311	100	111
MLW-1	11,536	14,295	11,062	2,483	8,673	9,075	4,448	1,854	1,004	4,596	607	514	572	1,180	951	700
Harmonic mean ( $\mu\text{g/L}$ )	9,129	3,077	3,233	1,584	1,556	1,987	1,422	1,215	636	1,448	356	419	450	235	239	223

**N.O: not observed.**

### **3.3 Methods**

In this part, the relationship between the contaminant source mass and dissolved concentration and the basic concept and mathematical descriptions of analytical solution are introduced.

#### **3.3.1 Relationship between the contaminant source mass and source mass flux**

As noted in Chapter 2, this study site have been contaminated for about 30 years ago since 1987. Due to no information for the history of contaminant source, it was hard to identify contamination characteristics of this study site. Therefore, the reasonable presumption for the initial source mass and dissolved concentration is necessary to predict the variation trend of source mass as time passed. Previous studies about field tests and experimental tests performed in different contamination sites indicated that, although the dissolved saturation concentration of TCE showed the range between 1,100,000 and 1,400,000  $\mu\text{g/L}$  depending on water temperature (Broholm and Feenstra, 1995; Pankow and Cherry, 1996; Broholm et al., 1999; Hunkeler et al., 2004; Parker et al., 2008), concentrations exceeding 10% of solubility are rarely investigated at DNAPL contaminated sites due to the heterogeneity of DNAPL distributions and the

solute partitioning into groundwater (Mackay et al, 1985; Mercer and Cohen, 1990; Parker and Park, 2004; Falta et al., 2005a; Miller et al., 2007; Hunkeler et al., 2011; Révész et al., 2014).

The source mass flux refers to the total dissolved contaminant mass flux ( $ML^{-2}T^{-1}$ ) originating from the main source zone under natural gradient conditions and discharging to the dissolved contaminant plume and it is generally used as the primary method for the evolution of the contaminant plume (Falta et al, 2005a; Fure et al., 2006; Chapman et al., 2007; Yang et al., 2011). Previous studies associated with the flux-based evaluation methods suggested that the source mass flux could be approximated by a power function of the DNAPL mass in the source zone (Rao et al., 2001; Parker and Park, 2004; Falta et al., 2005a). Also, the relationship between the residual NAPL mass and source concentration should be assumed considering the site specific NAPL distribution and heterogeneity.

The time-dependent contaminant discharge from DNAPL source zones associated with dissolution and other decay processes are estimated using analytical solutions proposed by Falta et al. (2005a). The relationship between the source mass discharge and source mass is given by:

$$\frac{C_s(t)}{C_o} = \left( \frac{M(t)}{M_o} \right)^\Gamma \quad (3-1)$$

where  $C_o$  is the initial TCE concentration,  $C_s(t)$  is the time dependent dissolved TCE concentration,  $M_o$  is an initial source zone mass,  $M(t)$  is the time-dependent source zone mass and  $\Gamma$  is an empirical parameter (Rao et al., 2001; Parker and Park, 2004; Falta et al., 2005a).

### 3.3.2. Analytical solutions for the source mass and dissolved concentration

A DNAPL source zone is the place directly released by DNAPL and their dimensions may be on the order of tens of meters. However, the plume zone located at downgradient from the source zone can be extended over hundreds or thousands of meters along the groundwater flow path if there is no natural or artificial reduction of the source zone mass.

A mass balance in the source zone can be formulated considering reduction of DNAPL mass by dissolution with additional first-order decay of the DNAPL by other processes except for the dissolution (Falta et al., 2005a):

$$\frac{dM}{dt} = -\frac{V_d A C_o}{M_o^\Gamma} M^\Gamma - \lambda_s M \quad (3-2)$$

where  $C_o$  the initial estimated DNAPL concentration,  $M_o$  is an initial

estimated source zone mass,  $\lambda_s$  is the decay constant at the source zone,  $V_d$  is an average darcy velocity,  $A$  is a cross sectional area of a control plane perpendicular to the regional groundwater flow direction and  $\Gamma$  is an empirical parameter (Rao et al., 2001; Parker and Park, 2004; Falta et al., 2005a). The source decay term accounts for biodegradation processes at aerobic and anaerobic conditions that can reduce the source mass as time passed.

If there is no biological or abiotic degradation of contaminant in the source zone, DNAPL source mass is only reduced by dissolution process ( $\lambda_s=0$ ). In this case, Eq (3-2) can be integrated (Parker and Park, 2004; Zhu and Sykes, 2004; Falta et al., 2005a) to get:

$$M(t) = \left\{ \frac{(\Gamma-1)V_d A C_o}{M_o^\Gamma} t + M_o^{1-\Gamma} \right\}^{\frac{1}{1-\Gamma}} \quad (3-3)$$

and

$$C_s(t) = \frac{C_o}{M_o} \left\{ \frac{(\Gamma-1)V_d A C_o}{M_o^\Gamma} t + M_o^{1-\Gamma} \right\}^{\frac{\Gamma}{1-\Gamma}} \quad (3-4)$$

### 3.3.3 Effect of partial source reduction on source mass flux

As noted above, the time-dependent depletion of contaminant in the source zone by biodegradation, dissolution, and other degradation processes can be calculated. As well, the effects of partial DNAPL source reduction by remedial action on the source mass flux can be estimated. In this latter estimation, an assumption that the initial DNAPL leakage happened at  $t=0$ , consider a source remedial action from  $t_1$  (start point) to  $t_2$  (finish point), during which a fraction,  $X$  of the  $t_1$  DNAPL mass is eliminated. With this scenario, Eqs (3-3) and (3-4) apply to the period before remedial action begins,  $0 \leq t < t_1$ . The source mass during the remedial action period can be estimated using Eq (3-5) with an assumption that the source mass is reduced as a linear function of time for  $0 \leq t \leq t_1$ :

$$M(t) = M_1 - XM_1 \left( \frac{t-t_1}{t_2-t_1} \right) \quad (3-5)$$

where  $M_1$  is the mass from Eq (3-3) at  $t = t_1$ . Also, the source concentration during this period can be calculated using Eq (3-1).

After the remedial action ( $t > t_2$ ), the source mass and concentration at the point of starting with the post-remedial action mass,  $M_2$  can be calculated

with new Eq (3-6):

$$M_2 = (1 - X)M_1 \quad (3-6)$$

A post-remedial action source concentration is given by:

$$C_2 = C_o \left( \frac{(1-X)M_1}{M_o} \right)^\Gamma \quad (3-7)$$

Then, the time variable is changed with  $(t - t_2)$  to rescale the time to begin at the end of the remedial action period. Using this method, Eq (3-3) becomes:

$$M(t) = \left\{ \frac{-V_d A C_2}{\lambda_s M_2^\Gamma} t + \left( M_2^{1-\Gamma} + \frac{V_d A C_2}{\lambda_s M_2^\Gamma} \right) e^{(\Gamma-1)\lambda_s(t-t_2)} \right\}^{\frac{1}{1-\Gamma}} \quad (3-8)$$

Where  $M_2$  is calculated from Eq. (3-6), and  $M_1$  is calculated by Eq. (3-2) with a time of  $t_1$ . The time dependent source concentration after the remedial action becomes:

$$C_s(t) = C_2 \left( \frac{M(t)}{M_0} \right)^\Gamma \quad (3-9)$$

### **3.4 Results and discussions**

#### **3.4.1 Determination of input parameters for analytical solution**

Based upon the usage history of solvents through personal communications, it is presumed that a residual NAPL existing in the finger type at the unsaturated zone and upper saturated zone is in more persuasive condition than a pool type which is formed by the leakage of a large quantity of NAPL to the deep bedrock aquifer because NAPL had been abandoned little by little for a long period. This assumption can be supported by results of diffusion sampler installed with depths at the main source zone which show that concentration data around the alluvial layer is higher than at the bedrock aquifer (Yang and Lee, 2012). Therefore, it is assumed that TCE contamination rarely affects the underneath of the bedrock aquifer.

It is reasonable to decide the value of empirical parameter ( $\Gamma$ ) depending on distributions of NAPL.  $\Gamma$  is an indicator representing the relationship between dissolved TCE concentration and residual NAPL mass and, also is determined according to the distribution of NAPL in the contaminated

sites. Therefore, various relationships between residual NAPL mass and dissolved TCE concentration can be represented depending on the change of  $\Gamma$  value (Figure 3-1). As shown in Figure 3-1, when  $\Gamma$  is 1.0, the relationship between the dissolved concentration and residual mass has a linear relationship. However, in a real field,  $\Gamma$  has the value greater than 1 at a “pool dominant” area when NAPL met the impermeable layer and then is distributed with the forms of several horizontal lenses (“pools”) that are connected by vertical “fingers” (Anderson et al., 1992; Keuper et al., 1993). Also,  $\Gamma$  has the value smaller than 1 at “NAPL blob dominant” area when the spilled NAPL vertically migrates and then is mainly trapped in the pores (Parker and Park, 2004). From the results of researches associated with the history of spilled contaminant and the source identification performed at this study site, it can be suggested that a small amount of residual DNAPL trapped in pores dominantly existed in this study site. Therefore, it is reasonable to assume that the empirical parameter ( $\Gamma$ ) has the range of value between 1.5 and 2.0. In this study, the value of empirical parameter ( $\Gamma$ ) is assumed with 1.7 which means that the main source zone of this study site is “residual NAPL dominant source” area.

Concentrations of redox-sensitive parameters analyzed at the main source zone showed high levels of dissolved oxygen (DO) and oxidation-reduction potential (ORP) which are indicative of aerobic and oxidation

conditions within the source area. Based on the above results, biodegradation of TCE is rarely investigated at the source zone except for cometabolic degradation of TCE at extremely limited area (Lee et al., 2015). Therefore, the decay constant ( $\lambda_s$ ) may be disregarded at the main source zone.

All parameters including the empirical parameter ( $\Gamma$ ) and the decay constant ( $\lambda_s$ ) were summarized in Table 3-2. In case of Darcy velocity, velocity ( $V_d$ , m/year) value was determined considering proper values of hydraulic conductivity (range between  $2.0 \times 10^{-4}$  cm/s and  $2.4 \times 10^{-3}$  cm/s) and hydraulic gradient (range between 0.002 and 0.005). Also, a cross section (A) was the rectangular sub-area formed by discretizing the cross-sectional area perpendicular to groundwater flow between two adjacent wells aligned along the source transect line in the main source zone considering the depth of bedrock at the saturated zone.

Because the distribution of TCE concentration showed seasonal fluctuation and high level of TCE temporarily detected at local area, harmonic mean values of total 16 TCE concentration data collected at 7 representative monitoring wells which had shown the continuous high level of TCE during 6 years from August 2010 to November 2015 were used to minimize these effects and then know overall pattern of TCE distribution (Table 3-1).

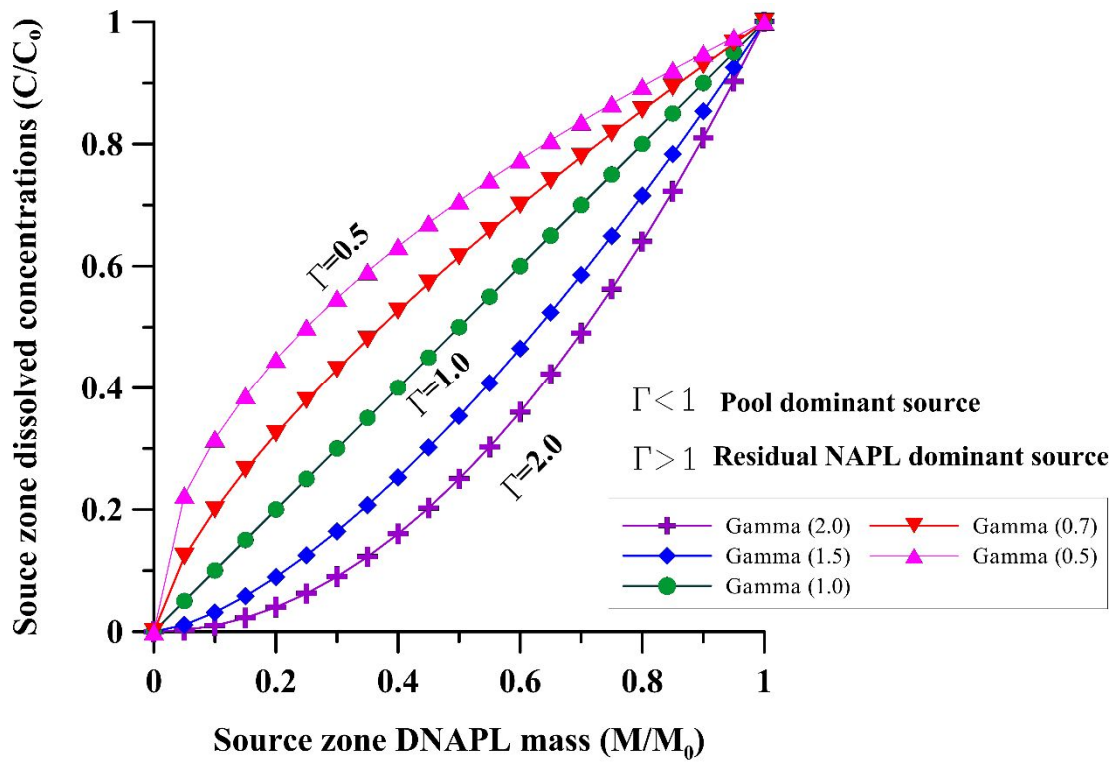


**Figure 3-1** Relationship between source zone DNAPL mass and source zone dissolved concentration data.

**Table 3-2.** Parameters used in analytical solution for estimating the initial source mass and dissolved concentration.

Parameter	Value	Parameter	Value
Decay constant ( $\lambda_s$ )	0	Cross sectional area ( $A$ , $m^3$ )	500
Darcy velocity ( $V_d$ , m/year)	6.0	Empirical parameter ( $\Gamma$ )	1.7

### **3.4.2 Estimation of the initial residual source mass and dissolved concentration**

To estimate the initial TCE residual source mass ( $M_o$ ) and verify the applied dissolved TCE concentration ( $C_o$ ), the tracing procedures which find the reasonable values well matched with the real field concentration data is required. Through the above procedures, the change of residual TCE mass after the remedial action ends can be predicted.

#### **3.4.2.1 Tracing the initial TCE residual source mass ( $M_o$ )**

The estimation of initial residual source mass was carried out with the following procedure. Firstly, TCE concentration data with harmonic mean is prepared and then plotted on semi-log scale (Figure 3-2). Secondly, three sets of TCE concentration data can be calculated using Eq (3-4) with three initial TCE source mass values (500, 1,000, 1,500 kg). In this process, it was assumed that the initial dissolved TCE concentration is 150,000  $\mu\text{g/L}$ . Estimated TCE concentration data of each source mass is plotted on the previous field data graph (Figure 3-3). As shown in Figure 3-3, when 1,000 kg is assumed as the initial residual source mass among three data curves of each initial residual source mass, data curve was well matched with the distribution of field TCE

concentration data until before intensive remedial action. Therefore, it is supposed that NAPL mass of 1,000 kg was spilled on a surface of the main source zone. In Figure 3-3, although about 900 kg as initial mass value looks like a more reasonable mass value than 1,000 kg, because this study only estimates the initial mass value with three types of source mass, more detailed approximate value will be performed at a further study.

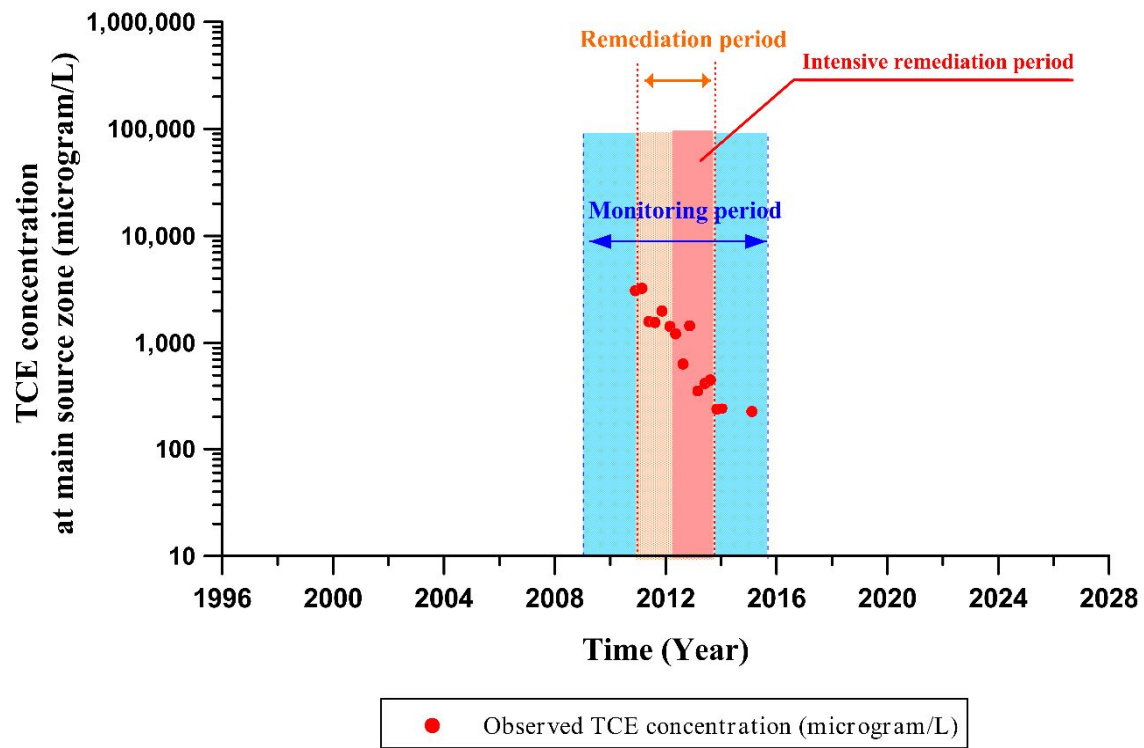


**Figure 3-2.** Field concentration data obtained from 2010 to 2015 for TCE plot on semi-log scale.

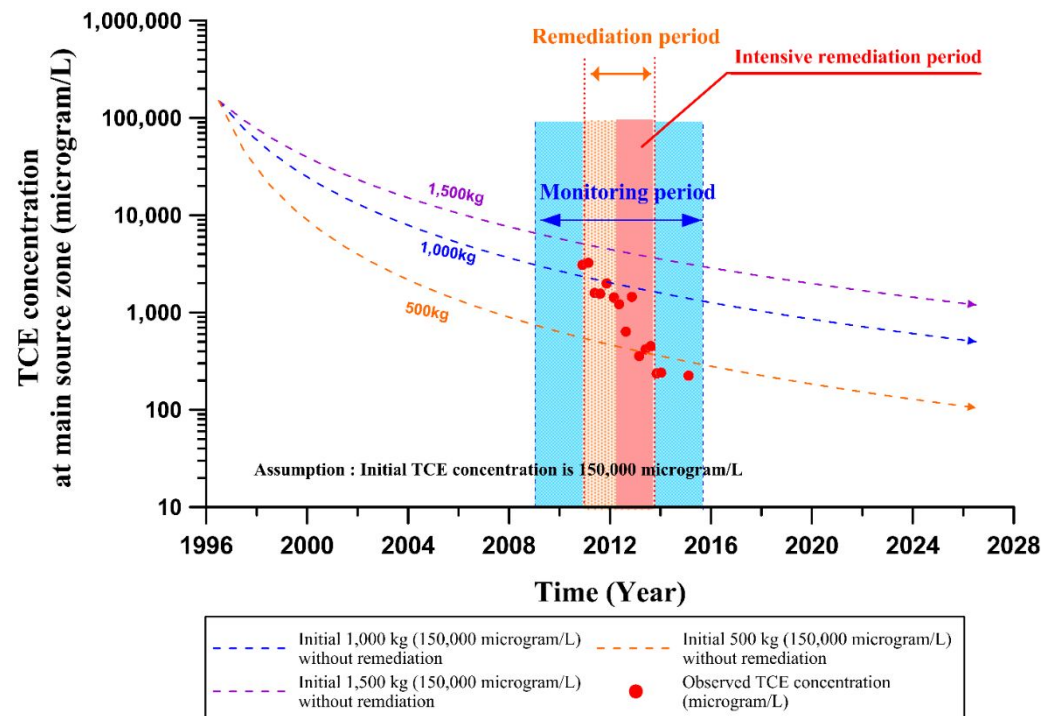


**Figure 3-3.** Matching of estimated data of each initial residual source mass (500, 1000, 1500 kg) data to field concentration data before the remedial action. (Assumption: initial TCE concentration is 150,000  $\mu\text{g/L}$ )

### **3.4.2.2 Verification procedure for the applied initial dissolved TCE concentration ( $C_o$ )**

Generally, when TCE had been spilled at many contaminated sites, initial TCE concentrations in groundwater were shown a range between 50,000 and 200,000  $\mu\text{g/L}$  at the main source areas (Wang and Zhang, 1997; Basu et al., 2006; Révész et al., 2014). In this study, it was considered that the above range is suitable as the range of input value for estimating the initial TCE dissolved concentration ( $C_o$ ).

The verification procedure which is similar with estimating the initial residual source mass was performed. Firstly, TCE concentration data with harmonic mean is prepared and then is plotted on semi-log scale (Figure 3-2). Secondly, three TCE concentration curves acquired using Eq (3-4) with total three initial dissolved TCE source concentration values (100,000, 150,000, 200,000  $\mu\text{g/L}$ ) among the range between 50,000 and 200,000  $\mu\text{g/L}$ , fit to the field data. In this procedure, it is assumed that the initial TCE source mass is 1,000 kg because this value is already estimated by tracing the initial source mass. As shown in Figure 3-4, each estimated TCE concentration data is plotted on the previous field data graph represented in Figure 3-2. Concentration curve estimated with 150,000  $\mu\text{g/L}$  as the initial dissolved TCE concentration is well

matched with the distribution of field TCE concentration data until before intensive remedial action. Although it looks like 200,000  $\mu\text{g/L}$  curve is better matched with field data than 150,000  $\mu\text{g/L}$  curve, this initial concentration value is not used as a reasonable value because estimated data curve is not matched with initial concentration values of field data. These results indicated that the initial dissolved TCE concentration had been distributed with the range between 100,000 and 200,000  $\mu\text{g/L}$  at the initial stage. Therefore, concentration value (150,000  $\mu\text{g/L}$ ) applied in tracing the initial residual source mass is reasonable as the input value. As NAPL is discharged to groundwater, the source mass has decreased and then the amount dissolving into the flowing groundwater has gradually decreased. Eventually, it can be estimated that the present dissolved TCE concentration was distributed through these processes.

From the procedure finding the initial source mass, residual mass and dissolved concentration data as time passed can be predicted. In this chapter, data considering the case of no remediation were calculated. Variations of residual source mass and dissolved concentration before and after the intensive remedial action will be discussed in Chapter 5.

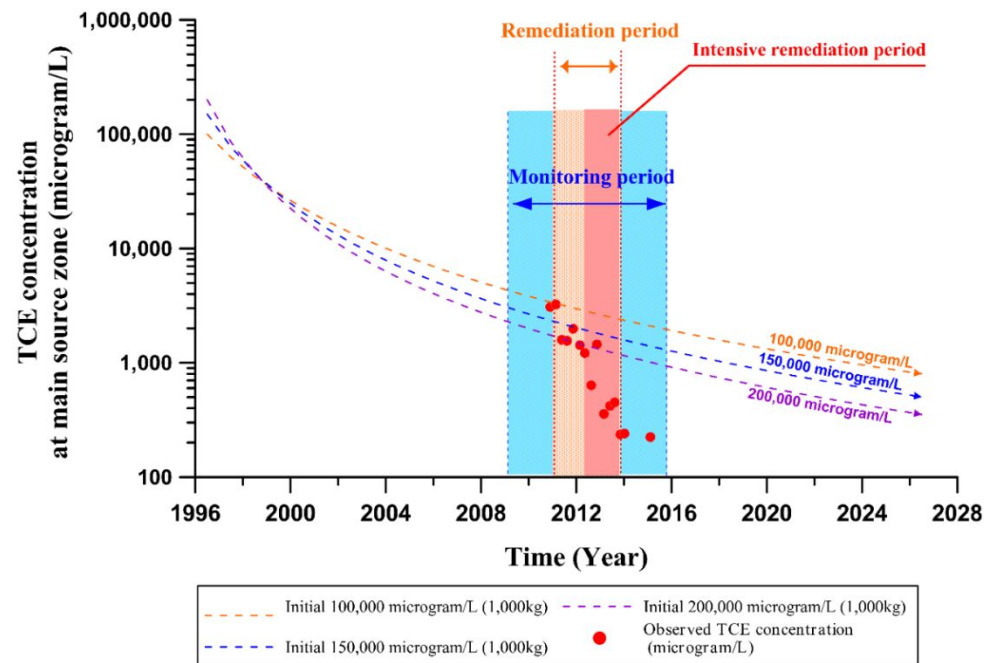


**Figure 3-4.** Matching of estimated data of each initial dissolved TCE source concentration (100,000, 150,000 and 200,000  $\mu\text{g/L}$ ) data to field concentration data until before the remedial action. (Assumption: initial TCE mass is 1,000 kg)

### 3.5 Conclusions

The study site of this study is located in an industrial complex of Wonju city, Korea. Contamination by TCE was detected and had been investigated for contaminant identification and remediation. The precise information for initial source mass and dissolved concentration was unknown at the source zone. These absence of information for contaminant source spilled at DNAPL contaminated sites leads to the deterioration of the groundwater quality and the inefficient augmentation of remedial action. Analytical solutions which can consider the time-dependent exponential reduction of contaminant were used to estimate the unknown initial TCE source mass and dissolved concentration and to predict the residual source mass and dissolved concentration as time passed.

The results of analytical solution used for the source identification indicated that contaminant source had been spilled with approximately 1,000 kg of the source mass and 150,000  $\mu\text{g/L}$  dissolved concentration at the initial stage. Quantitative evaluation method applied in this study have been proven to be useful tools in estimating the unknown contaminant source mass and dissolved concentration at the initial spilled stage of the DNAPL contaminated site using long-term monitoring data.

**CHAPTER 4.**

**EVALUATION OF THE FATE AND**

**TRANSPORT OF CHLORINATED ETHENES**

**IN A COMPLEX GROUNDWATER SYSTEM**

# CHAPTER 4. EVALUATION OF THE FATE AND TRANSPORT OF CHLORINATED ETHENES IN A COMPLEX GROUNDWATER SYSTEM

## Abstract

Chlorinated ethenes such as trichloroethylene (TCE) are common and persistent groundwater contaminants. If contaminated groundwater discharges to a stream, then stream water pollution near the contamination site also becomes a problem. In this respect, the fate and transport of chlorinated ethenes around a stream in an industrial complex were evaluated using the concentration of each component, and hydrogeochemical, microbial, and compound-specific carbon isotope data. Temporal and spatial monitoring reveal that a TCE plume originating from main and local source zones continues to be discharged to a stream. Groundwater geochemical data indicate that aerobic conditions prevail in the upgradient area of the studied aquifer, whereas conditions become anaerobic in the downgradient. The TCE molar fraction is high at the main and local source zones, ranging from 87.4 to 99.2% of the total volatile organic compounds (VOCs). An increasing trend in the molar fraction of *cis*-1, 2-dichloroethene (*cis*-DCE) and vinyl chloride (VC) was observed in

the downgradient zone of the study area. The enriched  $\delta^{13}\text{C}$  values of TCE and depleted values of *cis*-DCE in the stream zone, compared to those of the source zone, also suggest biodegradation of VOCs. Microbial community structures in monitoring wells adjacent to the stream zone in the downgradient area were analyzed using 16S rRNA gene-based pyrosequencing to identify the microorganisms responsible for biodegradation. This was attributed to the high relative abundance of dechlorinating bacteria in monitoring wells under anaerobic conditions farthest from the stream in the downgradient area. The multilateral approaches adopted in this study, combining hydrogeochemical and biomolecular methods with compound-specific analyses, indicate that contaminants around the stream were naturally attenuated by active anaerobic biotransformation processes.

## 4.1 Introduction

Industrial solvent trichloroethylene (TCE) is among the most common chlorinated compounds found in groundwater contamination. In Korea, TCE and tetrachloroethylene (PCE) are the main components of the dense non-aqueous phase liquids (DNAPLs) found in the groundwater of industrial areas, and groundwater contaminated by DNAPLs is often associated with nitrate

contamination (KMOE, 2010). Because chlorinated solvents have relatively low solubility in water and a low tendency to sorb, long contaminant plumes form and may reach surface water bodies. In the study area, a TCE plume originating from an upgradient source zone in an industrial complex passes through local sources in a downgradient area, and is discharged to a stream. Therefore, it is necessary to conduct an intensive study to evaluate the effect of contaminant plumes on stream water quality.

In order to assess the risk of exposure through groundwater, many field studies have been performed to quantify the mass discharge levels of chlorinated contaminant plumes at transects assigned along groundwater flow path, and have used the concentrations of a contaminant and its byproducts to understand various natural attenuation (NA) mechanisms, such as physical, geochemical, and microbial degradation (Kao and Prosser, 1999; Chapman et al., 2007; Basu et al., 2009; Yang et al., 2011). Recently, compound-specific isotope analysis (CSIA) and molecular biological analysis have been proposed as complementary tools for assessing the degree of reductive dechlorination (Hunkeler et al., 1999; Song et al., 2002; Nijenhuis et al., 2007; Imfeld et al., 2008; Abe et al., 2009; Hunkeler et al., 2009; Courbet et al., 2011; Hunkeler et al., 2011; Imfeld et al., 2011; Lojkaseck-Lima et al., 2012; Chiu et al., 2013; Damgaard et al., 2013; Kotik et al., 2014). Specially, studies combining

molecular biology and isotope fractionation (Nijenhuis et al., 2007; Imfeld et al., 2008; Imfeld et al., 2011) have been performed to evaluate dehalogenation in complex models of the discharge of halogenated groundwater to open water bodies. In general, the method used for microbial community analysis (Imfeld et al., 2008; Abe et al., 2009; Damgaard et al., 2013; Courbet et al., 2011; Hunkeler et al., 2011) is quantitative, real-time polymerase chain reaction (qPCR) which provides quantitative evaluation of target primers such as Dehalococcoides (Dhc). On the other hand, the pyrosequencing method (Kotik et al., 2013) can assess the composition and spatial distribution of entire microbial communities. In the present study, pyrosequencing rather than real-time qPCR for microbial community analysis was used because the present study focused on the microbial community structures and the distribution of potential dechlorinators.

The CSIA method uses differences in the reaction rates between molecules with light and heavy isotopes, and evaluates the amount of heavy isotope enrichment in the remaining substrate. Use of both CSIA and nucleotide sequence analysis can thus provide guidelines for microbial ecology, and can be used to indicate the trend of biological processes (Marley et al., 1992; Chen et al., 2005).

Previous studies relating to isotope analysis have been performed at the

present study site, but they have been focused on source identification and allocation (Kaown et al., 2014a). In this study, compound-specific carbon isotope ratio data for TCE and its daughter product (*cis*-DCE) are used to find evidence for biodegradation in the upgradient and downgradient areas of the study site. This study focuses particularly on the stream zone at the border of the contaminant plume, where degradation reactions are able to control the evolution of the plume, as observed by Wilson et al. (2004).

Each microbial community has different characteristics and is formed through the interaction between other microorganisms according to the surrounding environment (Watson et al., 2010). For this reason, it is more important to gain an understanding of microbial communities rather than each type of microorganism. In recent years, analysis of 16S rRNA genes has been used to understand the presence and activity of key organisms such as Dehalococcoides, and to confirm the presence of microorganisms responsible for dechlorination processes at TCE- or PCE-contaminated sites (Fennell et al., 2001; Miller et al., 2007; Nijenhuis et al., 2007; Imfeld et al., 2008; Abe et al., 2009; Maphosa et al., 2010; Imfeld et al., 2011; Tiehm and Schmidt, 2011; Kotik et al., 2014). In relation to evaluating the natural attenuation of chlorinated ethenes, the possibility of biodegradation based on geochemical data (groundwater concentration and isotopic ratio of chlorinated contaminants)

around the downgradient in the study area has previously been suggested (Kaown et al., 2014a). However, although the potential of biodegradation has been proposed, further investigation is required to obtain more detailed evidence of biodegradation, such as the presence and distribution of dechlorinating bacteria. In addition, where there is a contaminated site adjacent to the stream (such as at the study site), it is important for water resource management to assess whether the stream water has been affected by the contaminant plume.

Therefore, the main objectives of this study are to evaluate the fate of chlorinated ethenes associated with biodegradation in groundwater around the stream through an understanding of the spatial relationship between hydrogeochemical conditions and the composition and distribution of microbial communities, including dechlorinating bacteria; and also to investigate transport of the contaminant plume that could influence the quality of stream water. In this study, versatile approaches are used in combination with carbon isotope, hydrogeochemical, and microbial community analyses to gain an insight into the fate of the contaminant, and its transport around the stream.

## **4.2 Study site**

The study site is located approximately 120 km east of Seoul, Korea. As shown in Figure 4-1, the Wonju stream flows from southeast to northwest at the eastern area of the site, and is an important source of irrigation water for a paddy field. The Road Administrative Office (RAO) of Gangwon Province is situated within this site, together with the Woosan Industrial Complex (WIC). The RAO is located at the western area of the study site on a low hill surrounded by small mountains, and forests. A large industrial company is based at the industrial complex, together with approximately 40 public, commercial, and residential buildings. There is an unpaved region in the downgradient area (not related to the stream zone) where groundwater recharge can actively occur during precipitation events, and as this is the only area where groundwater can permeate the subsurface to recharge the aquifer. Only a small amount of rainfall can be recharged into the subsurface over the study area (Yang et al., 2011; Kaown et al., 2014a). Previous reports show that the aquifer at the study site has strong hydrogeological heterogeneity (KMOE, 2010; Yang et al., 2011; Yang et al., 2012; Kaown et al., 2014a). A water treatment facility was previously installed near the Wonju stream to enable stream water treatment at a depth of 3-4 m below the ground surface. However, that facility ceased operation since 2010. The dominant groundwater flow direction is from the RAO to the Wonju stream.

Boring log data show that the aquifer at the study site consists of weathered and highly fractured Jurassic biotite containing granite, with soil and alluvial deposits overlying weathered rocks (Baek and Lee 2001; Yu et al., 2006). The thickness of the aquifer is 10–15 m, and the alluvial deposits thicken near the stream zone, where they measure 3–4 m. During the summer, the depth of the water table has been measured as approximately 8–10 m below surface level (bsl) at RAO in the upgradient area, and 1–3 m bsl in the downgradient area. The observed water table levels during the winter range from 11 to 13 m bsl in RAO, and approximately 2–3 m bsl in the downgradient area. Therefore, the water table in groundwater wells at the RAO shows high seasonal variations, with a range of approximately 3 m throughout the year. Hydraulic gradients around the main source area have been measured as between 0.013 and 0.023, but are much lower in the industrial complex area and the area around the stream, with a narrower range of between 0.008 and 0.011. These differences in hydraulic gradients can result from topographic and hydrogeological conditions at the study site. The much more pronounced hydraulic gradients and wider hydraulic ranges observed at the main source area are due to the site's hilltop location and the heterogeneity of the aquifer. The porosity has been measured as between 0.29 and 0.31 at the main source area and the industrial complex, and from 0.30 to 0.35 around a stream. Kaown et al. (2014b) previously estimated

groundwater flow velocities at the study site by means of  $^3\text{H}$ - $^3\text{He}$  analysis. The groundwater flow velocities ( $1.9 \times 10^{-6}$  to  $2.1 \times 10^{-5}$  m/s) estimated around a stream were about ten times slower than those for the main source area ( $9.8 \times 10^{-6}$  to  $1.2 \times 10^{-4}$  m/s). According to the results from pumping and slug tests conducted in this study, the hydraulic conductivity values range between  $2.0 \times 10^{-4}$  cm/s and  $2.4 \times 10^{-3}$  cm/s and values in the area around the stream range between  $6.5 \times 10^{-4}$  cm/s and  $4.2 \times 10^{-3}$  cm/s.

Previous researches have reported that the groundwater at this site is contaminated by multiple DNAPL components, such as trichloroethylene (TCE), chloroform (CF), and tetrachloride (CT) (Yang and Lee, 2012; Kaown et al., 2014a). The main source of the contaminants is located inside the RAO. Local TCE sources of groundwater contaminants exist near GW-10, GW-11, and GW-19 wells, which are located in the downgradient area. Site monitoring and investigation was performed intensively from 2009 to 2013 as part of a research program for the Korea Ministry of the Environment (KMOE). Yang and Lee (2012) revealed that the study site was contaminated with multiple chlorinated contaminants; in particular, small contaminant sources were identified through a seasonal hydraulic impact analysis, historical approach, and chemical fingerprinting. The results of mass discharge of TCE and *cis*-DCE across transects assigned along the groundwater flow path show that the source

plumes have been effectively contained via remedial actions in the upgradient area. However, in the downgradient area the decreased TCE mass flux and the continuous detection of *cis*-DCE indicate biodegradation of TCE (Lee et al., 2013).

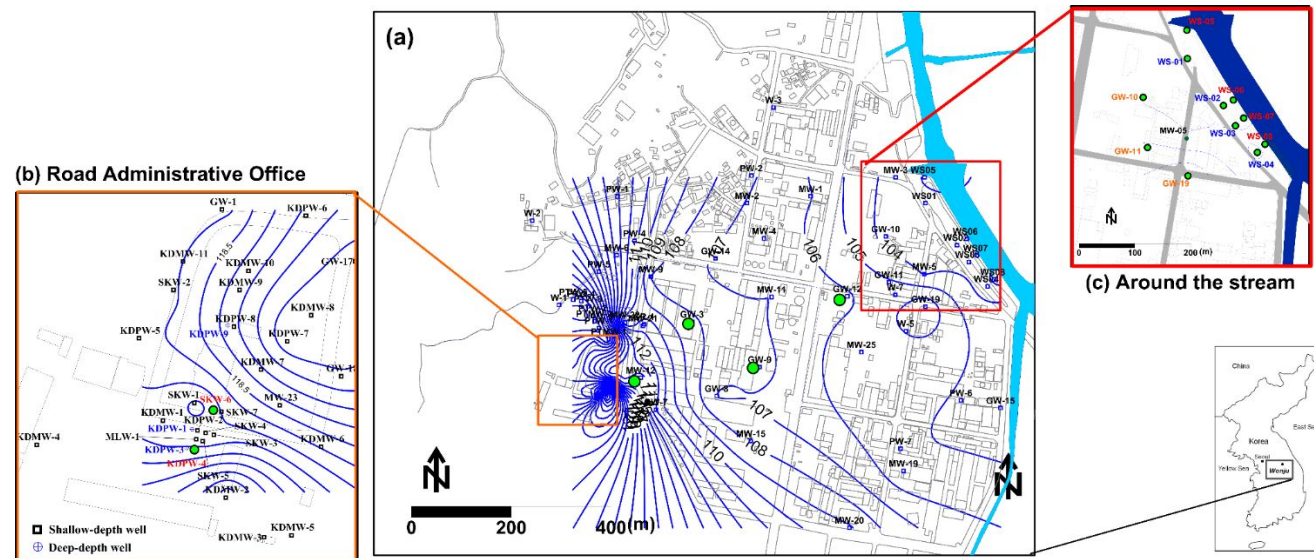


**Figure 4-1.** Location of the study site and layout of groundwater sampling wells (a). Blue lines indicate the contour lines of the measured groundwater level (in meters) conducted in November 2015. The location of wells installed at (b) the Road Administrative Office (RAO); and (c) around the stream. Green open circles represent the monitoring wells used in this study.

## 4.3 Methods

### 4.3.1. Water sampling and water quality analysis

During the period November 2011 to February 2013, groundwater and stream water samples were collected from the Wonju stream and 17 of the 100 monitoring wells installed throughout the study site using a submersible and controllable quantitative pump (MP1, Grundfos, Bjerringbro, Denmark), for chemical, microbiological, and isotopic analyses. All water samples were collected in a closed flow-through cell. Water samples for analysis of chlorinated contaminants were directly collected from the continuous water stream into 40 mL amber glass vials sealed with Teflon-lined septa with no headspace, and samples collected for TCE, *cis*-DCE and VC were directly sampled in identical vials. At the same time, measurements for temperature, pH, dissolved oxygen (DO), electrical conductivity (EC), oxidation-reduction potential (ORP), and total dissolved solid (TDS) were performed to evaluate the geochemical properties of the groundwater on-site. All samples were stored at 4 °C prior to laboratory analysis, with at least 10% of samples collected in duplicate. Gas chromatograph/mass spectrometer (GC/MS) (Saturn 2100T, VARIAN) was used for the analysis of chlorinated contaminants such as TCE,

CT and CF. Water quality parameters such as cations ( $\text{Ca}^{2+}$ ,  $\text{K}^+$ ,  $\text{Mg}^{2+}$ ,  $\text{Na}^+$ ,  $\text{Si}^{4+}$ ,  $\text{Fe}^{2+}$ , and  $\text{Mn}^{2+}$ ) were analyzed by inductively coupled plasma optical emission spectroscopy (ICP-OES) (VISTA-MPX, Varian, Palo Alto, California), while anions ( $\text{F}^-$ ,  $\text{Cl}^-$ ,  $\text{NO}_3^-$ ,  $\text{SO}_4^{2-}$ ,  $\text{HCO}_3^-$ , and  $\text{CO}_3^{2-}$ ) were analyzed by ion chromatography (IC) (761 Compact, Metrohm, Herisau, Switzerland), and dissolved organic carbon (DOC) by the UV persulfate method (Phoenix 8000, Tekmar Dohrmann, USA) was measured at Sangji University, Korea. Samples from several wells were temporally analyzed for  $\text{NO}_3^-$ ,  $\text{SO}_4^{2-}$ ,  $\text{Fe}^{2+}$  and  $\text{Mn}^{2+}$  to evaluate the stability of redox conditions at the site by comparing the data with results from previous samples obtained following well installation. In addition, water sampling for carbon isotope analysis was performed in February 2013 at 10 monitoring wells. The samples for  $\delta^{13}\text{C}$  of TCE and *cis*-DCE analysis were collected in triplicate in 40-mL amber vials fitted with septa and were preserved by the addition of NaOH. The analytical process and determination of values used for  $\delta^{13}\text{C}$  were those described in Kaown et al. (2014a) and Hunkeler and Aravena (2000).

For the carbon isotope analysis, 10 representative wells were selected from the monitoring wells situated between the source zone and the stream. The  $\delta^{13}\text{C}$  values of the contaminant compounds were determined at the Environmental Isotope Laboratory (EIL) at the University of Waterloo, Canada.

The minimum concentrations of TCE in the carbon isotope analysis were approximately 30 µg/L. The  $\delta^{13}\text{C}$  values of TCE ( $\delta^{13}\text{C}_{\text{TCE}}$ ) were then reported relative to Vienna Pee Dee Belemnite ( $\delta^{13}\text{C}_{\text{VPDB}}$ ) (Coplen, 1996), with an analytical precision of  $\pm 0.3\text{‰}$  using the delta notation given by  $\delta^{13}\text{C} = (\text{R}/\text{R}_{\text{std}} - 1)1000(\text{‰})$ ; here R and  $\text{R}_{\text{std}}$  are the isotope ratios of the sample and the  $\delta^{13}\text{C}_{\text{VPDB}}$  standard, respectively.

#### **4.3.2. Microbial community analysis**

Water samples (20 L each) were collected around the stream for the microbial community analysis. Samples were then filtered using a 0.22-µm filter (Millipore, Bedford, MA, USA), after which the filters were exfoliated using distilled water and subjected to total DNA extraction using a DNeasy Plant Mini Kit (Qiagen, Valencia, CA, USA) (Nübel et al., 1997). Amplification was carried out using a C1000 Touch thermal cycler (BioRad, Hercules, CA, USA) in a final volume of 50 µL, using 10× Taq buffer dNTP mixture (Takara, Shiga, Japan). The amplification condition was the same as that given in Hur et al., (2013). An AMPure Bead Kit (Agencourt BioScience, Beverly, MA, USA) was used to mix and purify equimolar concentrations of each amplified product. After emulsion PCR, the beads were recovered and then deposited on a 454 picotiter plate; sequencing was then completed using a Roche/454 GS Junior

system under the manufacturer's instructions (Chun Lab). The pyrosequencing procedure of genomic DNA extracted from water samples was performed as described in Undo et al. (2010) and Kou et al. (2015). Additionally, the taxonomic assignment of each pyrosequencing read was performed by comparing it to sequences stored in the EzTaxon database (which contains 16S rRNA gene sequences of type strains that have valid published names and representative species-level phylotypes of either cultured or uncultured entries in the database (<http://www.eztaxon-e.org>)), using BLASTN searches and pairwise similarity comparisons (Chun et al., 2007; Jeong et al., 2013).

## **4.4 Results and discussion**

### **4.4.1 Spatial distribution of contaminants**

The groundwater quality throughout the entire study site has been monitored since 2004, and a systematic and intensive groundwater quality monitoring was performed from 2009 to 2013 under funding from the KMOE (Yang et al., 2011; Lee et al., 2013; Kaown et al., 2014a). Based on the groundwater analytical results from November 2011 to February 2013, the TCE plume was found to originate from the RAO, and extend to the stream along the

groundwater flow path (Figure 4-2). The front edge of the plume was found at approximately 812 m downgradient from the main source zone in the RAO. In the main source zone, a maximum TCE concentration of up to 15,748  $\mu\text{g/L}$  was observed in August 2009, during sampling surveys (Yang et al., 2011), and concentrations then decreased along the groundwater flow path during the observation period. In the downgradient area, anomalously high TCE concentrations of between 36 and 122  $\mu\text{g/L}$  were observed at the GW-10 and GW-11 wells, which were known to be located near the local TCE source. In the upgradient area, the concentration of *cis*-DCE (which is a biodegradation byproduct of TCE) was found to range between non-detectable and 57  $\mu\text{g/L}$  from November 2011 to February 2013; in the downgradient area, wells GW-19, WS-3, and WS-4 showed high concentrations of 178 to 538  $\mu\text{g/L}$ . As previously noted, there was no previously recorded history of DCE use, and therefore, based on evidence identified from this study, the presence of the DCE isomer in groundwater at this site was considered to be due to the biotransformation of TCE via reductive dechlorination. In particular, only VC, which is a metabolite, was detected in the downgradient area.

Locally high VC concentrations of between 12 and 56  $\mu\text{g/L}$  were observed at wells WS-2 and WS-4 from February 2013 to September 2013 (Table 4-1). The coexistence of *cis*-DCE and VC around the stream where TCE

was detected indicates active biodegradation of TCE around the stream. Although high TCE levels were persistent from the source zone to the middle of the contaminant plume, the VOCs' molar fraction of TCE degradation products constantly increased toward the downgradient area, especially around the stream from 2012 to 2013 (Figure 4-2).

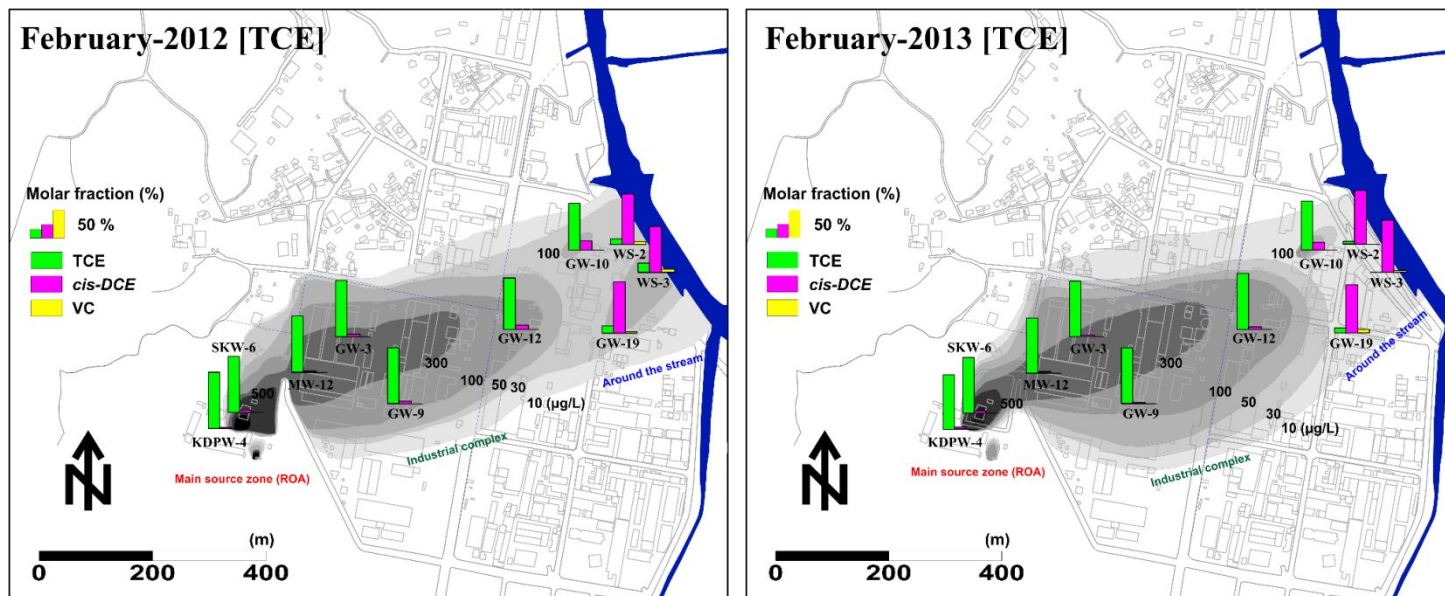


Figure 4-2. Spatial distribution of TCE in groundwater samples obtained at February 2012 and 2013, and molar fraction (%) of each contaminant.

**Table 4-1.** Concentrations ( $\mu\text{g/L}$ ) of TCE, *cis*-DCE and VC in groundwater obtained at the study site (February 2013; August 2013; September 2013).

Well name.	February 2013			August 2013			September 2013		
	TCE ( $\mu\text{g/L}$ )	<i>cis</i> -DCE ( $\mu\text{g/L}$ )	VC ( $\mu\text{g/L}$ )	TCE ( $\mu\text{g/L}$ )	<i>cis</i> -DCE ( $\mu\text{g/L}$ )	VC ( $\mu\text{g/L}$ )	TCE ( $\mu\text{g/L}$ )	<i>cis</i> -DCE ( $\mu\text{g/L}$ )	VC ( $\mu\text{g/L}$ )
GW-10	113	12	N.D.	66	7	N.D.	100	15	1
GW-19	25	194	7	7	26	8	16	127	8
WS-1	2	8	N.D.	N.D.	5	3	1	3	2
WS-2	11	241	1	3	47	56	4	74	43
WS-3	1	302	5	2	68	1	3	94	6
WS-4	2	32	N.D.	1	59	3	1	113	12
WS-5	N.D.	N.D.	N.D.	N.D.	N.D.	N.D.	N.D.	N.D.	N.D.
WS-6	N.D.	N.D.	1	1	1	1	N.D.	N.D.	N.D.
WS-7	N.D.	N.D.	1	N.D.	31	11	N.D.	N.D.	N.D.
WS-8	N.D.	N.D.	N.D.	1	N.D.	N.D.	N.D.	N.D.	N.D.
SW-3	N.D.	N.D.	N.D.	N.D.	N.D.	N.D.	N.D.	N.D.	N.D.

N.D.: Not detected

#### 4.4.2 Hydrogeochemistry

Concentrations of redox-sensitive parameters analyzed from the main source zone to the stream are shown in Figure 4-3a. Concentrations of DO were observed from November 2011 to February 2013; values ranged from 0.02 to 1.45 mg/L in the downgradient area, in contrast to the higher values found in the upgradient area (KDPW-4: 2.12 to 7.01 mg/L) and in the stream water (SW-3: 1.45 to 8.93 mg/L). Low levels of DO are indicative of anaerobic conditions within the downgradient area adjacent to the stream (Figure 4-3a). However, it is of note that the redox condition is characterized by aerobic conditions in most of the study area, except in the streamside zone in the downgradient area. This difference can be explained by site-specific conditions; most of the upgradient area is directly recharged by rainfall through areas such as forest and grassland, whereas most of the downgradient area is covered by a paved surface and industrial buildings, and there is no implication by rainfall events. According to a comparison of ORP distribution between the source area and the downgradient area, values in the source area ranged between 89.0 and 324.1 mV at well KDPW-4, while monitoring wells located around the stream showed declines in values of ORP ranging between -211.1 and 51.5 mV. This reflects the change in the redox condition from oxidizing to reducing conditions, and

also indicates the occurrence of biodegradation processes, which subsequently provokes the decrease in ORP values (Figure 4-3b). Nitrate ( $\text{NO}_3^-$ ) levels varied considerably along the groundwater flow path (Figure 4-3c); concentrations ranged between 9.63 and 18.55 mg/L in the upgradient area, and between non-detectable and 6.62 mg/L in the downgradient area. This result reveals nitrate reduction to be the dominant biodegradation pattern within the local area around the stream (Figure 4-3c). Compared with values of ferrous ion ( $\text{Fe}^{2+}$ ) ( $<0.03$  mg/L) and manganese ( $\text{Mn}^{2+}$ ) ( $<0.01$  mg/L) measured at wells KDPW-4 and SKW-6 located in the main source area, the values of  $\text{Fe}^{2+}$  and  $\text{Mn}^{2+}$  around the stream increased to 13.98 mg/L at well WS-4 and 5.09 mg/L at WS-6, respectively. This result suggests that iron and manganese reduction was an active process around the stream (Figure 4-3d and 4-3e). Concentrations of sulfate ( $\text{SO}_4^{2-}$ ) in the groundwater ranged between 1.28 and 89.46 mg/L around the stream, and it was therefore evident that an intensive  $\text{SO}_4^{2-}$  reducing process was not occurring at the study site.

An analysis of the geochemical data indicates that the heterogeneity of aquifer and recharge patterns at this study site (KMOE, 2010; Yang et al., 2011; Yang et al., 2012; Kaown et al., 2014a) is closely related to the heterogenic geochemical conditions. The upgradient areas of the study site showed aerobic condition with high concentrations of DO and  $\text{NO}_3^-$ , indicating oxidizing

conditions. In addition, concentrations of TCE accounted for between 97.2% and 99.2% of the molar fraction of total VOCs. These results meant that the strong oxidants  $O_2$  and  $NO_3^-$  have not been fully consumed as electron acceptors in the upgradient area. Furthermore, anaerobic condition with high concentrations of  $Fe^{2+}$  and  $Mn^{2+}$  and low concentrations of DO and  $NO_3^-$  was found in the streamside zone of the downgradient area, within which the TCE molar fraction accounted for 0.2 to 8.2% of the total VOCs found around the stream, as presented in Table 4-2 and Figures 4-2 and 4-3. The change of geochemical parameters in the downgradient area indicates that TCE started to serve as electron acceptor following consumption of the oxidants  $O_2$  and  $NO_3^-$ . The trend of the redox condition and the distribution of the VOC's molar fraction from the main source zone to the stream indicated that reductive dechlorination was occurring in the downgradient area, especially around the stream.

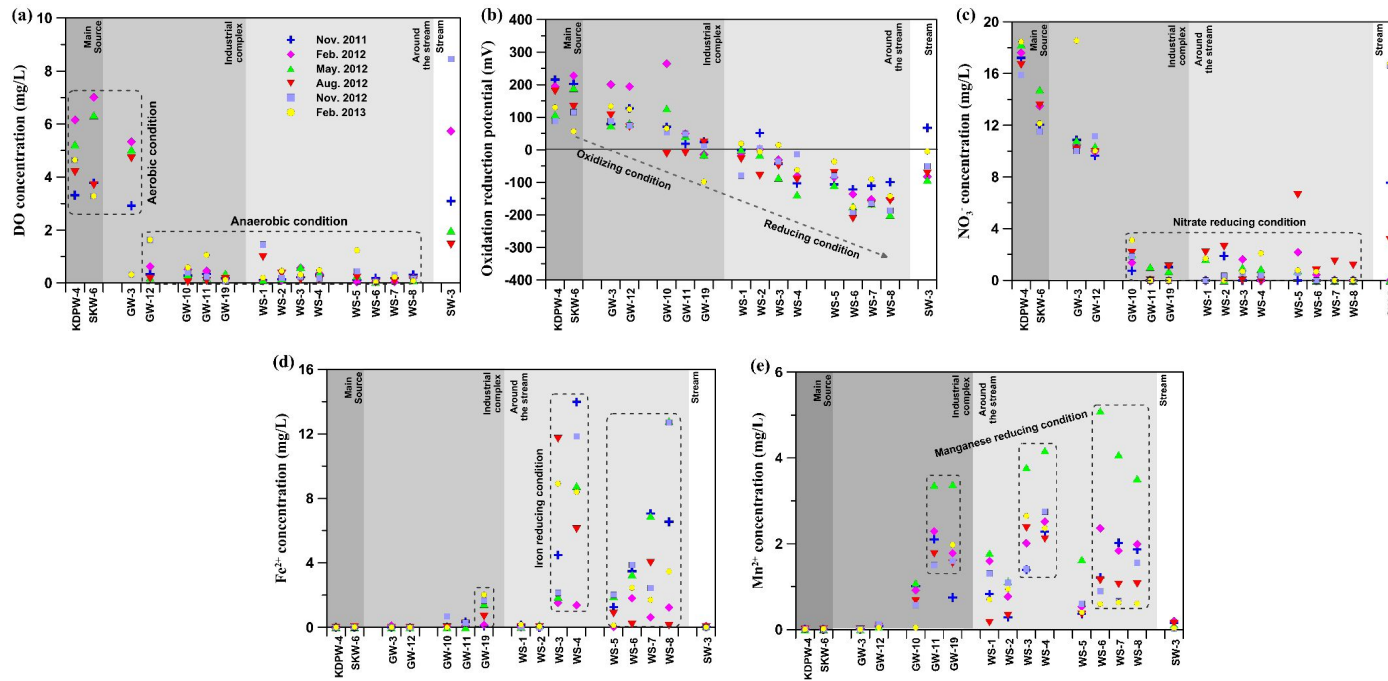


**Figure 4-3.** Seasonal variations of Dissolved Oxygen (DO, mg/L),  $\text{NO}_3^-$  (mg/L),  $\text{Fe}^{2+}$  (mg/L),  $\text{Mn}^{2+}$  (mg/L) concentrations and Oxidation Reduction Potential (ORP, mV) in groundwater samples, measured in November 2011, February, May, August, and November 2012, and February 2013.

**Table 4-2.** Concentrations ( $\mu\text{g/L}$ ) and carbon isotope ( $\delta^{13}\text{C}$ ) values (‰) of TCE and *cis*-DCE in groundwater obtained at study site (February 2013)

Well name	Distance from the source zone (m)	TCE	<i>cis</i> -DCE	VC	$\delta^{13}\text{C}$ TCE	$\delta^{13}\text{C}$ <i>cis</i> -DCE	$\delta^{13}\text{C}$ VC	Molar fraction	Molar fraction	Molar fraction
		( $\mu\text{g/L}$ )	( $\mu\text{g/L}$ )	( $\mu\text{g/L}$ )	(‰)	(‰)	(‰)	(TCE, %)	( <i>cis</i> -DCE, %)	(VC, %)
KDPW-4	0	1,508	27	N.D.	-22.8	-23.8	N.M.	97.7	2.3	0.0
SKW-6	21	2,018	31	N.D.	-24.7	N.M.	N.M.	98.0	2.0	0.0
MW-12	125	94	2	N.D.	-24.4	N.M.	N.M.	97.2	2.8	0.0
GW-3	271	360	2	N.D.	-24.0	-26.8	N.M.	99.2	0.8	0.0
GW-9	362	172	2	N.D.	-24.1	N.M.	N.M.	98.5	1.5	0.0
GW-12	570	194	3	N.D.	-24.1	N.M.	N.M.	97.9	2.1	0.0
GW-10	692	113	12	N.D.	-24.4	-27.9	N.M.	87.4	12.6	0.0
GW-19	712	25	194	7	-19.2	-26.8	-35.2	8.2	86.3	5.5
WS-2	814	1	241	1	-18.4	-27.9	-33.5	3.2	96.2	0.6
WS-3	823	1	302	5	-17.7	-29.1	-29.3	0.2	96.8	3.0

N.M.: Not measured; N.D.: Not detected

#### 4.4.3 Compound-specific carbon stable isotope analysis

The measured  $\delta^{13}\text{C}$  values of TCE and *cis*-DCE are shown in Table 4-2. Most of the measured  $\delta^{13}\text{C}$  values of TCE ranged from -24.7‰ to -17.7‰ (mean value, -22.4‰). The observed  $\delta^{13}\text{C}$  of *cis*-DCE values ranged from -29.1‰ to -23.8‰ (mean value, -27.1‰). It was apparent that the values of  $\delta^{13}\text{C}$  were affected by whether or not degradation of TCE had occurred, and it appeared that generally the  $\delta^{13}\text{C}$  values of TCE were depleted in the upgradient area (Figure 4-4a). The SKW-6 well in the main source zone showed the highest concentrations of dissolved TCE (2,018  $\mu\text{g/L}$ ), and the least-enriched  $\delta^{13}\text{C}$  signatures were found at this site (Table 4-2). This evidence supports the hypothesis that the isotopic fractionating processes of biodegradation have a minimal impact at this source well. Uncommonly, the isotopic values of TCE at KDPW-4 well in the main source area were slightly enriched (Figure 4-4a). However, this isotope pattern is estimated to be related to the cometabolic degradation of TCE under aerobic conditions (Chu et al., 2004; Tiehm and Schmidt, 2011), because KDPW-4 well is located in the upgradient area which is composed of the heterogeneous aquifer and *cis*-DCE was continuously detected during the monitoring period (Kaown et al., 2014a). The enrichment of  $\delta^{13}\text{C}$  TCE values accompanied by declining TCE molar fraction was observed;

this is a typical trend for TCE biodegradation. In the study area, the most-enriched  $\delta^{13}\text{C}$  TCE values (-17.7‰) compared to the source values were found in the groundwater sampled from WS-3 well, which is located in the vicinity of the stream (Figure 4-4a). This isotope pattern is in agreement with the VOC molar distribution, which showed that *cis*-DCE represented 96.8% of the remaining total VOCs in this well, thereby indicating that an appreciable mass of TCE had been transformed to *cis*-DCE (Table 4-2, Figure 4-2). In the downgradient area (and in particular around the stream), where much lower TCE concentration were observed than in the source area, relatively higher byproducts of TCE such as *cis*-DCE and VC were detected. At wells WS-2 and WS-3, which are located around the stream, the *cis*-DCE comprised more than 86% of the total VOCs, and VC represented 5% of this amount (Table 4-2, Figure 4-2); these data also support the conclusion that TCE was biodegraded to *cis*-DCE and VC in the downgradient area. The  $\delta^{13}\text{C}$  values for *cis*-DCE at these wells were depleted compared to values at the main source area, which was consistent with the expectation that *cis*-DCE was formed by the degradation of TCE (Figure 4-4b). This change of isotope pattern in relation to location also corresponded with the VOCs' molar distribution shown in Figure 4-2 and 4-4b. In particular, at well GW-10, which is located around the local source, relatively depleted  $\delta^{13}\text{C}$  for *cis*-DCE was detected (Figure 4-4b).

The enriched  $\delta^{13}\text{C}$  value (-17.7‰) of TCE, and the presence of byproducts such as *cis*-DCE and VC representing 96.8% and 3.0% of the total molar fraction in well WS-3 indicated that TCE biodegradation has proceeded beyond *cis*-DCE.

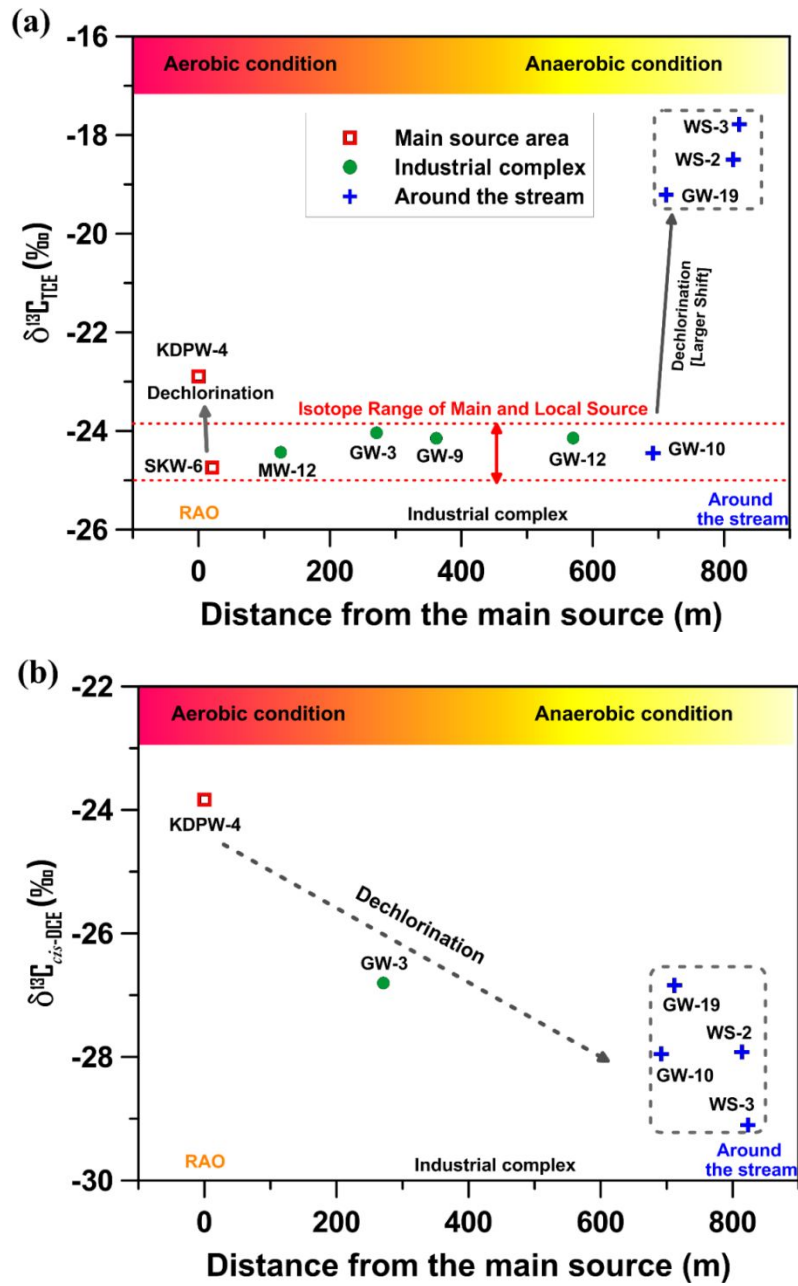


**Figure 4-4.** (a)  $\delta^{13}\text{C}$  value (‰) of TCE, and (b) *cis*-DCE with distance (m) from the main source zone.

#### **4.4.4 Microbial community structures and distribution of potential dechlorinators**

The pyrosequencing method used in this study is widely applied in various fields of metagenomics as it provides a sufficient DNA sequence read-length for analysis. The microbial community structure of eight groundwater samples and one stream water sample were analyzed using 16S rRNA gene-based pyrosequencing. The numbers of analyzed sequences, the operational taxonomic units (OTUs), estimated species richness (Chao 1 and ACE), diversity indices (Shannon and Simpson), and the estimated sample coverage for a 16S rRNA library of samples are summarized in Table 4-3. The number of sequences for each sample was within the 4837–7597 (Table 4-3). The diversity index indicated that among the samples, microbial diversities were highest at well WS-7 and lowest at well GW-10. Well GW-10 showed the highest concentration of TCE among the analyzed samples. This is related to the fact that bacterial community diversity is generally low under stressed conditions, and exists closest to the plume center when polluted by chemical contaminants (Fahrenfeld et al., 2014).

Dendrograms provide grouping of the samples based on microbial community similarities (Figure 4-5). The hierarchical clustering of the bacterial

communities of wells GW-10, WS-1, WS-2, and GW-19 showed similarities, and they were thus classified as Group-A; wells WS-4, WS-6, and WS-7 were classified as Group-B. The phylogenetic distributions of each sample at the phylum, class, and order levels are summarized in Table 4-4. Microbial community structures of all samples were dominated by Betaproteobacteria, which accounted for 24.3–78.5% of all sequences assigned to this class of Proteobacteria. The abundance of Betaproteobacteria was higher at well WS-2 (representing 78.5% of all sequences), which also had the highest *cis*-DCE concentration (214  $\mu\text{g/L}$ ). Sequences belonging to Alphaproteobacteria were the second-largest segment of all sequences. However, the abundance of Deltaproteobacteria peaked at well GW-19 (4.1% in all sequences), and TCE reductive dechlorination had been actively proceeding at this well. Planctomycetacia and Verrucomicrobiae were mostly detected in stream water (SW-3).

The phylogenetic distribution indicated that bacterial communities were similar at wells GW-10 and GW-19, and at wells WS-6 and WS-7. When grouped by the monitoring well, the bacterial community structure varied in relation to the distance from the source area. For example, the majority of orders identified in the proximate GW-10 well (48.5% order diversity) were related to the order Burkholderiales, whereas, at well WS-6 most of the orders

were related to Methylophilales (38.1%) (Figure 4-6). Members of Burkholderiales were most abundant in all groups, showing a relative abundance of between 10.3% and 49.8 %. Similar distributions were published by Miller et al. (2007) and Kotik et al. (2013) when analyzing the bacterial community structures within TCE-contaminated site; in their study sites, the major bacterial sequences were also related to the order Burkholderiales.

The genus *Sterolibacterium* was the most abundant in samples from Group A, particularly at well WS-2, and accounted for 8.1–39.7% of all sequences. Members of the order Methylophilales and Methylococcales, which are obligate methanotrophs (Kotik et al., 2013), were most abundant in samples from Group B (particularly at well WS-6), and accounted for 2.3–38.1% and 7.7–16.6%, respectively (Figure 4-6). Members of the order Nitrosomonadales, which include the genus *Nitrosomonas* that oxidizes ammonia into nitrite in a process called nitrification, also exhibited increased abundances in group B, especially at well WS-7.

In relation to biotic reductive dechlorination, it is important to know which type of dechlorinating microbial communities are present, so as to provide evidence for biodegradation (Abe et al., 2009; Miller et al., 2009; Conrad et al., 2010; Kotik et al., 2013). Therefore, a heat map gradient and hierarchical cluster analysis were used to identify the difference in relative

abundance for all sequences between the microbial communities in each group, as separated by a dendrogram, and then to detect any dechlorinating bacteria (Figure 4-7).

Members of the genus *Polaromonas* appeared to be the most significant of the bacterial groundwater communities around the local source area. The bacteria were most abundant at well GW-10, which is installed near the local source, and accounted for 23.0% of all sequences (Figure 4-7). However, the bacteria were less abundant at wells WS-4 (0.1%) and WS-6 (0.1%), which were located further from the local source. Under aerobic condition, *Polaromonas*-related bacteria actively oxidize *cis*-DCE for use as a carbon source at concentrations of a few mg/L (Coleman et al., 2002; Jeon et al., 2004). At this study site, *Polaromonas*-related bacteria showed an increased abundance trend at well GW-10 (Group A), which contained a high level of TCE and low concentrations of *cis*-DCE (12 µg/L) and VC (1 µg/L) which are measured intermittently (Table 4-2). Based on the dechlorinating feature of *Polaromonas* and the presence of *cis*-DCE and VC, that the findings suggest that *Polaromonas*-related bacteria actively dechlorinate *cis*-DCE as a carbon source at well GW-10. A substantial number of known organohalide-respiring bacteria were detected to the most absent in the DNA data sets from all three groups. A detailed analysis found that the highly specialized organohalide respirers within

the genera Dehalococcoides, Dehalobacter, and Dehalobium were represented in extremely small numbers, or were not detected. The limitation of the above-mentioned dehalogenators performing a sequential anaerobic dechlorination at this study site is closely related to the heterogeneous nature of the aquifer, which leads to partially anaerobic conditions in the downgradient area. Therefore, it was assumed that dehalogenators were detected in small numbers in the downgradient area because the fluctuating redox conditions are not suitable for anaerobic organohalide-respiring bacteria. However, some of the more versatile genera or organohalide respirers, which use various electron acceptors and donors (Maphosa et al., 2010), were detected, albeit in small numbers. For instance, the genus Geobacter, which is one of the most important dechlorinating bacteria involved in the process of TCE to *cis*-DCE and acts as a metal-reducing bacterium (Sung et al., 2006), was relatively abundant at well GW-19 under anaerobic conditions, accounting for 1.9% of all sequences (Figure 4-7). The presence of the genus Geobacter correlated with the detection of *cis*-DCE and VC at well GW-19, and correlated with a larger shift in the carbon isotope composition of both TCE and *cis*-DCE. In addition, molar fractions for TCE, *cis*-DCE, and VC (0.2%, 96.8%, and 2.9%) at this well provide supporting evidence that the genus Geobacter was actively reductive dechlorinating TCE to *cis*-DCE.

Nitrosomonas-related bacteria, which are capable of cometabolically degrading a variety of halogenated organic compounds, including TCE, benzene, and VC (Arciero et al., 1989) were the most abundant at well WS-7 and accounted for 8.7% of all sequences. The presence of Nitrosomonas-related bacteria correlated with the detection of low levels of VC (1-11  $\mu\text{g/L}$ ) at well WS-7 compared to well WS-2 (1-56  $\mu\text{g/L}$ ) (Table 4-1). This study assumed that Nitrosomonas-related bacteria intermittently participate in the degradation of TCE and VC because *cis*-DCE and VC were not consistently detected. *Curvibacter* which is a TCE-degrading bacteria (Kuo et al., 2014) showed a high relative abundance (>5%) at well WS-4, which contained high concentrations of *cis*-DCE and low levels of VC, accounting for 23.1% of all sequences (Figure 4-7). It has been suggested that this species is potentially involved in the degradation of TCE and VC. Methanotrophs such as *Methylothera* and *Methylobacter*, which utilize methane as the sole source of carbon and energy, participate in cometabolic TCE degradation (Koh et al., 1993; van Hylckama and Janssen, 2001; Kotik et al., 2013). The genus *Methylobacter* appears to be significant members of the bacterial groundwater communities of Group B, which consisted of wells installed near the stream, accounting for 10.3% of all sequences (Figure 4-7). Especially, the species *M. tundripaludum*, which is a methane-oxidizing bacterium showed high relative

abundance (6.2% of all sequence) at well WS-4, which contained a high concentration of *cis*-DCE (32  $\mu\text{g/L}$ ) and low levels of TCE (1 to 2  $\mu\text{g/L}$ ) and VC (1 to 12  $\mu\text{g/L}$ ) under anaerobic conditions (Table 4-1). It is likely that the high abundance of methylotrophs under anaerobic conditions near the stream is a consequence of the metabolic activity of archeal methanogens, thereby generating methane, and a carbon and energy source for methylotrophic bacteria mentioned by Kotik et al. (2013).

It is of interest that SW-3 was assigned to an isolated location (Group C), which suggests that its bacterial community was distinct from all others. These group classifications were closely related to the results of the flowmeter test carried out in the survey area (Lee et al., 2015), which showed that groundwater located around wells GW-10 and GW-19 (that were installed around the local source) moved towards the stream with two dominant flow directions. One of these flow directions was towards the location of the installed wells WS-1 and WS-2, which assigned to Group-A on the basis of hierarchical clustering. The other flow direction was towards the location of wells WS-4, WS-6, and WS-7, which are assigned to Group-B. From these results, it is suggested that the direction of groundwater flow is closely related to the distribution of microbial communities around the stream, which thus indicates that the microbial communities in the study area are influenced by

both the hydrogeological characteristics and the distribution of the chlorinated ethenes related to anaerobic conditions. Although microbial community structure analyses were performed along the groundwater flow path during one time sampling, it is considered that the findings for the microbial community structure can be usefully applied to assess the biodegradation of chlorinated ethenes in the study area.

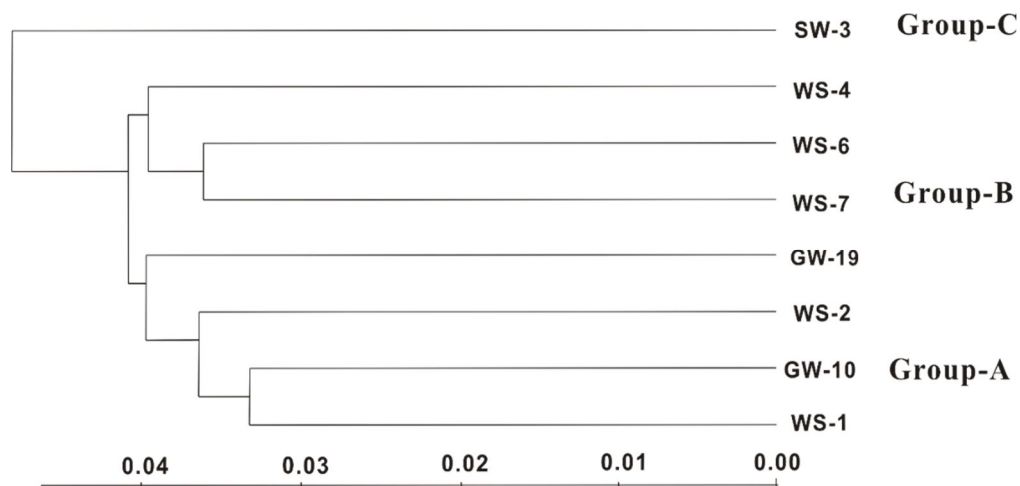


**Figure 4-5.** Hierarchical clustering of clone libraries from eight samples.

**Table 4-3.** Observed and estimated bacterial diversity in groundwater samples

Sample	Total reads	OTUs (CD-HIT)	Estimated species richness		Diversity indices		Goods Lib. Coverage
			Ace (CD-HIT)	Chao1 (CD-HIT)	Shannon (CD-HIT)	Simpson (CD-HIT)	
GW-10	7218	1172	3220	2374	5.17	0.03	0.91
GW-19	6225	1038	2258	1959	5.74	0.01	0.92
SW-3	5370	1095	2525	1975	5.86	0.01	0.90
WS-1	5213	1294	3865	2796	5.97	0.01	0.85
WS-2	4387	851	1674	1411	5.56	0.02	0.91
WS-4	7163	1063	2547	2044	5.29	0.02	0.92
WS-6	7597	1290	3162	2450	5.63	0.01	0.91
WS-7	5171	1355	3409	2529	6.24	0.01	0.86

**Table 4-4.** Most active microbial community structures with groups A, B, C, as determined by ratios of relative abundance of DNA reads at phylum, class, and order levels.

		Relative abundance (%) - Group A				Relative abundance (%) - Group B			Relative abundance (%) - Group C
		WS-1	GW-10	WS-2	GW-19	WS-7	WS-6	WS-4	SW-3
Phylum	<i>Proteobacteria</i>	67.6	76.0	95.5	70.0	80.1	85.0	91.1	51.3
	<i>Actinobacteria</i>	3.2	0.6	0.5	3.3	4.0	2.0	0.5	7.3
	<i>Verrucomicrobia</i>	0.4	0.3	0.0	0.4	0.2	0.7	0.0	10.6
	<i>Acidobacteria</i>	2.3	0.8	0.8	1.3	1.3	0.4	0.1	0.1
	<i>Bacteroidetes</i>	0.4	0.5	0.0	5.2	1.4	5.9	0.1	6.6
	<i>Firmicutes</i>	0.8	0.1	0.0	1.0	1.0	0.2	0.0	0.1
Class	<i>Alphaproteobacteria</i>	18.0	9.5	8.1	14.7	18.0	7.6	1.6	16.4
	<i>Betaproteobacteria</i>	43.1	59.8	78.5	40.2	49.3	57.1	74.3	24.3
	<i>Gammaproteobacteria</i>	4.0	4.9	7.9	10.7	9.5	18.1	13.9	9.1
	<i>Deltaproteobacteria</i>	2.0	1.4	0.8	4.1	3.0	2.0	1.2	1.2
	<i>Actinobacteria</i>	2.7	0.1	0.3	3.2	3.4	1.8	0.4	5.7
	<i>Acidobacteria</i>	0.2	0.1	0.1	0.0	0.0	0.0	0.0	0.0
	<i>Sphingobacteria</i>	0.3	0.1	0.0	1.2	0.7	4.4	0.0	3.2
	<i>Planctomycetacia</i>	0.6	0.0	0.0	0.1	0.2	0.2	0.0	14.9
	<i>Verrucomicrobiae</i>	0.3	0.1	0.0	0.1	0.2	0.6	0.0	10.2
	Order	<i>Burkholderiales</i>	27.5	48.5	35.4	33.1	23.6	10.3	49.8

<i>Sterolibacterium_</i> <i>o</i>	11.9	8.1	39.7	0.3	7.9	3.9	1.8	3.3
<i>Methylophilales</i>	1.0	0.6	0.6	0.9	2.3	38.0	10.1	0.9
<i>Methylococcales</i>	0.5	2.3	6.9	0.3	7.6	16.6	13.6	0.0
<i>Sphingomonadales</i>	9.2	5.2	2.7	7.5	6.2	4.2	0.1	3.5
<i>Rhizobiales</i>	4.7	1.3	3.1	0.4	3.7	0.7	1.1	3.7
<i>Rhodocyclales</i>	0.4	0.0	0.8	5.0	0.9	3.0	1.2	0.3
<i>Pseudomonadales</i>	0.4	1.9	0.3	7.8	0.0	0.0	0.0	1.2
<i>Nitrosomonadales</i>	0.0	0.1	0.0	0.0	9.4	0.4	0.0	1.3
<i>Verrucomicrobiales</i>	0.1	0.0	0.0	0.0	0.1	0.4	0.0	10.0
<i>Chloroflexi_</i> <i>uc_</i> <i>o</i>	0	0.0	0.0	0.0	0.0	0.0	0.0	0.0
<i>Desulfuromonadales</i>	0.2	0.1	0.0	2.8	0.6	0.3	0.0	0.0

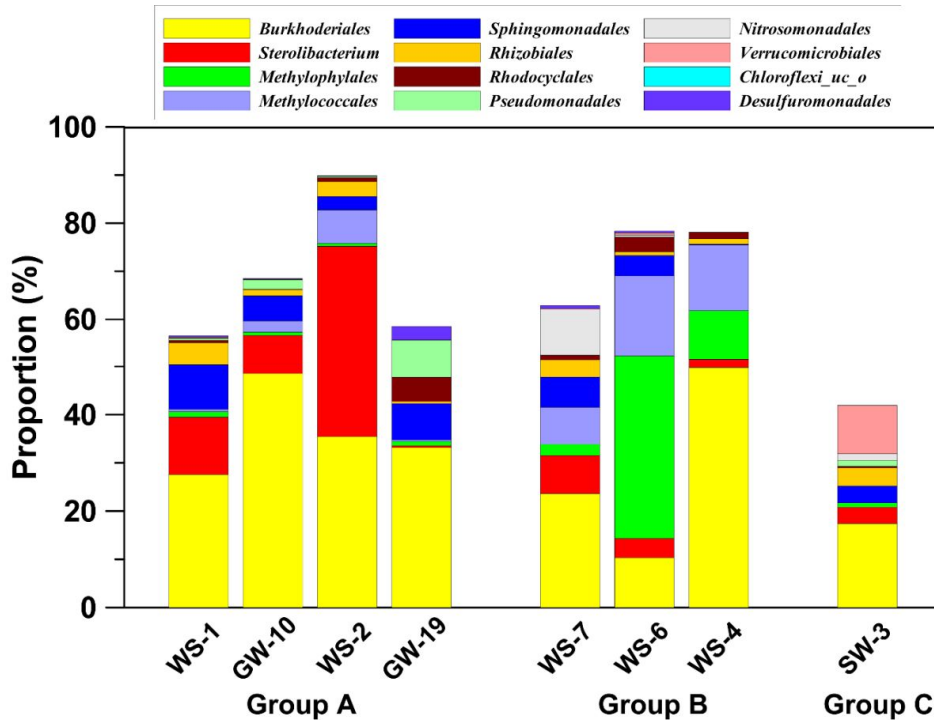


**Figure 4-6.** Phylogenetic classification and distribution of the dominant bacterial sequences at the order level.

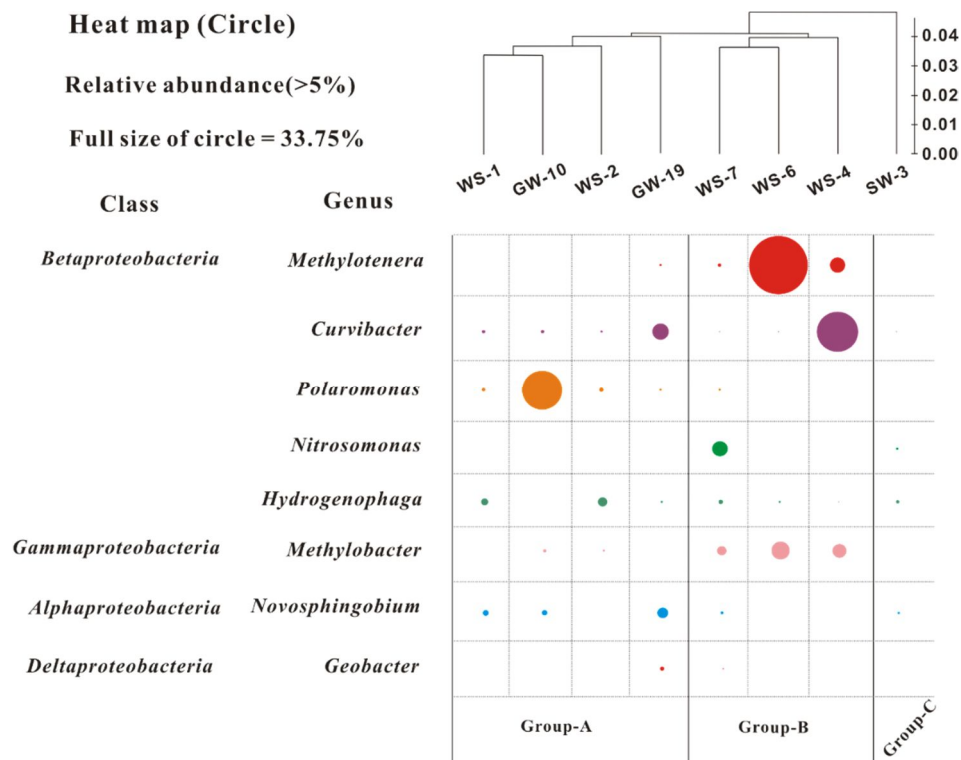


**Figure 4-7.** Comparison of bacterial community structures at each monitoring well. DNA-derived 16S rRNA gene reads were classified at the genus level. The heat map shows the relative abundance (>5%) of the most prominent taxonomic groups of the most abundant phyla.

## 4.5 Conclusions

Groundwater contaminated with chlorinated ethenes near a stream is a potential source of streamwater pollution. Hydrochemical, isotopic, and microbial data of groundwater near the stream in the study site were analyzed to investigate the fate of chlorinated ethenes. An analysis of groundwater near the stream indicated a zone characterized by partial anaerobic conditions and reductive dechlorination. Additionally, the enriched  $\delta^{13}\text{C}$  value of TCE, and the presence of metabolites such as *cis*-DCE and VC around the stream supported the transformation of TCE and *cis*-DCE to VC. Although the investigated microbial groundwater communities were highly complex, some dominant genus and species (i.e. *Polaromonas*-related bacteria; *Geobacter*; *Nitrosomonas*-related bacteria; *Curvibacter*; Methanotrophs such as *Methylothera* and *Methylobacter*) were detected, and these dechlorinating bacteria may have contributed to the aerobic and anaerobic biodegradation of chlorinated ethenes (i.e. reductive dechlorination, and metabolic and cometabolic oxidation). The detected location of putative reductive dechlorinating bacteria around the stream correlated with the detected position of *cis*-DCE and VC, as well as with the position of a larger shift in the carbon isotope composition of both TCE and *cis*-DCE. This reductive dechlorination to VC was also investigated at locations

where iron-, manganese-, and nitrate-reducing processes were observed. In addition, phylogenetic groups of microbial communities were found to be closely related to the direction of local groundwater flow around the stream. Although 16S rRNA gene-based pyrosequencing was only used in this study to demonstrate the presence of a gene, not the activity of a process, there was good agreement between the detection of microbial communities and the location appeared to be under anaerobically degradable conditions.

The multilateral approach implicit in hydrogeochemical and biomolecular methods in relation to compound-specific isotope analysis indicated that the TCE plumes were naturally attenuated by active aerobic and anaerobic dechlorination of TCE to VC around the stream. As a result, the TCE plumes dispersed near the stream, and had no appreciable effects on the streamwater quality. The polyphasic approach used in this study was considered useful in evaluating the development and degradation of the contaminant plume, as well as in investigating the effect of contaminated groundwater on surrounding surface water bodies.

**CHAPTER 5.**

**EFFECTS OF IN SITU REMEDIATION**

**REPRESENTED ON LONG-TERM**

**MONITORING DATA**

## **CHAPTER 5.**

# **EFFECTS OF IN SITU REMEDIATION REPRESENTED ON LONG-TERM MONITORING DATA**

### **Abstract**

In this chapter, a study finding evidence of remediation represented on monitoring data before and after in site remedial action was performed with various quantitative evaluation methods such as mass discharge analysis, statistical trend analysis, and analytical solutions. Remediation technologies such as soil vapor extraction, soil flushing, biostimulation, and pump-and-treat have been applied to eliminate the contaminant sources of trichloroethylene (TCE) and to prevent the migration of TCE plume from remediation target zones.

At each remediation target zone, temporal monitoring data before and after the application of remedial actions showed that the aqueous concentrations of TCE plume presented at and around the main source areas decreased significantly as a result of remedial actions. The TCE concentration of the

plumes at the downstream area remained unchanged in response to the remedial actions at the initial stage, and then, after remediation, its variation slightly represented on the monitoring data. Prior to the remediation action, the concentration and mass discharges of TCE at all transects were affected by seasonal recharge variation and residual DNAPLs sources. After the remediation, the effect of remediation took place clearly at the main source zone and industrial complex. By tracing a time-series of plume evolution, a greater variation in the TCE concentrations was detected at the plumes near the source zones compared to the relatively stable plumes in the downstream. The difference in the temporal profiles of TCE concentrations between the plumes in the source zone and those in the downstream could have resulted from the intensive remedial actions taken at the source zones.

The removal amount of the residual source mass during the intensive remedial action was estimated to evaluate the efficiency of the intensive remedial action using analytical solution. From results of quantitative evaluation using analytical solution, it is assessed that the intensive remedial action had effectively performed with removal efficiency of 70% for the residual source mass during the remediation period. Analytical solution which can consider and quantify the impacts of partial mass reduction have been proven to be useful tools for quantifying unknown contaminant source mass

and dissolved concentration at the DNAPL contaminated site and evaluating the efficiency of remediation using long-term monitoring data.

The polyphasic approach used in this study was taken into account useful in finding evidences represented on the long-term monitoring data collected at the pre- and post-remedial action, as well as in evaluating the efficiency of remedial actions.

## **5.1 Introduction**

Trichloroethylene (TCE) is one of the most frequently detected contaminants at high concentrations due to its widespread usage as a degreasing and cleaning agent in various commercial applications in the industrial area of Korea. Due to its hazard effect in human health (Gist and Burg, 1995), effective remediation methods of groundwater sites contaminated with chlorinated ethenes such as TCE need to be established (Jackson, 2004). The Korea Ministry of Environment (KMOE) commenced intense monitoring at selected contaminated sites within industrial complexes and near chemical storage facilities. The Woosan Industrial Complex (WIC) is a typical example of an intensely monitored contaminated site, which has drawn considerable attention from KMOE as well as the public media (Yang et al., 2012). With the financial

support from KMOE, a project team called ‘SEEDS groundwater research team’ has initiated a 5-year Geo-Advanced Innovative Action (GAIA) project on the development of remediation technologies to eliminate and restore contaminated groundwater at WIC.

The remediation methods for decontamination of chlorinated ethenes on a field scale include soil vapor extraction (SVE), soil flushing, pump-and-treat, and injection of nanoscale zerovalent iron (nZVI) (Gordon, 1998; Mackay et al., 2000; Rivett et al., 2006; Wei et al., 2010; McCray et al., 2011). Long-term monitoring data have been used to evaluate the occurrence of natural attenuation or the long-term effectiveness of remediation techniques (McGuire et al., 2004; McGuire et al., 2006; Phillips et al., 2010). Previous studies have assessed the remediation efficiency based on the monitoring data, most of which were obtained from near-source zones. For the better management of groundwater resources, the intensive monitoring of water systems on a catchment scale (from a contaminant source to the downstream region) is required for the groundwater quality protection (Conant et al., 2004; Chapman et al., 2007). Moreover, mass flux approaches (monitoring the concentration of contaminants in aqueous phase due to source zone DNAPL-groundwater mass transfer) have been used to evaluate the source zone remediation efficiency (Soga et al., 2004; Brusseau et al., 2013) and to understand the natural

attenuation mechanisms (Chapman et al., 2007; Basu et al., 2009). The spatial and temporal variations of mass fluxes at contaminated sites can provide an effective tool for evaluating the effectiveness of remediation technologies and for envisioning the temporal evolution of contaminant plumes (Einarson and Mackay, 2001).

Statistical analyses for the detection and assessment of noteworthy trends in contaminant concentration monitoring data associated with contaminant remediation can be classified as parametric and non-parametric methods (Lee et al., 2006; Choi et al., 2009). Parametric trend tests require data to be independent and normally distributed, while non-parametric trend tests require only that the data be independent. Sen's slope estimator has been widely applied in hydrogeological time series (Hirsch et al., 1982; Yue and Wang, 2002; Lee et al., 2006; Lee et al., 2008; Choi and Lee, 2009; Machiwal and Jha M.K., 2015).

As noted in Chapter 3, analytical solution for approximating the time-dependent contaminant discharge from DNAPL source zones developed by Falta et al. (2005a) is also used to assess the impacts of partial source depletion by the intensive remedial action during the whole remediation period and to predict the residual source mass and dissolved concentration as time passed.

In this study, the TCE concentration in plumes near WIC and its mass

discharge were monitored at three transects perpendicular to the dominant groundwater flow path, and they were evaluated along with nineteen rounds of groundwater quality data at about 100 monitoring wells from May 2009 to November 2015. In RAO, several remediation actions such as pump-and-treat, soil flushing, and development of an in-situ reactive zone using nZVI injection have been employed to clean up the TCE contaminant source and to prevent the spread of the contaminant plume from the source zone.

The purpose of this study is to assess the efficiency of the remedial actions applied at the study site using various evaluation methods such as statistical trend analysis, mass discharge analysis, and analytical solutions based on the long-term data showing the variation of TCE concentration.

## **5.2 Materials and methods**

### **5.2.1 Site description and history**

The study site is located in Wonju city, about 120-km eastward of Seoul, Korea. As shown in Figure 5-1, this site covers the Road Administrative Office (RAO) of Gangwon Province, Woosan industrial complex (WIC), with the Wonju stream flowing from west to east. In the western part of the study area,

RAO is located at the altitude of 135 m above the mean sea level (msl) and surrounded by small mountains, forest, and grass areas. Groundwater recharge is likely to occur through unpaved regions around the RAO. Most area of WIC is paved (91% of the area) and located at the downhill of the RAO with relatively low altitude (118 m, msl). Due to the paved surfaces, only a small portion of rainfall is recharged into groundwater. The dominant groundwater flow direction is from the RAO to the Wonju stream.

The study area has been heavily contaminated by multiple DNAPL components such as trichloroethylene (TCE) and tetrachloride (CT) (Yang et al., 2012) (Figure 2-5 in Chapter 2). During the GAIA project period, the intensive monitoring of groundwater quality data has been performed using 101 monitoring wells (51 wells pre-existed before the GAIA project were and newly installed 50 wells). Figure 5-1 shows the location of groundwater monitoring wells in this area.

For the first 2 years of the GAIA project period (years 2009–2010), 8 potential source locations responsible for various plumes were identified by Yang et al. (2014), and they also reported that some DNAPL sources existed above the groundwater table, which sporadically affects the groundwater quality by recharge.

Several remediation technologies have been employed to eliminate the

contamination sources. For the remediation of the main source area (A zone), soil vapor extraction, soil flushing, and biostimulation techniques were applied. Also, nZVI was injected to reduce the TCE concentration near another source area (B zone). In the C zone, pump-and-treat method was implemented to prevent the migration of TCE plumes from the RAO to WIC and reduce dissolved TCE concentration (see Figure 2-6 in Chapter 2).

To evaluate the effectiveness of the remedial actions, the concentrations of TCE, CT and CF dissolved in groundwater have been monitored for 5 years. The TCE concentrations were compared before and after implementing the remediation actions.

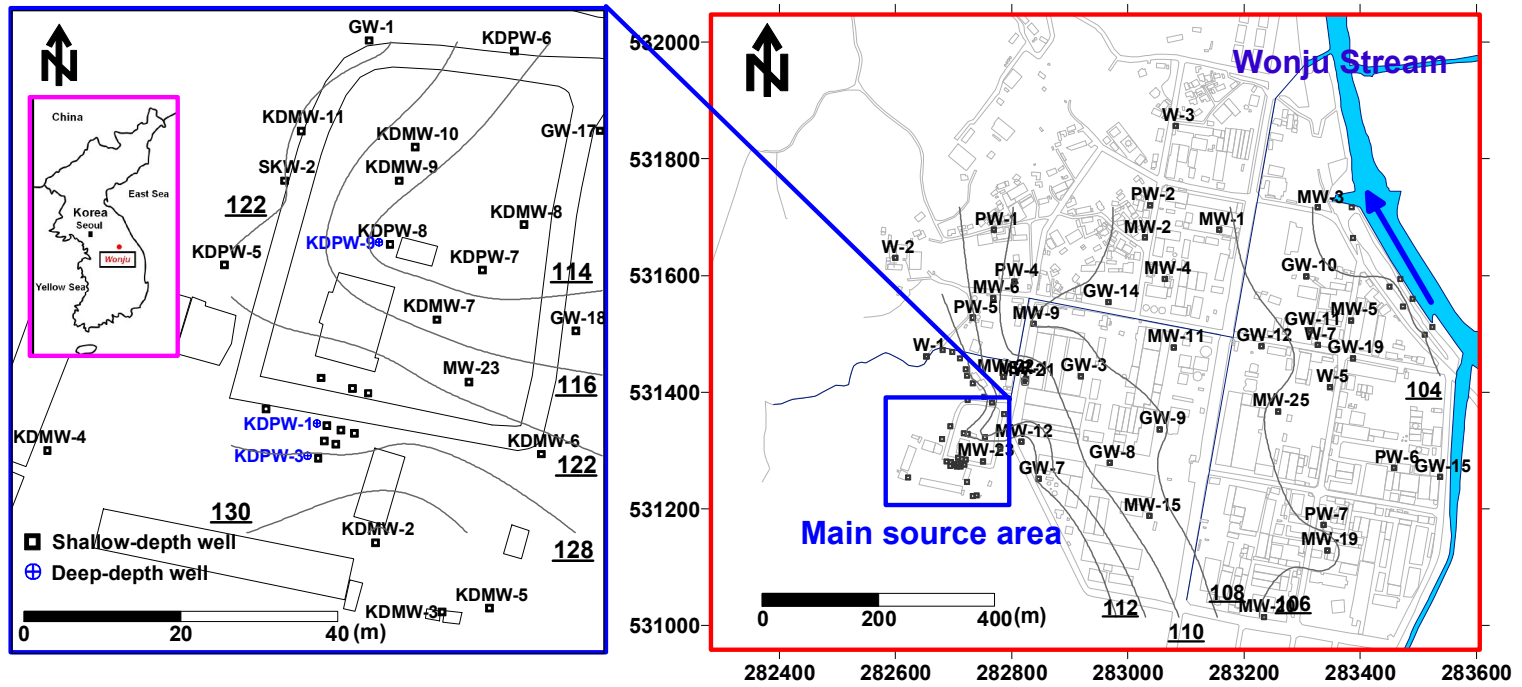


Figure 5-1. Location of study area showing main source area, monitoring wells, and groundwater level measured in August 2013.

### 5.2.2 Groundwater sampling and water quality analysis

Nineteen rounds of groundwater sampling were taken at approximately 100 monitoring wells from May 2009 to November 2015. Especially, the long-term monitoring data were collected to evaluate the effectiveness of the applied techniques such as soil flushing and SVE. Prior to groundwater sampling, at least three well-volumes were purged using a low-rate submersible pump attached to a polyethylene hose, and a new hose was replaced at each sampling point to avoid the potential cross-contamination. All groundwater samples were collected in a closed flow-through cell. At the same time, measurements for temperature, pH, dissolved oxygen (DO), electrical conductivity (EC), oxidation reduction potential (ORP) and total dissolved solid (TDS) were performed to evaluate the geochemical properties of groundwater in the field. Also, the groundwater samples for analysis of chlorinated contaminants were directly collected from a continuous water stream into 40 ml amber glass vials sealed with Teflon-lined septa with no headspace. All samples were stored at 4 °C prior to laboratory analysis, with at least 10% of them collected in duplicate. GC/MS (Saturn 2100T, VARIAN) was used for the analysis of chlorinated organic contaminants- TCE, CT and CF. Water quality parameters such as cations ( $\text{Ca}^{2+}$ ,  $\text{K}^+$ ,  $\text{Mg}^{2+}$ ,  $\text{Na}^+$ ,  $\text{Si}^{4+}$ ,  $\text{Fe}^{2+}$ ,  $\text{Mn}^{2+}$ ), anions ( $\text{F}^-$ ,  $\text{Cl}^-$ ,  $\text{NO}_3^-$ ,  $\text{SO}_4^{2-}$ ,

HCO<sub>3</sub><sup>-</sup>, CO<sub>3</sub><sup>2-</sup>, dissolved organic carbon (DOC) were measured at off-site laboratories.

### 5.2.3 Mass discharge

A mass discharge is an important parameter used for designing an effective remediation scheme and evaluating its performance. The mass discharge of the main contaminant TCE along the groundwater flow path was calculated according to Einarson and Mackay (2001) and Chapman et al. (2007) as follows:

$$M_d = \sum_{i=1}^n C_i q_i A_i \quad (1)$$

where  $M_d$  is the total TCE mass discharge in mass per time;  $C_i$  is the linearly interpolated TCE concentration in mass per volume;  $n$  is the number of vertical section which is assigned within a transect and  $A_i$  is the rectangular sub-area formed by discretizing the cross-sectional area of groundwater flow between two adjacent wells aligned along the transect line. The specific discharge of groundwater ( $q_i$ ) was estimated using the Darcy's law (i.e.,  $q_i = Ki$ ), where  $K$  is a hydraulic conductivity and the hydraulic gradient ( $i$ ) for each sampling event

was calculated with observed head data measured at wells around each transect.

#### **5.2.4 Statistical trend analysis**

##### **5.2.4.1 Interpretation for temporal changes of contaminant concentration represented by remedial action**

Statistical analyses for the detection and assessment of noteworthy trends in contaminant concentration monitoring data associated with contaminant remediation can be classified as parametric and non-parametric methods (Lee et al., 2006; Choi et al., 2009). Parametric trend tests require data to be independent and normally distributed, while non-parametric trend tests require only that the data be independent. In this study site, Sen's slope estimator of various non-parametric methods was applied to detect and assess the effect of remedial action represented on the long-term TCE concentration monitoring data.

##### **5.2.4.2 Sen's slope estimator method**

Non-parametric trend analyses such as Sen's slope estimator and Mann-Kendall test automatically permit missing data but is not affected by

gross data errors and outliers (Yue and Wang, 2002). Especially, if a linear trend is present in a time series, then the true slope (change per unit time) can be estimated using a simple non-parametric procedure proposed by Sen (1968). To check the existence of the trend in collected data, the slope estimates of  $N$  pairs of data are first computed by:

$$Q_i = \frac{x_j - x_k}{j - k} \quad \text{for } i = 1, \dots, N \quad (1)$$

where  $x_j$  and  $x_k$  are data values at times  $j$  and  $k$  ( $j > k$ ), respectively.

The median of these  $N$  values of  $Q_i$  is Sen's estimator of slope. If  $N$  is odd, then Sen's estimator is computed by:

$$Q_{med} = Q_{[(n+1)/2]} \quad (2)$$

If  $N$  is even, then Sen's estimator is computed by

$$Q_{med} = \frac{1}{2} (Q_{[N/2]} + Q_{[(n+2)/2]}) \quad (3)$$

The  $Q_{med}$  sign reflects data trend reflection, while its values indicates the steepness of the trend. Finally,  $Q_{med}$  is generally tested with a two-sided

test at the  $100(1-\alpha)$  % confidence interval and the true slope may be obtained with the non-parametric test (Partal and Kahya, 2006; Tabari et al., 2011). In this study, the confidence interval was calculated at 95% confidence level ( $\alpha = 0.05$ ) as follows (Gilbert 1987):

$$C_\alpha = Z_{1-\alpha/2} \sqrt{Var(S)} \quad (4)$$

where  $Z_{1-\alpha/2}$  is obtained from the standard normal distribution and the variance  $Var(S)$  has been calculated as follows:

$$Var(S) = \frac{[n(n-1)(2n+5) - \sum_{i=1}^m t_i(t_i-1)(2t_i+5)]}{18} \quad (5)$$

where  $n$  is the number of data points,  $m$  is the number of tied groups and  $t_i$  denotes the number of ties of extent  $i$ . A tied group is a set of sample data having the same value. In case where the sample size  $n > 10$ , the standard normal variable  $Z$  is computed by:

$$Z = \begin{cases} \frac{S-1}{\sqrt{Var(S)}} & \text{if } S > 0 \\ 0 & \text{if } S = 0 \\ \frac{S+1}{\sqrt{Var(S)}} & \text{if } S < 0 \end{cases} \quad (6)$$

Positive values of  $Z$  indicate increasing trends while negative  $Z$  values show decreasing trends. Then,  $M_1 = (N - C_\alpha)/2$  and  $M_2 = (N + C_\alpha)/2$  are calculated. The lower and upper limits of the confidence interval,  $Q_{min}$  and  $Q_{max}$ , are the  $M_1$ th largest and the  $(M_2 + 1)$ th largest of the  $N$  ordered slope estimates (Gilbert, 1987). The null hypothesis is rejected if the two limits ( $Q_{min}$  and  $Q_{max}$ ) is different than zero.

## **5.3 Results and discussion**

### **5.3.1 Variations in TCE concentration and its mass discharge**

Groundwater of the study area is contaminated by chlorinated solvents, mainly TCE with other chlorinated organics including carbon tetrachloride, chloroform and their degradation by-products. Six representative wells were selected along the groundwater flow direction from the main source area (A Zone) to the Wonju stream. Periodically monitored concentrations of chlorinated organic pollutants for sixteen times were plotted to evaluate their temporal variations (Figure 5-2). The highest TCE concentration of 15,748  $\mu\text{g/L}$  was observed at KDPW-02 (August 2009), the monitoring well at the

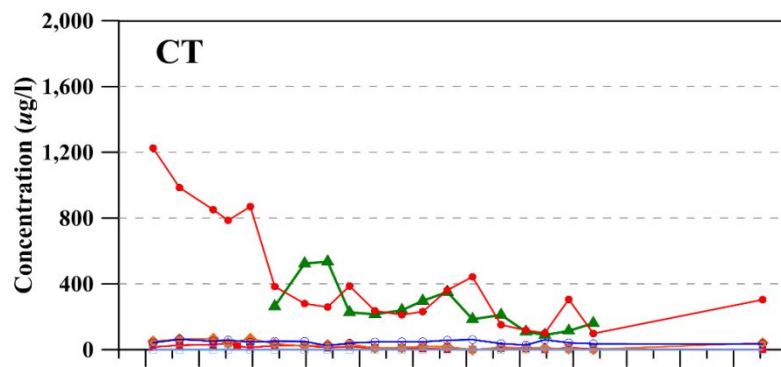
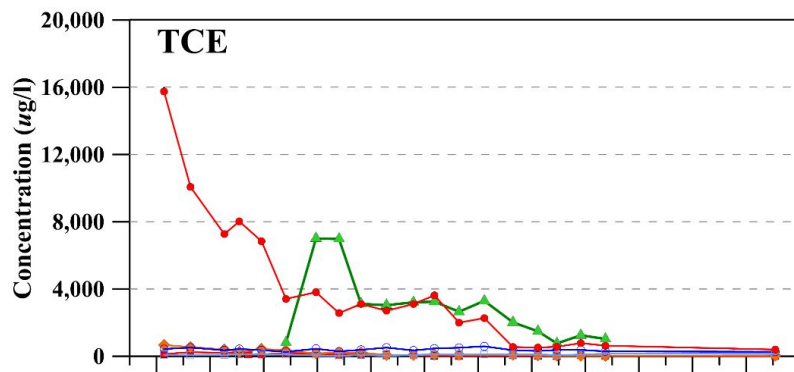
main source area. The highest TCE concentrations at SKW-6, GW-1, MW-22, GW-3, and GW-10 were 7,007 (February 2011), 593 (October 2007), 748 (August 2004), 574 (August 2008), and 112  $\mu\text{g/L}$  (May 2010), respectively, indicating that the contaminants migrate along the groundwater flow direction. The TCE concentration in the main source area gradually decreased over time during the early monitoring period (years 2009–2011), while it dramatically decreased from the end of year 2012 due to the effect of remediation. The most recently measured TCE concentration at KDPW-2 (November 2015) was 399  $\mu\text{g/L}$ . In the downstream, slightly lower TCE concentrations were observed at GW-1 and MW-22, while the concentrations were maintained in the range of range of 66–377  $\mu\text{g/L}$  at GW-3 and GW-10. The CT and CF concentrations at KDPW-2 showed the similar temporal pattern to the TCE concentration over the period, but they were lower compared to the TCE concentration (Figure 5-2).

The mass discharge of TCE across the source transect decreased since the remediation actions were implemented (see Figures 5-3 and 5-4). Before the remediation actions, the maximum mass discharge was estimated to be 26.58 g/day. However, after the start of the remediation actions, the mass discharge was decreased to 0.99 g/day at November 2015 (Figure 5-4). The calculated mass discharges of TCE at transects-1 and -2 were correlated with the seasonal variation due to recharge event, but they were gradually affected by the

remediation actions (Figure 5-3b and 5-4). In transect-1, the mass discharges before and after the implementations of the remediation actions were estimated to be 15.81 (November 2012) and 3.86 g/day (November 2015), respectively (Figure 5-4). Similarly, the mass discharges at transect-2 were estimated to be 3.57 g/day (November 2011) for before-the-remediation and 0.03 g/day for after-the-remediation (November 2015) (Figure 5-4). Based on these distributions of mass discharges, over half of TCE plumes crossing the source transect would reach the middle of the industrial complex (Figures 5-4 and 5-5).

The minimal presence of the TCE degradation products such as *cis*-DCE and VC suggests that little transformation of TCE occurred over a 200 meter long path between the main source area and transect-1 (Figure 5-3b and 5-4). However, near the stream, the biodegradation of TCE may explain the decreased TCE mass flux and the continuous detection of *cis*-DCE near the stream zone (Figure 5-4).

The effect of the remediation actions taken at the main source area was evident at the transect-1 during the monitoring period. Therefore, from the results of mass discharge, mass discharge method using long-term monitoring data is effectively applied to observe the reduction of the TCE mass discharge across transects-1 and 2 located at downstream as a result of the remediation actions.



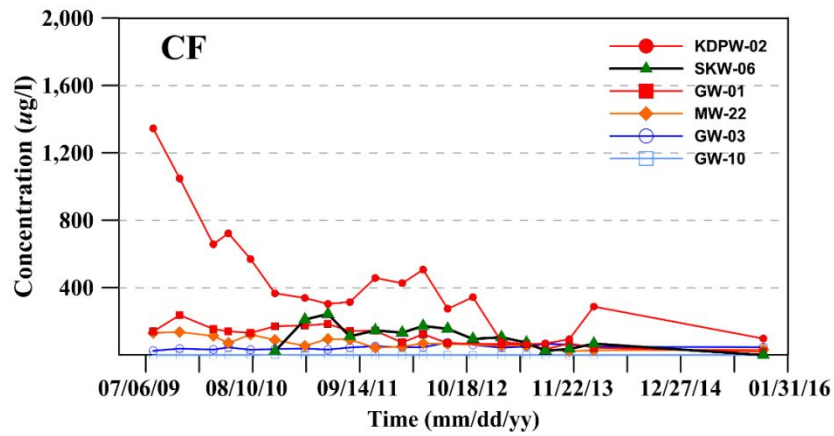
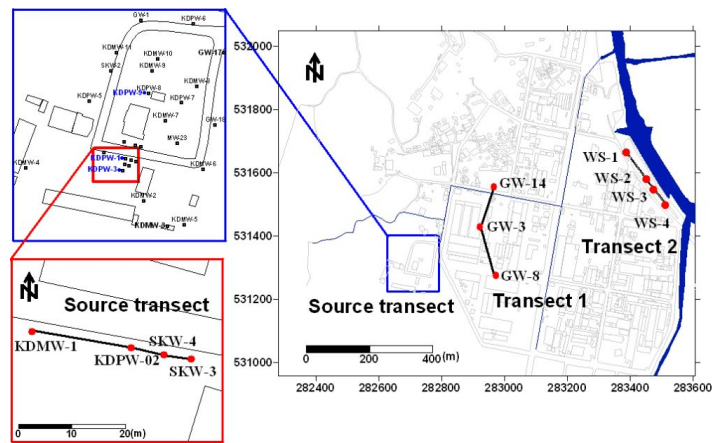
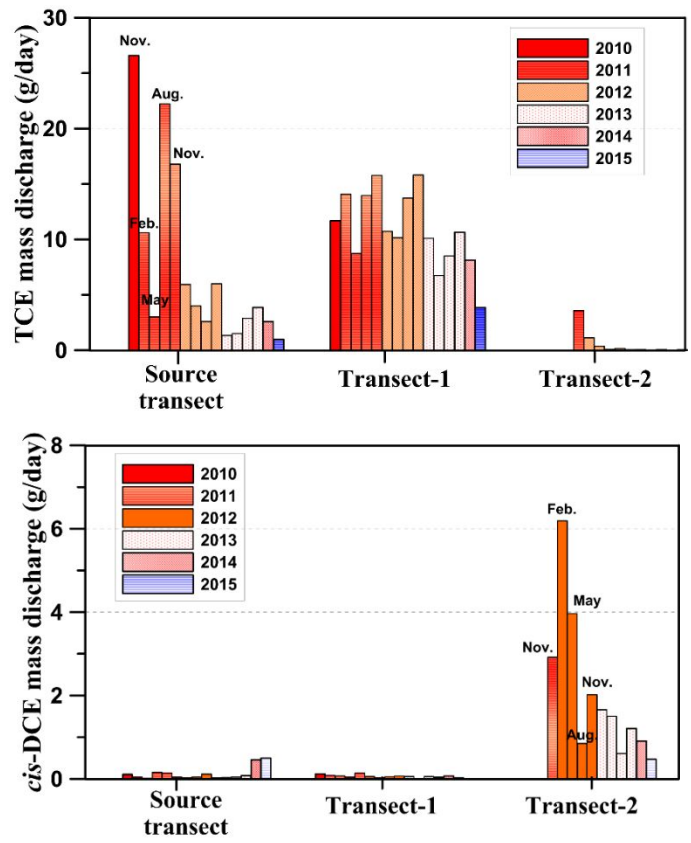


Figure 5-2. Seasonal concentration changes of multiple-DNAPL contaminants at selected wells along a groundwater flow path.



(a)



(b)

**Figure 5-3.** Study site showing the transect lines for mass discharge (a) and temporal mass discharge of TCE and *cis*-DCE plume at each transect (b).

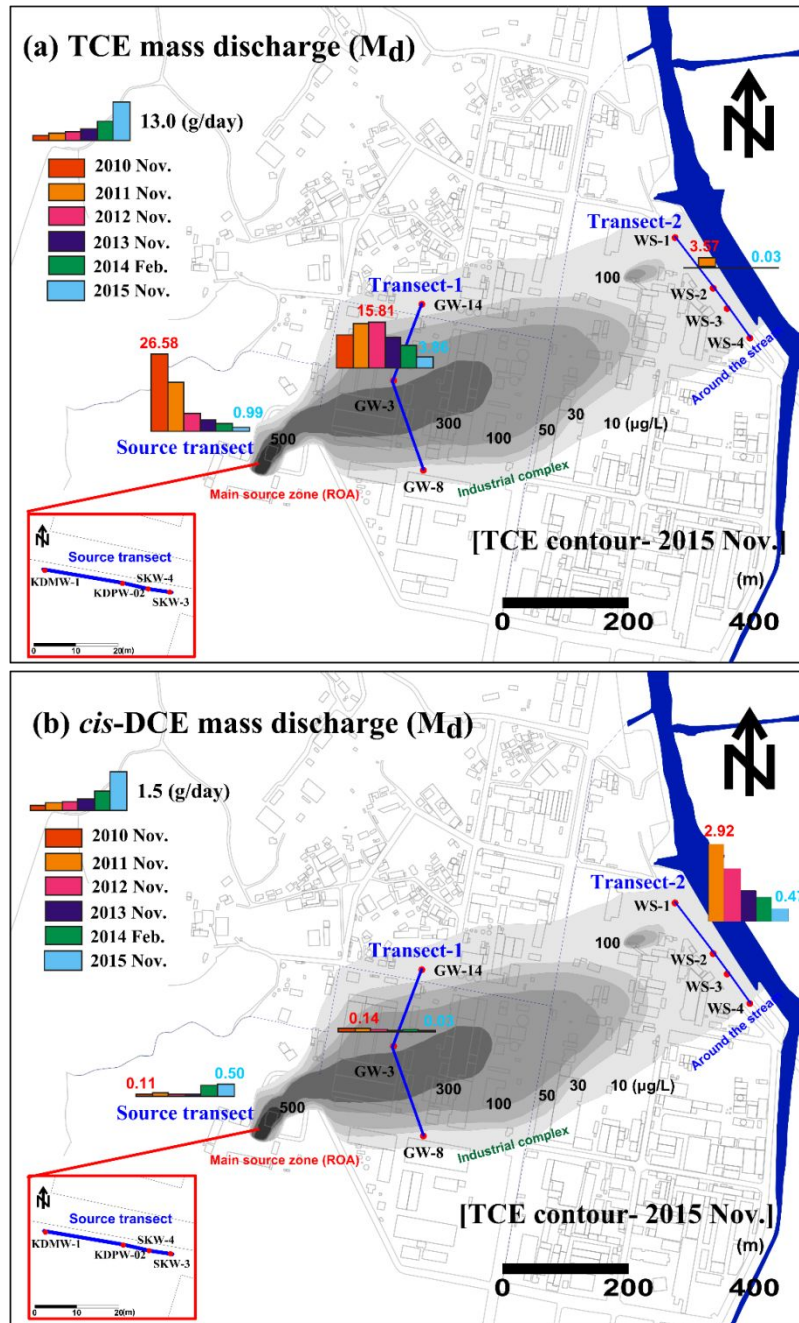
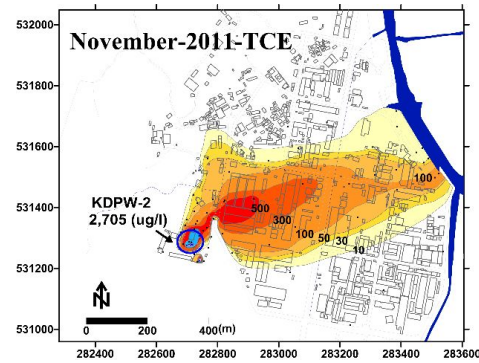


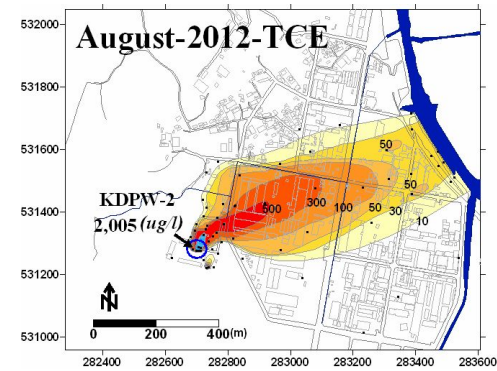
Figure 5-4. Variation of TCE (a) and *cis*-DCE (b) mass discharge from 2010 to 2015.

### **5.3.2 Comparison of TCE contaminant plumes**

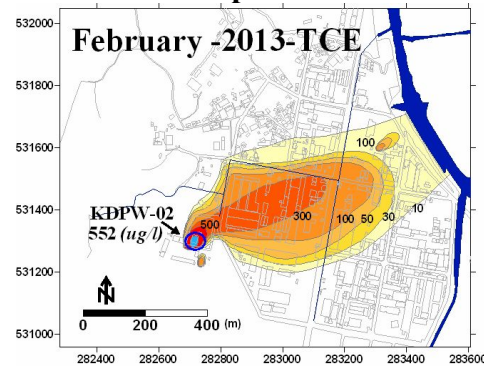
In Figure 5-5, the temporal changes in the distribution of TCE plumes can be readily seen from the water quality data of the samples collected in November 2011, November 2012, February 2013, and November 2013. The four TCE plumes in Figure 5-5 exhibit considerably larger variations in the TCE concentrations near the source zone than in the downstream. Before the remediation actions applied, several high concentration levels of TCE (2,705  $\mu\text{g/L}$  in November 2011 and 2,005  $\mu\text{g/L}$  in August 2012) were observed in the plume placed at the main source area. During the remediation, the size of the TCE plume at the downgradient did not change significantly, but the TCE concentration in the plume at the main source area showed the apparent decrease (e.g., from 552  $\mu\text{g/L}$  in February 2013 to 399  $\mu\text{g/L}$  in November 2015). From these results, it is assumed that the TCE plume representing the high concentration level became smaller in size than previous plumes due to the effect of remedial action.



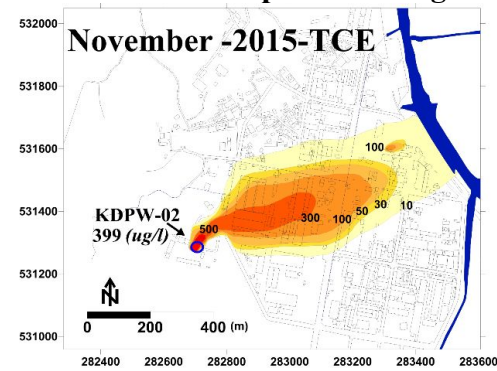
(a) TCE contaminant plume at November 2011



(b) TCE contaminant plume at August 2012



(c) TCE contaminant plume at February 2013



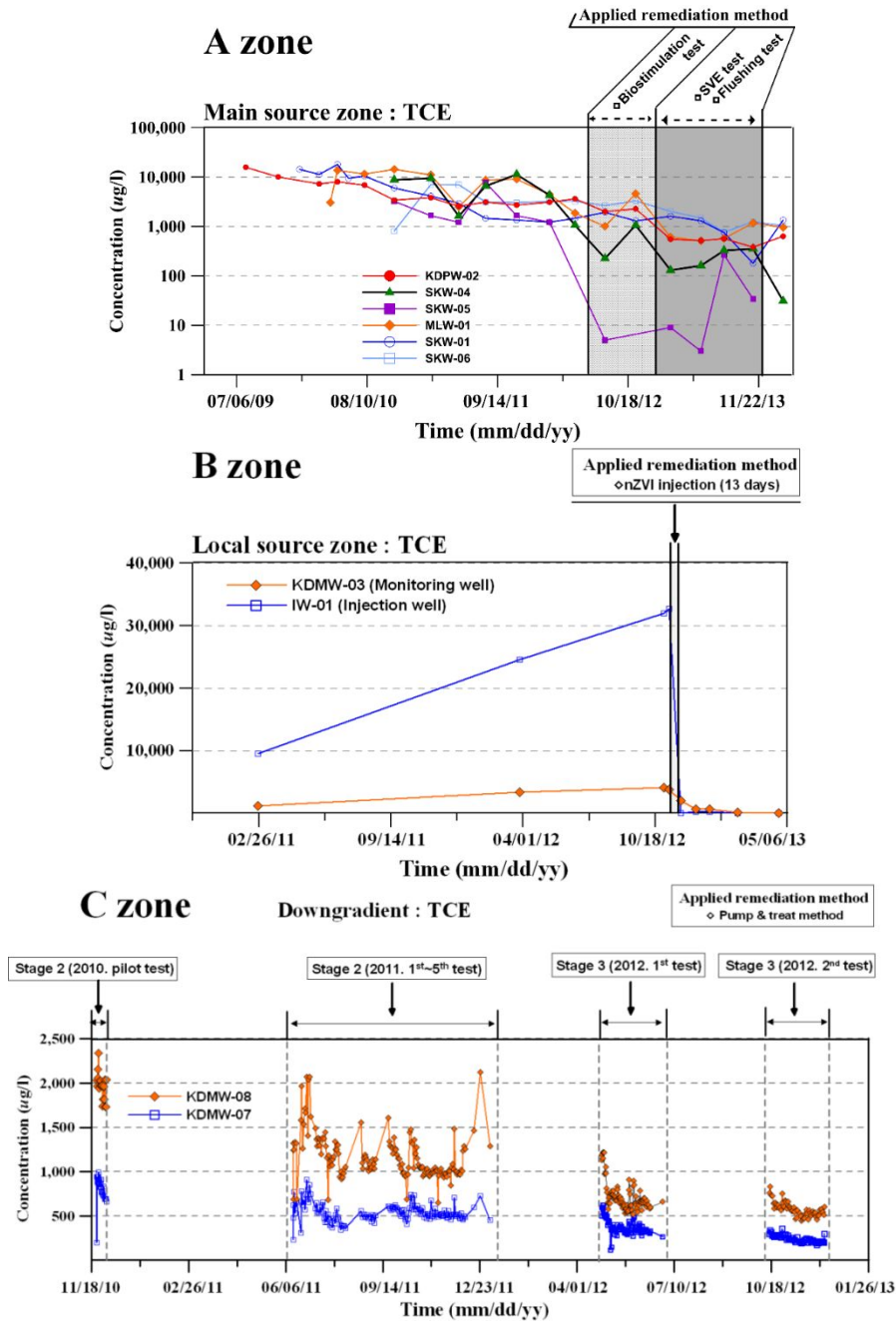
(d) TCE contaminant plume at November 2015

Figure 5-5. Comparison of TCE plumes observed from November 2011 to November 2015.

### **5.3.3 TCE concentration monitoring at each remediation target zone**

Since remediation technologies were employed to cleanup several target areas the variations of TCE concentration were monitored (Figure 5-6). In case of A zone where the highest TCE contamination was encountered, biostimulation, SVE, and flushing methods were applied at the main source area. Before the application of the remediation technologies, monitoring wells in the main source area showed high TCE concentration levels whereas, after the remediation actions applied, the overall TCE concentration was lowered. Especially, at SKW-04, the TCE concentration fell from maximum 11,282 to 31  $\mu\text{g/L}$ . In case of B zone, nZVI injection was applied to a local source zone which has the maximum TCE concentration of 32,729  $\mu\text{g/L}$ . As a result of nZVI injection, the most dramatic change was observed for the TCE concentration; for example, the maximum TCE concentration dropped below the drinking water standard (3  $\mu\text{g/L}$ ) during the 13-day remediation period. At C zone located in the downward of the main source area, a pump-and-treat method was performed to prevent the further migration of the contaminants from A and B zones. The pump-and-treat method was operated periodically 10 times for the 4 year duration from 2010 to 2013. According to the monitoring data at the pumping wells of KDPW-07 and KDPW-08, TCE concentrations showed gradual decreases due to the remediation action. The initial TCE

concentrations in the groundwater were 899  $\mu\text{g/L}$  at KDPW-07 and 2,022  $\mu\text{g/L}$  at KDPW-08. Over the course of the remediation, the TCE concentrations were decreased to 122  $\mu\text{g/L}$  at KDPW-07 and 485  $\mu\text{g/L}$  at KDPW-08. Based on the mass discharge data of TCE at each well, the cumulative mass removal of TCE was estimated to be 5.49 kg over the remediation period. These results indicated that the pump-and-treat method exercised at C zone was effective for preventing the migration of the TCE plume from the RAO to WIC.



**Figure 5-6.** Results of TCE concentration monitoring observed at each remediation target zone.

#### **5.3.4 Evaluating the efficiency of intensive remedial action**

As noted in Chapter 2, various remediation technologies had been performed in the main source zone. Especially, the intensive remedial action was carried out at the hot source zone from November 2012 to November 2013. The efficiency of the intensive remedial action can be evaluated with the reduction rate of source mass estimated from analytical solution which proposed for estimating the initial TCE source mass and dissolved concentration.

Evaluating procedure is similar with estimating the initial TCE mass and concentration, while, to assess the effect of remedial action, analytical solution was used to apply the effect of source mass depletion against the period of pre- and post-remedial action. Therefore, Eqs. (3-3) and (3-4) which estimate the DNAPL source mass and concentration only removed by dissolution without biological or abiotic degradation use until the period before intensive remedial action begins (1996 to 2011). And then, Eqs. (3-6) and (3-7) considering the effect of partial source mass depletion set to the intensive remedial action period (2012 to 2013). Also, a post-remediation residual source mass and dissolved concentration calculate using Eqs. (3-8) and (3-9). When Eqs (3-6) through (3-7) are used, a fraction,  $X$  is important parameter which can

be directly related with the efficiency of the remedial action because these values mean the reduction rate of source mass from the start of the remedial action to the end point of remediation. Therefore, new values of source mass and dissolved concentration reflected the reduction of source mass were calculated using Eqs. (3-6) through (3-9) from the start point of remediation to the future period

#### **5.3.4.1 Estimation of source mass reduction rate**

TCE concentration of the main source zone after the remedial action dramatically decreased compared to the pre-remediation (Lee et al, 2013). From the results of TCE concentration monitoring before and after remediation, different three fraction (X) values (50, 60, 70 %) which mean the reduction rate of source mass are proposed to evaluate the efficiency of intensive remedial action. To acquire the reasonable value of mass reduction rate, tracing the data curves correlated with the distribution of field concentration data is required. Herein, the estimated data curves can be obtained from analytical solution with different fraction (X) values (50, 60, 70 %) which means the partial source mass depletion (Figures 5-7 through 5-12). From results obtained with the initial source mass (1,000 kg) and dissolved concentration (150 ppm) for three mass

reduction rates, it is determined that 70 % of fraction (X) is a reasonable value for the partial mass reduction rate during the intensive remedial action (Figure 5-9, 5-12 and 5-13). Also, the residual source mass and dissolved concentration over time after remedial action ends are predicted. As represented on Table 5-1, in case of no remedial action, the dissolved source concentration ( $1,902 \mu\text{g/L}$ ) at the pre-remedial action (2012) decreased up to  $502 \mu\text{g/L}$ , and residual source mass ( $76.60 \text{ kg}$ ) will be decreased up to  $35.00 \text{ kg}$  (54 % reduction) at 2026. However, if 70% of the residual source mass removed during the intensive remediation, the dissolved source concentration dropped to  $279 \mu\text{g/L}$  and the residual source mass removed to  $24.81 \text{ kg}$  (70 % reduction) at 2013 after the remedial action ends. These values will be decreased up to  $139 \mu\text{g/L}$  and  $15.25 \text{ kg}$  (80 % reduction) at 2026. The source mass ( $1,000 \text{ kg}$ ) at the initial spilled stage removed up to 98.5 % of initial mass at 2026 (Table 5-1).

From the above results, it is evaluated that the intensive remedial action had effectively performed with removal efficiency of 70 % for the residual source mass during the remediation period at the main source zone of this study site. Therefore, if monitoring data before and after remedial action can be obtained from contaminated sites, removal efficiency and the prediction of future mass and concentration according to the remedial action can be estimated using analytical solution applied in this study.

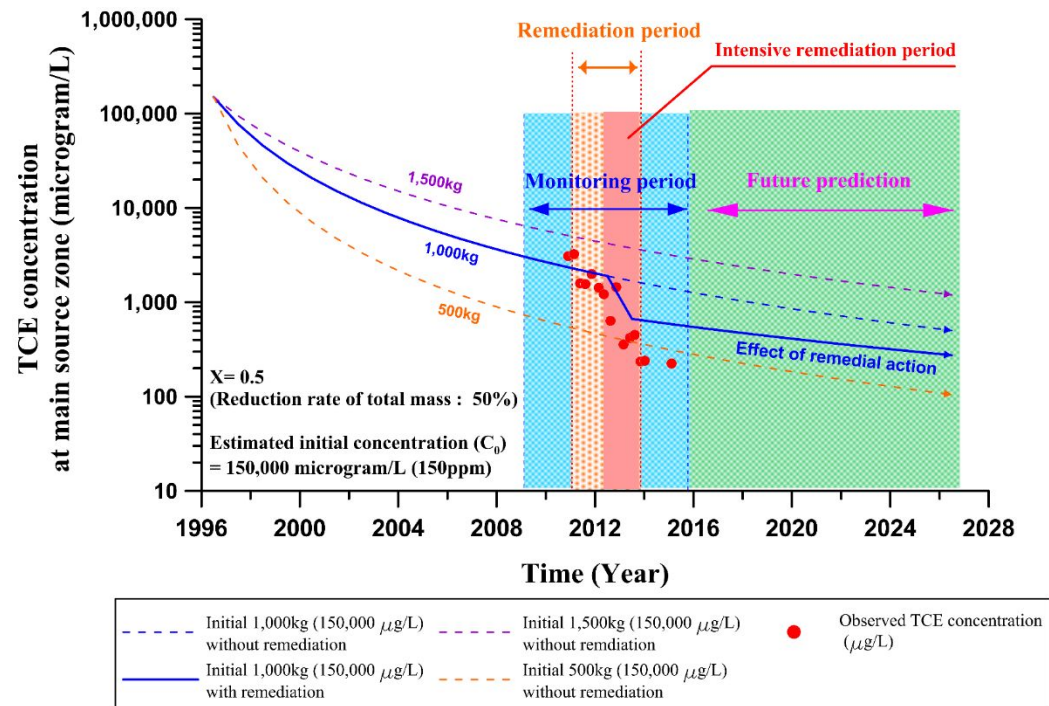


**Figure 5-7.** Matching of data estimated with initial TCE source mass (1,000 kg) considering the source mass depletion to field concentration data. (Assumption: fraction ( $X$ ) is 0.5)

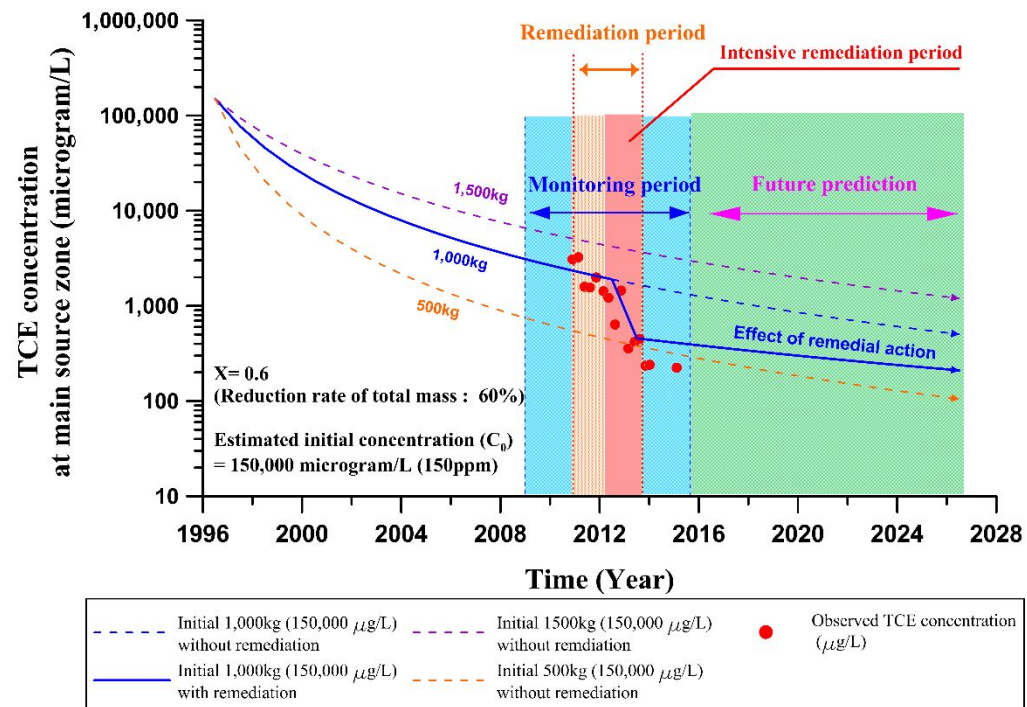


**Figure 5-8.** Matching of data estimated with initial TCE source mass (1,000 kg) considering the source mass depletion to field concentration data. (Assumption: fraction ( $X$ ) is 0.6)

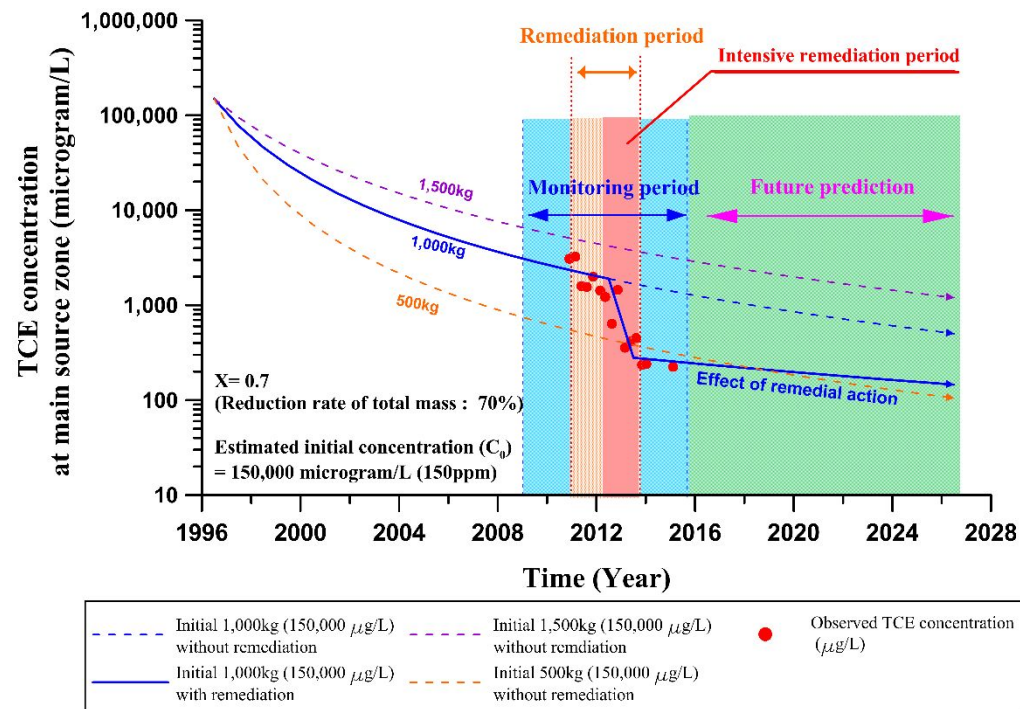


**Figure 5-9.** Matching of data estimated with initial TCE source mass (1,000 kg) considering the source mass depletion to field concentration data. (Assumption: fraction ( $X$ ) is 0.7)

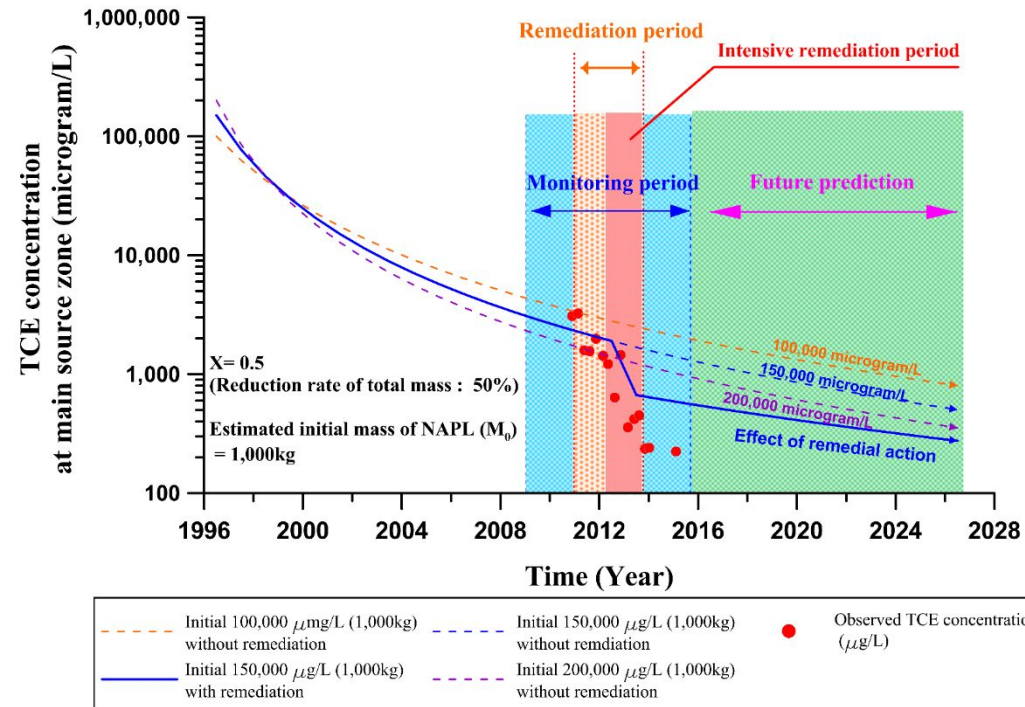


**Figure 5-10.** Matching of data estimated with initial dissolved TCE source concentration (150,000  $\mu\text{g/L}$ ) data considering the source mass depletion to field concentration data. (Assumption: fraction ( $X$ ) is 0.5)

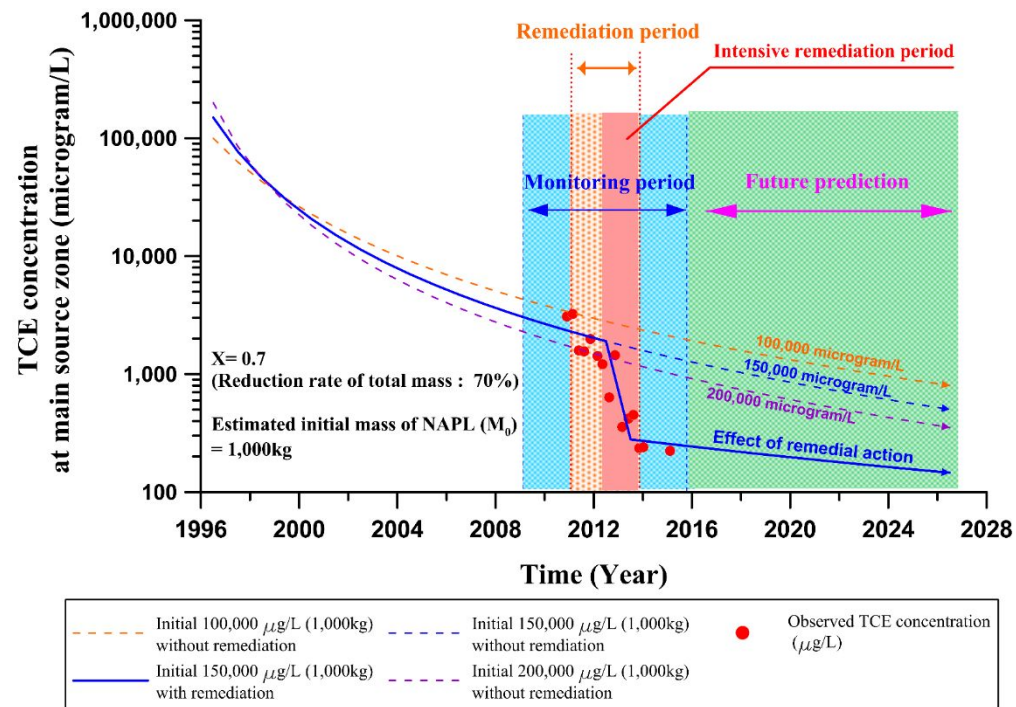


**Figure 5-11.** Matching of data estimated with initial dissolved TCE source concentration (150,000  $\mu\text{g/L}$ ) data considering the source mass depletion to field concentration data. (Assumption: fraction ( $X$ ) is 0.6)

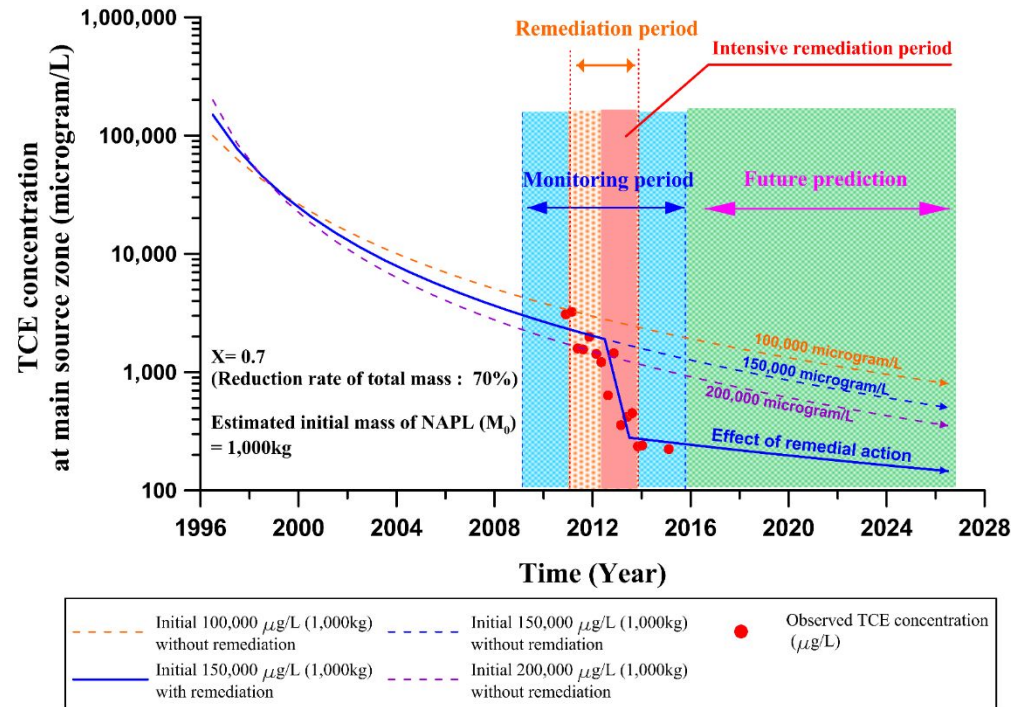


**Figure 5-12.** Matching of concentration data estimated with initial dissolved TCE source concentration (150,000  $\mu\text{g/L}$ ) data considering the source mass depletion to field concentration data. (Assumption: fraction ( $X$ ) is 0.7)

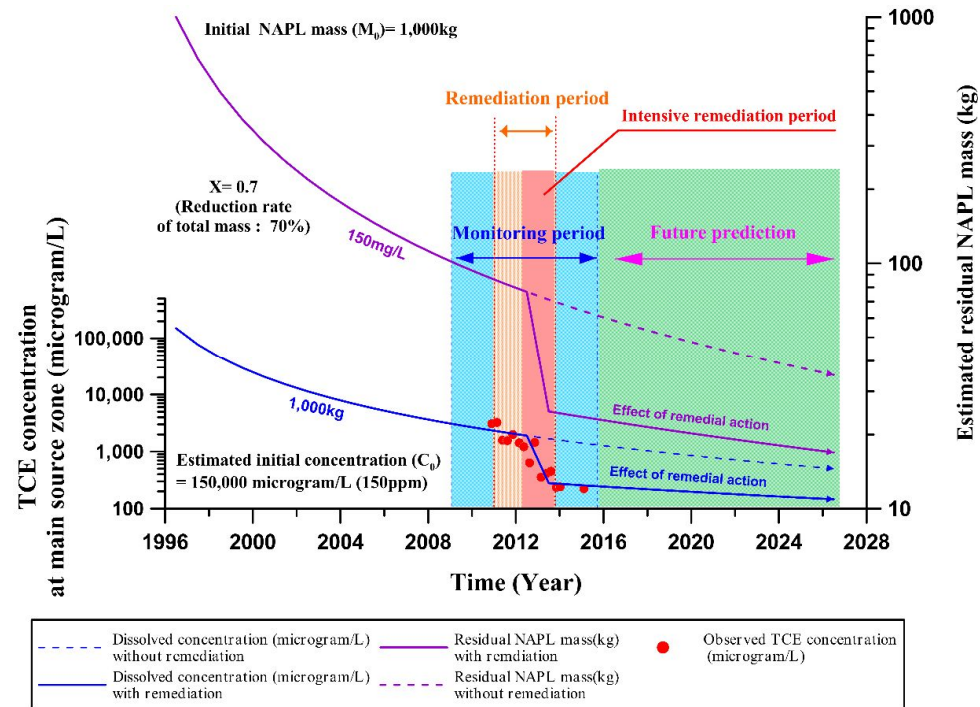


**Figure 5-13.** Results estimated with initial dissolved TCE source concentration ( $150,000 \mu\text{g/L}$ ) and source mass ( $1,000 \text{ kg}$ ) considering the partial source mass depletion. (Assumption: fraction ( $X$ ) is  $0.7$ )

**Table 5-1.** Estimated dissolved TCE concentration ( $\mu\text{g/L}$ ) and residual NAPL mass before and after remedial action

	<b>Initial spilled stage (1996)</b>	<b>Before remedial action (2009)</b>	<b>Start remediation (2010)</b>	<b>Before intensive remedial action (2012)</b>	<b>After the intensive remedial action (2013)</b>	<b>Prediction (2026)</b>
Dissolved concentration ( $\mu\text{g/L}$ )	150,000 $\mu\text{g/L}$	2,875 $\mu\text{g/L}$	2,485 $\mu\text{g/L}$	1,902 $\mu\text{g/L}$	279 $\mu\text{g/L}$	146 $\mu\text{g/L}$
Dissolved concentration ( $\mu\text{g/L}$ )				Without remediation	1,681 $\mu\text{g/L}$	502 $\mu\text{g/L}$
Residual NAPL mass (kg)	1,000 kg	97.67 kg	89.65kg	76.60 kg	22.98 kg (70 %) <sup>(1)</sup>	15.25 kg (80 %) <sup>(1)</sup>
Residual NAPL mass (kg)				Without remediation	71.23 kg (7 %) <sup>(1)</sup>	35.00 kg (54 %) <sup>(1)</sup>

<sup>(1)</sup> Reduction rate compared to 2012

### **5.3.5 Analyzing the trend in variation of contaminant concentration**

The remediation of contaminant source affects the concentration degradation of downgradient plume because its effect can decrease the contaminant mass of source zone for a short period, while, in a long-term perspective, source remediation decreases mass discharge from source discharging into groundwater. In other words, if mass discharge decreased by the removal of residual NAPL mass of contaminant source, in the long-held view, concentration of downgradient plume may show the decreasing trend due to the reduced influx of dissolved mass with high-level. However, when it considers the groundwater flow velocity according to the hydraulic gradient, the concentration variation does not simultaneously appear with the reduction of contaminant source. Partitioning into dissolved phase of solute from contaminant source leads to the reduction of mass discharge and thus the concentration reduction of contaminant source happens by inpouring of low-level groundwater from the upgradient. Therefore, to evaluate whether the remedial action is effectively applied in the contaminated sites, verification of remediation efficiency can be paired with the evaluation of natural attenuation through long-term monitoring of downgradient plume.

To identify whether the remedial action performed at the main source zone is affecting the downgradient plume, the study area was divided into three zones (main source zone, plume zone 1, plume zone 2) along the groundwater flow direction from RAO to Wonju stream (Figure 5-14). Fifty eight representative monitoring wells with data set whose length is greater than 5 years among the total 105 monitoring wells were selected (Table 5-2).

Results of TCE concentration monitoring data obtained during the study period showed the variation because of the pre- and post-remedial action. Therefore, to detect any trend of TCE concentration data before and after the implementation of remedial action, non-parametric trend analysis was conducted with long-term TCE monitoring data collected from 2010 to 2013. The non-parametric trend analyses can give us information on potential variation trend with confidence level (Salmi et al., 2002). Results of the non-parametric trend analyses for the TCE concentration data are given in Table 5-3. The trends were determined at a confidence level of 95%.

As shown in Figures 5-14 and 5-15, decreasing and increasing velocity ( $\mu\text{g}/\text{day}$ ) of TCE concentration and its spatial distribution are identified from each monitoring well data. Results of reduction velocity for TCE concentration obtained from Sen's slope estimator at both industrial complex (Plume zone 1) and around the stream (Plume zone 2) except for main source zone showed that

TCE concentration dominantly represented no trend until the pre-remedial action, while, if analysis period extended until the post-remedial action period, it was rapidly reduced at the border of the main source zone compared to around the stream (Figure 5-14). The intensive remedial actions such as SVE test, soil flushing test and nZVI test and the installation of hydraulic barrier for spreading obstruction of contaminant plume such as pump-and-treat remediation were conducted from 2011 to 2013 in the main source zone. Therefore, it is assessed that transport of contaminant plume was controlled by these efforts from 2011, and thus the remedial action performed at the main source zone has an effect to the Plume zone 1 located at downgradient area.

The reduction velocity of concentration in the main source zone before the remedial action showed bigger values (maximum value:  $-15.8 \mu\text{g/day}$ ) than after the remediation (maximum value:  $-7.71 \mu\text{g/day}$ ) (Figure 5-15). The distribution of contaminant concentration in this study site is affected by relationship between the groundwater-level fluctuation and residual DNAPL sources (Yang et al., 2012), therefore the seasonal variation of concentration shows a considerable fluctuation (Figure 5-16). As shown in Figure 5-16, the variation of TCE concentration until the pre-remediation shows the considerable decreasing trend, while the variation of concentration during the remediation showed a relative small range compared to the pre-remedial action

due to the concentration rebounding effect by the intensive remedial action such as the injection of water and surfactant. This hydrogeological relationship and the rebounding effect by intensive remedial action such as soil flushing test can affect this difference between the values of reduction velocity.

At the main source zone, most monitoring well did not show any significant trend at the pre-remedial action (Figure 5-15a), while, in case of analysis involving the post-remedial action, the influence of intensive remedial action performed at the main source zone was represented on monitoring wells which showed no trend before the remediation (Figure 5-15b). One specific monitoring well (KDMW-1) showed increasing trend during the analysis period. It is assumed that the reason why increasing trend before the remedial action showed is due to an impact of seasonal variations in hydrological stresses and spatial variations in geologic conditions (Yang et al., 2012). However, in case of the post-remediation, it is assumed that the concentration mounding effect which means the migration of high-level groundwater from remedial target zone to this monitoring well by the intensive remedial action, such as soil water flushing test and surfactant flushing test, leads to the increasing trend until the post-remedial action.

The results of Sen's trend analysis showed that 41% of whole 27 monitoring wells in the main source zone at the pre-remedial action period were

decreasing while 4% of them showed increasing trend. Large proportion (55%) of the monitoring wells did not show any significant trend (Figure 5-17). These trends were also represented at both plume zone 1 and plume zone 2 with each 79% and 92% proportion (Figure 5-18 and Table 5-3). However, trend of concentration data after the remediation showed considerable changes of zonal trend due to the intensive remedial action. At the main source zone, dominant trend dramatically changed to increasing trend with large proportion (85%), and also at plume zone 1 and plume zone 2, proportion of decreasing trend slightly increased up to 31% and 25%, respectively (Table 5-3). These variation in trend of TCE concentration before and after remedial action indicated that the intensive remedial action affected the most monitoring wells of main source zone and then its influence reached the vicinity of border between main source zone and plume zone 1.

From the results of the Sen's trend analysis, it is assessed that reduction velocity of concentration which is calculated using Sen's slope estimator is more quickly progressed in the main source zone due to the intensive remedial action compared to both plume zone 1 and plume zone 2. Overall trend in variation of TCE concentration at the whole study area showed that decreasing trend gradually increased and thus these evidences supported that the intensive remedial action had been effectively applied in the main source zone.

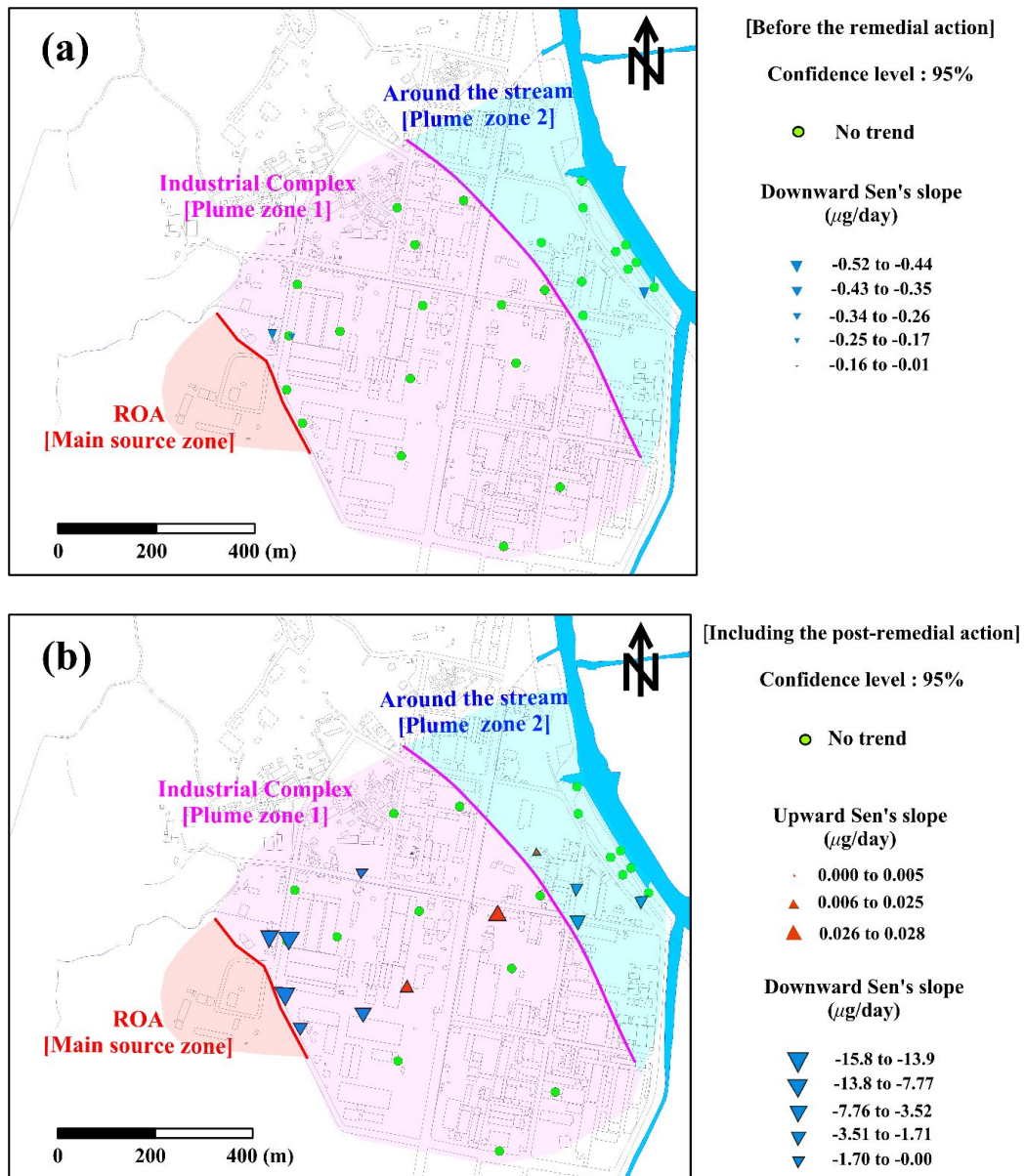


**Figure 5-14.** Spatial distribution of variation trend of TCE concentration with Sen's trend analysis at the industrial complex [Plume zone 1] and around the stream [Plume zone 2] until the pre-remedial action [from 2009 to 2012] (a) and whole study period involving the post-remedial action [from 2009 to 2015] (b).

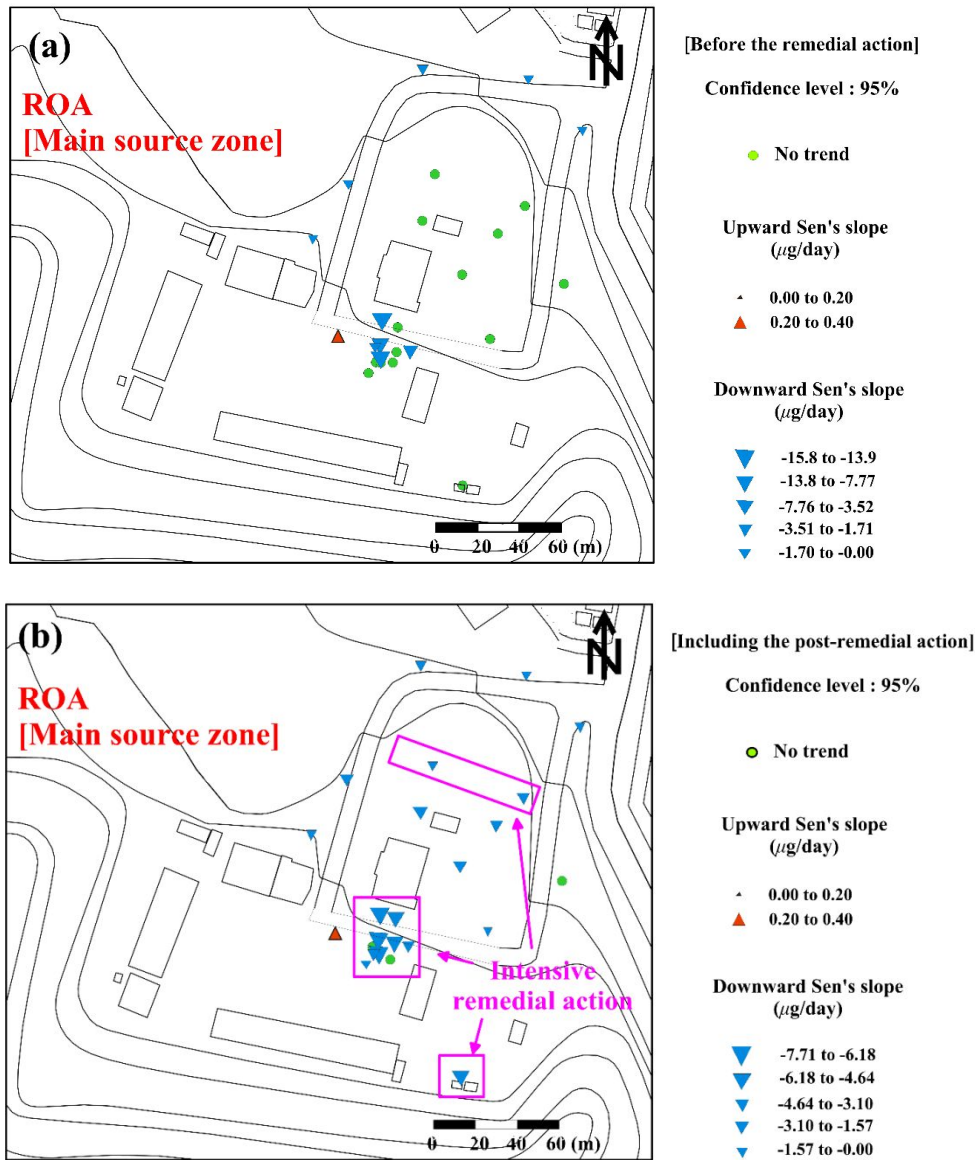


**Figure 5-15.** Spatial distribution of variation trend of TCE concentration with Sen's trend analysis at RAO [the main source zone] until the pre-remedial action [from 2009 to 2012] (a) and whole study period involving the post-remedial action [from 2009 to 2015] (b).

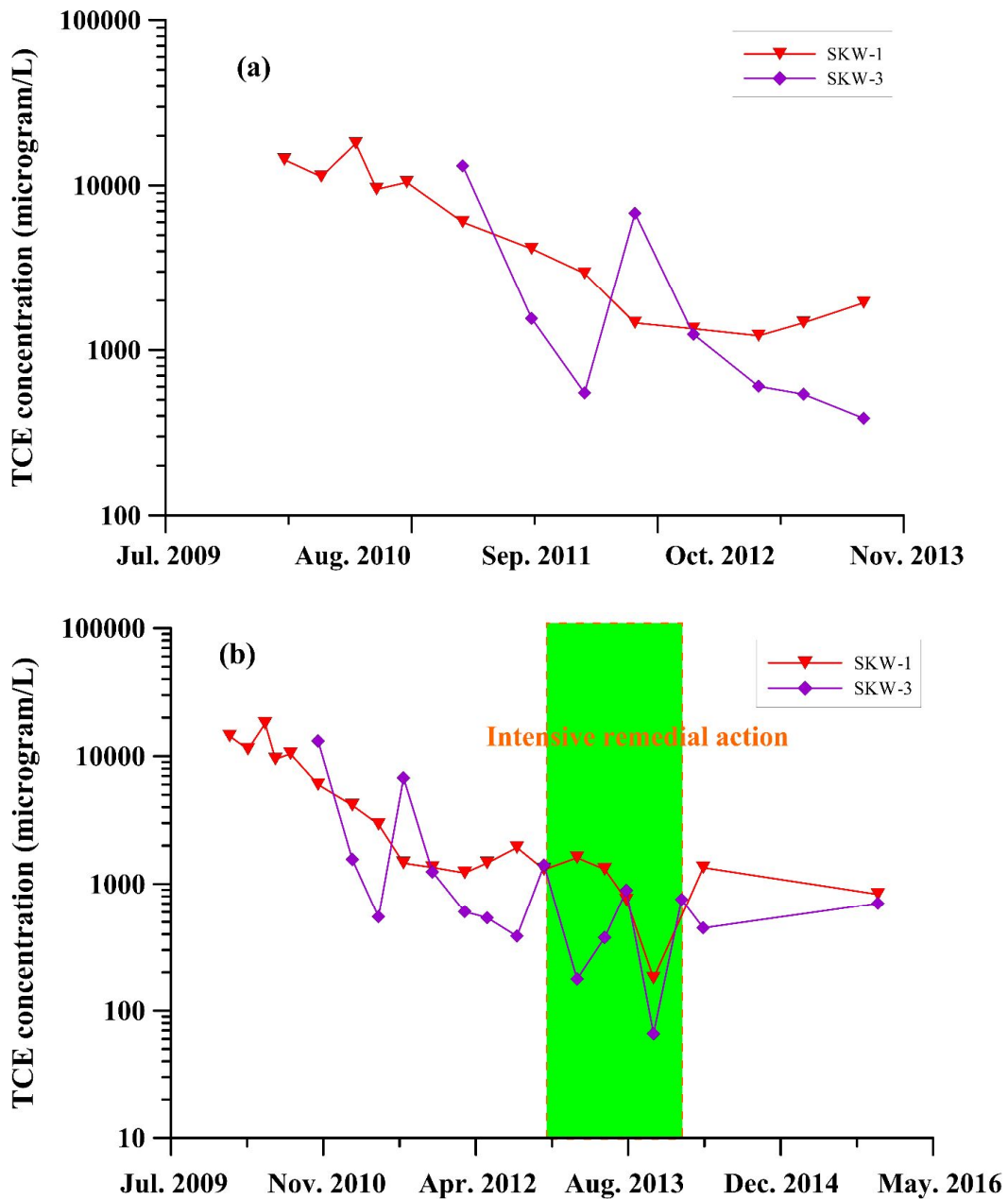


**Figure 5-16.** Temporal variations of TCE concentration at monitoring well conducted the intensive remedial action until the pre-remediation (a) and the post- remediation (b).

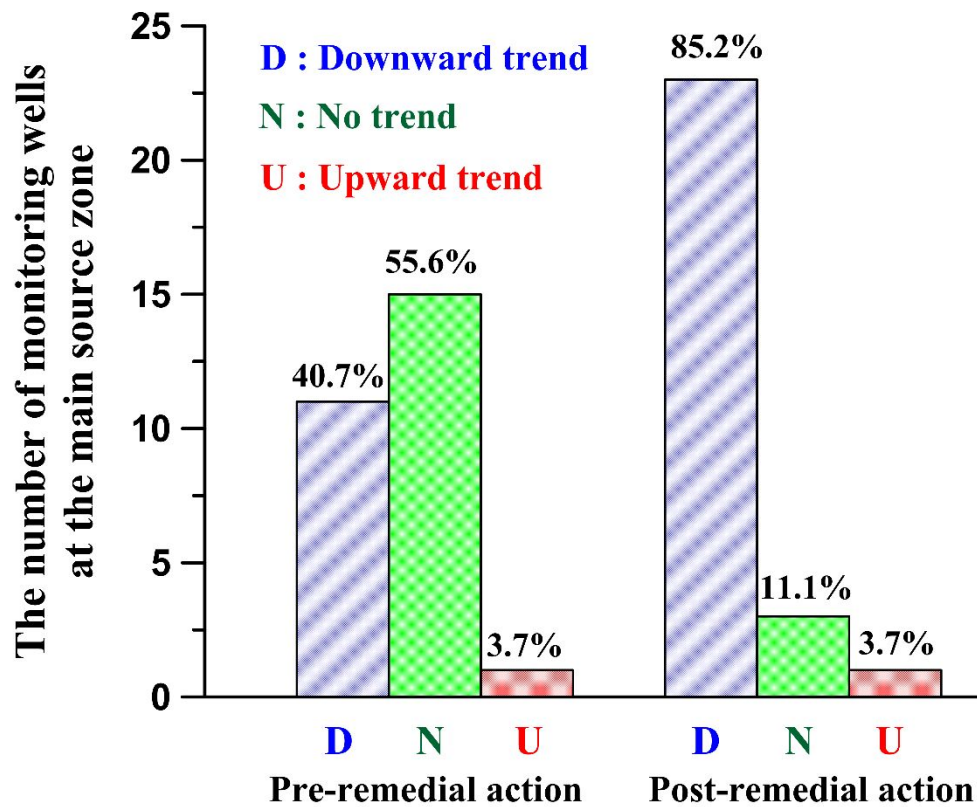
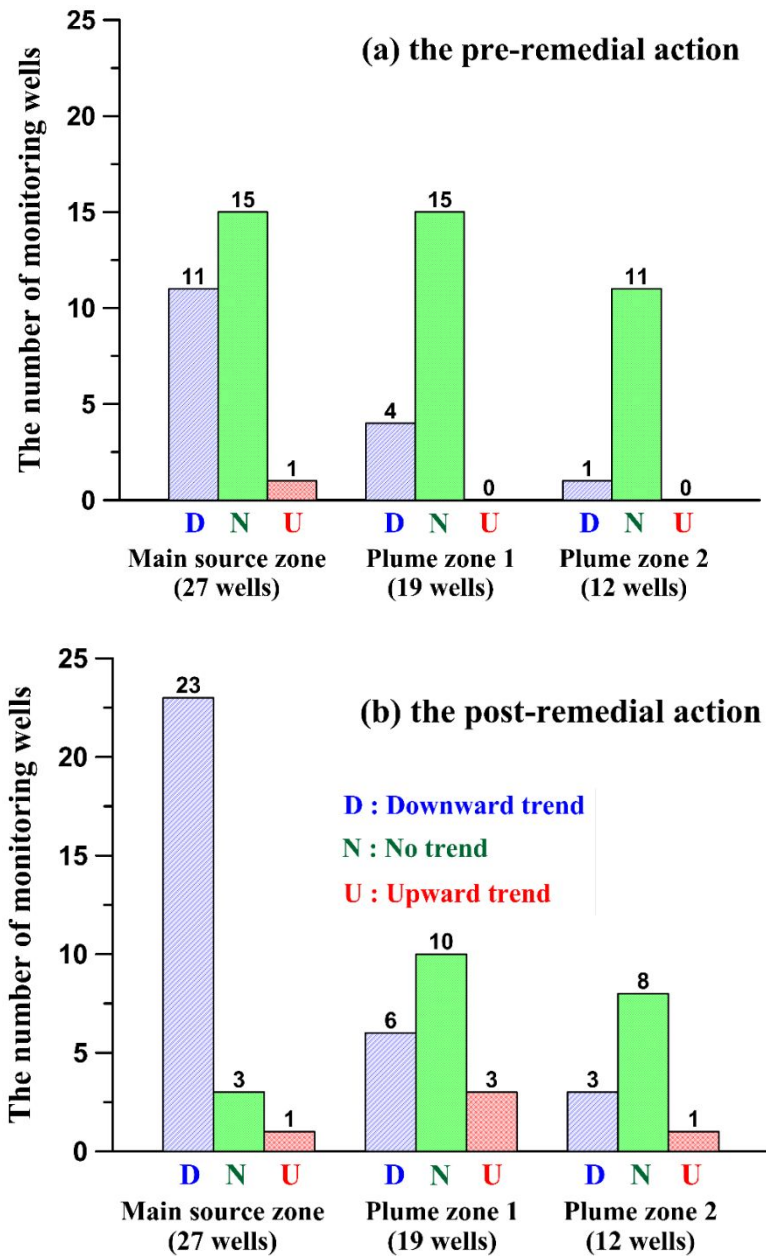


Figure 5-17. Distribution of the number of monitoring wells involving each significant trend until (a) the pre-remedial action and (b) the post-remedial action at the main source zone.



**Figure 5-18.** Zonal distribution of the number of monitoring wells involving each significant trend at (a) the pre-remedial action and (b) the post-remedial action.

**Table 5-2.** Number of monitoring well data for this study

Parameters	Total Number of monitoring well			Number of data set whose length is greater than 5 years		
	Main source zone	Industrial complex	Around the stream	Main source zone	Industrial complex	Around the stream
No. of data set	105			58		
	39	54	12	27	19	12

**Table 5-3.** Results of Sen's slope trend analysis for TCE concentration in main source zone and whole study area

Trend  (95% Confidence)	Pre-remedial action			Post remedial action		
	Main source zone	Industrial complex (Plume 1)	Around the stream (Plume 2)	Main source zone	Industrial complex (Plume 1)	Around the stream (Plume 2)
	<b>Decreasing</b>	41% (11 <sup>a</sup> /27 <sup>b</sup> )	21% (4/19)	8% (1/12)	85% (23/27)	31% (6/19)
<b>No trend</b>	55% (15/27)	79% (15/19)	92% (11/12)	11% (3/27)	53% (10/19)	67% (8/12)
<b>Increasing</b>	4% (1/27)	0% (0/19)	0% (0/12)	4% (1/27)	16% (3/19)	8% (1/12)

<sup>a</sup>Number of wells showing negative slope

<sup>b</sup>Number of wells analyzed

## **5.4 Summary and conclusion**

Temporal variations of TCE plumes and the mass discharge of TCE in groundwater at an industrial complex, Wonju, Korea were examined using various quantitative evaluation methods. Associated with the intensive remedial action, to evaluate the effectiveness of the remediation technologies applied, the variation in the TCE concentrations was analyzed and quantified using statistical trend analysis method based on the monitoring data. Additionally, the removal efficiency such as reduction rate of source mass and removed mass was estimated using analytical solutions.

TCE concentrations and its mass discharge through the source transect responded strongly to the applied remediation actions. However, as getting to the downstream from the main source area, the observed variations in the TCE concentration and its mass discharge were mainly controlled by hydrogeological parameters such as seasonally varied recharge. Although the TCE contamination in WIC was not attenuated to a great extent, our results through various evaluation methods indicated that the source plumes have been contained effectively. From the results of analytical solution, the TCE concentration in WIC is expected to decrease in the future as a result of the intensive source zone remediation. Also, it is assumed that the intensive

remedial action had been effectively performed with the removal efficiency of 70% for the residual source mass during the remediation period and the effect of remediation performed at source zone have been gradually presented at the downstream area until the present day.

This study demonstrates that long-term monitoring data collected at the pre- and post-remedial action can be utilized in planning the optimized remediation strategy and evaluating the efficiency of remedial action through selection of reasonable evaluation methods such as mass discharge method, statistical trend analysis method and analytical solution in a complex groundwater system discharging to the stream.

## **CONCLUDING REMARKS**

## CONCLUDING REMARKS

This study focuses on the characterization of chlorinated ethenes contamination using quantitative and qualitative evaluation methods in a complex groundwater system discharging to a stream. The study site is located at an industrial complex of Wonju city, Korea, adjacent to the stream. Contamination by trichloroethylene (TCE) was detected in 1990's and had been investigated for contaminant identification and remediation.

Due to the limited information of spilled TCE at the main source zone, it was very difficult to identify characteristics of TCE contamination, regarding the source identification such as tracing the initial source mass and dissolved concentration. For this reason, analytical solutions which can assess the impacts of partial mass depletion are applied. The results of quantitative evaluation using analytical solutions indicated that contaminant source had been spilled with approximately 1,000 kg of the source mass and 150,000  $\mu\text{g/L}$  dissolved concentration at the initial stage.

The fate and transport of chlorinated ethenes in a locally heterogeneous stream watershed was evaluated using qualitative evaluation method such as the concentration of each component, and hydrogeochemical, microbial, and compound-specific carbon isotope data. The multilateral approach implicit in

hydrogeochemical and biomolecular methods in relation to compound-specific isotope analysis indicated that the TCE plumes were naturally attenuated by active aerobic and anaerobic dechlorination of TCE to VC around the stream. As a result, the TCE plumes dispersed near the stream, and had no appreciable effects on the streamwater quality.

The evidences of in situ remediation represented on long-term monitoring data were assessed with quantitative evaluation methods using mass discharge analysis, Sen's trend analysis and analytical solutions. Long-term concentration monitoring data can be utilized as evidence in evaluating the evolution of plume and the efficiency of remedial action. As results from mass discharge analysis and Sen's trend analysis, a greater trend variation in TCE concentrations and mass discharge was detected at the plumes near the source zone compared to the relatively stable plumes in the downstream. The difference in temporal trends of TCE concentrations between the plumes in the source zone and those in the downstream could have resulted from remedial actions taken at the source zones. Results of Sen's trend analysis indicated that the intensive remedial action leads to rapid concentration reduction at the main source zone compared to the downgradient area and has an effect on the downgradient plume. Also, the efficiency of remedial actions was evaluated with analytical solution, and then the residual mass and dissolved concentration

were predicted. The results indicated that remedial actions performed at the mains source zone effectively remediated with the mass reduction rate of 70% during the performance period, and the residual mass and dissolved concentration will be gradually decreased until 2026.

The multilateral approach used in this study site involving a complex groundwater system from the main source zone corresponding to recharge area to groundwater discharge area such as stream was considered useful in evaluating the characteristics of contaminant source, the development and degradation of the contaminant plume, and the efficiency of remedial action, as well as in investigating the effect of contaminated groundwater on surrounding surface water bodies. From these results, it is enable to plan the systematic long-term plume management and to support in efficiently performing the decision-making process for an optimized remediation strategy.

## References

- Abe Y., Aravena R., Zopfi J., Parker B., Hunkler D., 2009. Evaluating the fate of chlorinated ethenes in streambed sediments by combining isotope, geochemical and microbial methods. *J. Contam. Hydrol.*, 107(1-2), 10-21.
- Aral, M.M. and Guan, J., 1996. Genetic algorithms in search of groundwater pollution sources. *Advances in groundwater pollution control and remediation*, M.M. Aral, ed., Vol. 9, Kluwer, Dordrecht, Netherlands, 9, 346-371.
- Aral, M.M. and Maslia, M.L., 2001. Identification of contaminant source location and release history in aquifers, *Journal of Hydrologic Engineering*, 6(3), 225-234.
- Arciero D., Vannelli T., Logan M., Hooper A.B., 1989. Degradation of trichloroethylene by the ammonia-oxidizing bacterium *Nitrosomonas europaea*. *Biochem Bioph RES CO.*, 159(2), 640-643.
- Baek, W., Lee J.Y., 2011. Source apportionment of trichloroethylene in groundwater of the industrial complex in Wonju, Korea: a 15-year distribute and perspective. *Water Environ. J.*, 25(3), 336-344.

Basu, N.B., Rao P.S.C., Poyer I.C., Nandy S., Mallavarapu M., Naidu R., Davis G.B., Patterson B.M., Annable M.D., Hatfield K., 2009. Integration of traditional and innovative characterization techniques for flux-based assessment of Dense –Non-Aqueous Phase Liquid (DNAPL) sites. *J. Contam. Hydrol.*, 105(3-4), 161-172.

Basu, N.B., Rao, P.S.C., Falta, R.W., Annable, M.D., Jawitz, J.W., Hatfield, K., 2008. Temporal evolution of DNAPL source and contaminant flux distribution: Impacts of source mass depletion, *J. Contam. Hydrol.*, 95, 93-109.

Basu, N.B., Rao, P.S.C., Poyer, I.C., Annable, M.D., Hatfield, K., 2006. Flux-based assessment at a manufacturing site contaminated with trichloroethylene, *J. Contam. Hydrol.*, 86(1-2), 105-127.

Broholm, K., Feenstra, S., 1995. Laboratory measurements of the aqueous solubility of mixtures of chlorinated solvent, *Environ Toxicol Chem*, 14(1), 9-15.

Broholm, K., Feenstra, S., Cherry, J.A., 1999. Solvent release into a sandy aquifer, 1. Overview of source distribution and dissolution behavior, *Environ.*

Sci. Technol., 33(5), 681-690.

Brusseau, M. L., Matthieu III, D. E., Carroll, K. C., Mainhagu, J., Morrison, C., McMillan, A., Russo, A., and Plaschke, M., 2013. Characterizing long-term contaminant mass discharge and the relationship between reductions in discharge and reductions in mass for DNAPL source areas, *J. Contam. Hydrol.*, 149, 1-12.

Chapman S.W., Parker B.L., Cherry J.A., Aravena R., Hunkeler D., 2007. Groundwater-surface water interaction and its role on TCE groundwater plume attenuation. *J. Contam. Hydrol.*, 91(3-4), 203-232.

Chen K.F., Kao C.M., Hsieh C.Y., Chen S.C., Chen Y.L., 2005. Natural biodegradation of MTBE under different environmental conditions: Microcosm and microbial identification studies. *B. Environ. Contam. Tox.*, 74(2), 356-364.

Chiu H. Y., Liu K.K., Chien H.Y., Surampalli R.Y., Kao C.M., 2013. Evaluation of Enhanced Reductive Dechlorination of Trichloroethylene Using Gene Analysis: Pilot-Scale Study. *J. Environ. Eng.*, 139(3), 428-437.

Choi, H.M. and Lee, J.Y., 2009. Parametric and non-parametric trend analysis for water levels of groundwater monitoring wells in Jeju island, *Journal of Soil and Groundwater Environmental*, 14(5), 41-50.

Chu K., Mahendra S., Song D.L., Conrad M.E., Alvarez-Cohen L., 2004. Stable carbon isotope fractionation during aerobic biodegradation of chlorinated ethenes. *Environ. Sci. Technol.*, 38(11), 3126-3130.

Chun J., Lee J., Jung Y., Kim M., Kim S., Kim B.K., Lim Y., 2007. ExTazon: a web-based tool for the identification of prokaryotes based on 16S ribosomal RNA gene sequences. *Int. J. Syst. Evol. Microb.*, 57, 2259-2261.

Coleman N.V., Mattes T.E., Gossett J.M., Spain J.C., 2002. Biodegradation of *cis*-dichloroethene as the sole carbon source by a beta-proteobacterium. *Appl. Environ. Microb.*, 68(6), 2726-2730.

Conant J. B., Cherry, J. A., and Gillham, R. W., 2004. A PCE groundwater plume discharging to a river: influence of the streambed and near-river zone on contaminant distributions, *J. Contam. Hydrol*, 73(1-4), 249-279.

Conrad M.E., Brodie E.L., Radtke C.W., Bill M., Delwiche M.E., Lee M.H., Swift D.L., Colwell F.S., 2010. Field evidence for co-metabolism of

trichloroethene stimulated by addition of electron donor to groundwater. *Environ. Sci. Technol.*, 44(12), 4697-4704.

Coplen T.B., 1996. New guidelines for reporting stable hydrogen, carbon, and oxygen isotope-ratio data. *Geochim. Cosmochim. Ac.*, 60, 3356-3360.

Courbet, C., Riviere, A., Jeannotat, S., Rinaldi, S., Hunkeler, D., Bendjoudi, H., de Marsily, G., 2011. Complementing approaches to demonstrate chlorinated solvent biodegradation in a complex pollution plume: Mass balance, PCR and compound-specific stable isotope analysis. *J. Contam. Hydrol.*, 126, 315-329.

Damgaard, I., Bjerg, P.L., Baelum, J., Scheutz, C., Hunkeler, D., Jacobsen, C.S., Tuxen, N., Broholm, M.M., 2013. Identification of chlorinated solvents degradation zones in clay till by high resolution chemical, microbial and compound specific isotope analysis. *J. Contam. Hydrol.*, 146, 37-50.

Einarson, M. D. and Mackay D.M., 2001. Predicting impacts of groundwater contamination. *Environ. Sci. Technol.*, 35(3), 66–73.

Enfield, C.G., Wood, A.L., Brooks, M.C., Annable, M.D., 2002. Interpreting

tracer data to forecast remedial performance. In: Thornton, S., Oswald, S. (Eds.), *Groundwater Quality: Natural and Enhanced Restoration of Groundwater Pollution*. IAHS, Sheffield, UK, 11-16.

Enfield, C.G., Wood, A.L., Espinoza, F.P., Brooks, M.C., Annable, M.D., Rad, P.S.C., 2005. Design of aquifer remediation systems: (1) describing hydraulic structure and NAPL architecture using tracers, *J. Contam. Hydrol.*, 81(1-4), 125-147.

Fahrenfeld N., Cozzarelli I.M., Bailey Z., Pruden A., 2014. Insights into biodegradation through depth-resolved microbial community functional and structural profiling of a crude-oil contaminant plume. *Microb. Ecol.*, 68 (3), 453-462.

Falta, R.W., Rao, P.S.C., Basu, N., 2005a. Assessing the impacts of partial mass depletion in DNAPL source zones: 1. Analytical modeling of source strength functions and plume response, *J. Contam. Hydrol.*, 78, 259-280.

Falta, R.W., Rao, P.S.C., Basu, N., 2005b. Assessing the impacts of partial mass depletion in DNAPL source zones: 2. Coupling source strength functions to plume evolution, *J. Contam. Hydrol.*, 79, 45-66.

Fennell D., Gossett J., 1998. Modeling the production of and competition for hydrogen in a dechlorinating culture. *Environ. Sci. Technol.*, 16(32), 2450-2460.

Freitas, J.G., Rivett, M.O., Roche, R.S., Durrant, M., Walker, C., Tellam, J.H., 2015. Heterogeneous hyporheic zone dechlorination of TCE groundwater plume discharging to an urban river reach, *J. Contam. Hydrol.*, 505, 236-252.

Fure, A.D., Jawitz, J.W., Annable, M.D., 2006. DNAPL source depletion: linking architecture and flux response, *J. Contam. Hydrol.*, 85, 118-140.

Gan, T.Y., 1998. Hydroclimatic trends and possible climatic warming in the Canadian Prairies, *Water Resource Research*, 34(11), 3009-3015.

Gehard, J.I., Pang, T., Kueper, B., 2007. Time scale of DNAPL migration in sandy aquifers examined via numerical simulation, *Groundwater*, 45, 147-157.

Gilbert, R.O., 1987. *Statistical Methods for Environmental Pollution*

Monitoring, John Wiley & Sons, New York.

Gist, G. L. and Burg J. R., 1995. Trichloroethylene – A review of the literature from a health effects perspective, *Toxicol. Ind. Health.*, 11(3), 253-307.

Gocic, M. and Trajkovic, 2013. Analysis of changes in meteorological variables using Mann-Kendall and Sen's slope estimator statistical tests in Serbia, *Global and Planetary Change*, 100, 172-182.

Gorden, M. J., 1998. Case history of a large-scale air sparging/soil vapor extraction system for remediation of chlorinated volatile compounds in ground water, *Groundwater Monit. R.*, 18(2), 137-149.

Gorelick, S.M., Evans, B., Remson, I., 1983. Identifying sources of groundwater pollution: An optimization approach, *Water Resource Research.*, 19(3), 779-790.

Hannesin, S.F.O. and Gillham, R.W., 1998. Long-term performance of an in situ "iron wall" for remediation of VOCs. *Groundwater*, 36(1), 164-170.

Harkness M., Spivack J., 2001. Stable carbon isotope evidence for intrinsic bioremediation of tetrachloroethene and trichloroethene at area 6, Dover Air Force Base. *Environ. Sci. Technol.*, 35(2), 261-269.

Henri C.V., Fernandez-Garcia D., de Barros F. P.J., 2016. Assessing the joint impact of DNAPL source-zone behavior and degradation products on the probabilistic characterization of human health risk, *Advances in Water Resources*, 88, 124-138.

Hirsch, R.M., Slack, J.R., Smith, R.A., 1982. Techniques of trend analysis for monthly water quality data. *Water Resource Research*, 18(1), 107-121.

Hunkeler D., Aravena R., 2000. Determination of compound-specific carbon isotope ratios of chlorinated methanes, ethanes, and ethenes in aqueous samples. *Environ. Sci. Technol.*, 34, 2839-2844.

Hunkeler D., Aravena R., 2009. *Environmental Isotopes in Biodegradation and Bioremediation*. Chapter 8, Investigating the origin and fate of organic contaminants in groundwater using stable isotope analysis. CRC press, Florida, 239-291.

Hunkeler D., Aravena R., Butler B.J., 1999. Monitoring microbial dechlorination of tetrachloroethen (PCE) in groundwater using compound-specific stable carbon isotope ratios: microcosm and field studies. *Environ. Sci. Technol.*, 37(4), 2733-2738.

Hunkeler, D., Abe, Y., Broholm, M.M., Jeannotat, S., Westergaard, C., Jacobsen, C.S., Aravena, R., Bjerg, P.L., 2011. Assessing chlorinated ethene degradation in a large scale contaminant plume by dual carbon-chlorine isotope analysis and quantitative PCR. *J. Contam. Hydrol.*, 119, 69-79.

Hunkeler, D., Chollet, N., Pittet, X., Aravena, R., Cherry, J.A., Parker, B.L., 2004. Effect of source variability and transport processes on carbon isotope ratios of TCE and PCE in two sandy aquifers, *J. Contam. Hydrol.*, 74(1-4), 265-282.

Hur M.S., Lee I.J., Tak B.M., Lee H.J., Yu J.J., Cheon S.U., Kim B.S., 2013. Temporal shifts in cyanobacterial communities at different sites on the Nakdong River in Korea. *Water Res.*, 47(19), 6973-6982.

Imfeld G., Aragonés C.E., Zeiger S., Eckstädt C.C.V., Paschke H., Trabitisch R., Weiss H., Richnow H.H., 2008. Characterization of in situ

biodegradation in a models subsurface flow constructed wetland treating 1,2-dichloroethenes along a vertical gradient. *Environ. Sci. Technol.*, 42, 7924-7930.

Imfeld G., Nijenhuis I., Nikolausz M., Zeiger S., Paschke H., Drangmeister J., Grossmann J., Richnow H.H., Weber S., 2008. Assessment of in situ degradation of chlorinated ethenes and bacterial community structure in a complex contaminated groundwater system. *Water Res.*, 42 (4-5), 871-882.

Imfeld G., Pieper H., Shani N., Rossi P., Nikolausz M., Nijenhuis I., Paschke H., Weiss H., Richnow H.H., 2011. Characterization of groundwater microbial communities, dechlorinating bacteria, and in situ biodegradation of chloroethenes along a vertical gradient. *Water Air Soil Pollut*, 211, 107-122.

Jackson, R. E., 2004. Recognizing emerging environmental Problems: The case of Chlorinated solvents in groundwater, *Technol. Cul.*, 45(1), 55-79.

Jawitz, J.W., Fure, A.D., Demmy, G.G., Berglund, S., Rao, P.S.C., 2005. Groundwater contaminant flux reduction resulting from nonaqueous phase liquid mass reduction, *Water Resource Research*, 41(10), W10408.

Doi:10.1029/2004WR003825.

James, M. M., Travis, M. M., Charles, J. N., 2005. Analysis of DNAPI source-depletion costs at 36 field sites, *Remediation*, 15(2), 9-18.

Jeon C.O., Park W., Ghiorse W.C., Madsen E.L., 2004. *Polaromonas naphthalenivorans* sp. Nov., a naphthalene-degrading bacterium from naphthalene-contaminated sediment. *Appl. Environ. Microb.*, 54, 93-97.

Jeong S., Moon H.S., Shin D., Nam K., 2013. Survival of introduced phosphate-solubilizing bacteria (PSB) and their impact on microbial community structure during the phytoextraction of Cd-contaminated soil. *J. Hazard. Mater.*, 263(2), 441-449

Kao C.M., Prosser J., 1999. Intrinsic bioremediation of trichloroethylene and chlorobenzene: field and laboratory studies. *J. Hazard. Mater.*, 69 (1), 67-79.

Kaown, D., Koh, D.C., Lee, K.K., 2011. Combined use of groundwater age data and compound-specific stable isotope data to determine in site degradation rate of chlorinated solvents, 2011 American Geophysical Union (AGU) fall meeting, Paper number (H41A-1004).

Kaown D., Shouakar-Stash, O., Yang, J.H., Hyun, Y.J., Lee, K.K., 2014a. Identification of multiple sources of groundwater contamination by dual isotopes. *Groundwater*, 52(6), 875-885.

Kaown D., Koh D.C., Solomon D.K., Yoon Y.Y., Yang, J.H., Lee, K.K., 2014b. Delineation of recharge patterns and contaminant transport using  $^3\text{H}$ - $^3\text{He}$  in a shallow aquifer contaminated by chlorinated solvents in South Korea. *Hydrogeology J.*, 22, 1041-1054.

KMOE (Korea Ministry of Environment). National wide groundwater monitoring reports in 2009, 2010.

Koh S., Bowman J.P., Sayler G.S., 1993. Soluble methane monooxygenase production and trichloroethylene degradation by a type I methanotroph, *Methylomonas methanica*. *Appl. Environ. Microbiol.*, 59, 960-967.

Kotik M., Davidová A., Voříšková J., Baldrian P., 2013. Bacterial communities in tetrachloroethene-polluted groundwaters: A case study. *Sci. Total Environ.*, 454–455 (0), 517-527.

Kuo Y.C., M.ASCE S.H.L., Wang S.Y., Chen S.H., F.ASCE C.M.K., 2014. Application of emulsified substrate biobarrier to remediate TCE-contaminated groundwater: pilot-scale study. *J. Hazard. Toxic Radioact. Waste.*, 18, 04014006-1 - 04014006-8.

Lee S.S., Kim H.M., Lee S.H., Yang J.H., Koh Y.E., Lee K.K., 2013. Evidences of in situ remediation from long-term monitoring data at a TCE-contaminated site, Wonju, Korea. *Journal of Soil and Groundwater Environment*, 18(6), 8-17.

Lee, S.S., Kaown, D., Lee, K.K., 2015. Evaluation of the fate and transport of chlorinated ethenes in a complex groundwater system discharging to a stream in Wonju, Korea, *J. Contam. Hydrol.*, 182, 231-243.

Lee, J.Y., Yi, M.J., Lee, J.M., Ahn, K.H., Won, J.H., Moon, S.H., Cho, M., 2006. Parametric and Non-parametric trend analysis of groundwater data obtained from national groundwater monitoring stations, *Journal of Soil and Groundwater Environment*, 11(2), 56-67.

Lee, J.Y., Yi, M.J., Song, S.H., Lee, G.S., 2008. Evaluation of seawater

intrusion on the groundwater data obtained from the monitoring network in Korea, *Water International*, 33(1), 127-146.

Lenczewski, M., Mckay, L., Pitner, A., Driese, S., Vulava, V., 2006. Pure-phase transport and dissolution of TCE in sedimentary rock saprolite. *Groundwater*, 44, 406-414.

Lojkasek-Lima P., Aravena R., Parker B.L., Cherry J.A., 2012. Fingerprinting TCE in a bedrock aquifer using compound-specific isotope analysis. *Groundwater*, 50(5), 754-764.

Machiwal, D. and Jha, M.K., 2015. Identifying sources of groundwater contamination in a hard-rock aquifer system using multivariate statistical analyses and GIS-based geostatistical modeling techniques, *J. Hydrol.*, 4, 80-110.

Mackay, D. M., Wilson, R. D., Brown, M. J., Ball, W. P. and Durfee, D. P., 2000. A controlled field evaluation of continuous vs. pulsed pump-and- treat remediation of a VOC-contaminated aquifer: site characterization, experimental setup, and overview of results, *J. Contam. Hydrol.*, 41(1-2), 81-131.

Mackay, D.M., Roberts, P.V., Cherry, J.A., 1985. Transport of organic contaminations in groundwater: Distribution and fate of chemicals in sand and gravel aquifers, *Environ. Sci. Technol.*, 19(5), 384-392.

Maphosa F., Smidt H., De Vos W. M., Röling W.F.M., 2010. Microbial community- and metabolite dynamics of an anoxic dechlorinating bioreactor. *Environ. Sci. Technol.*, 44, 4884-4890.

Marley M.C., Hazebrouck D.J., Walsh M.T., 1992. The application of in situ air sparging as an innovative soils and ground water remediation technology. *Groundwater Monit. R.*, 12(2), 137-145.

McCray, J. E., Tick., G. R., Jawitz, J. W., Gierke, J. S., Brusseau, M. L., Falta, R. W., Knox, R. C., Sabatini, D. A., Annable, M. D., Harwell, J. H., and Wood, A. L., 2011. Remediation of NAPL sources: lessons learned from field studies at hill and dover AFB, *Groundwater*, 49(5),727-744.

McGuire, T. M., Newell, C. J., Looney, B. B., Vangelas, K. M., and Sink, C. H., 2004. Historical analysis of monitored natural attenuation: A survey of

191 chlorinated solvent sites and 45 solvent plumes, *Remediation*, 15(1), 99-112.

McGuire, T. M., McDade, J. M., and Newell, C. J., 2006. Performance of DNAPL source depletion technologies at 59 chlorinated solvent-impacted sites, *Groundwater Monit. R.*, 26(1), 73-84.

Miller T.R., Franklin M.P., Halden R.U., 2007. Bacterial community analysis of shallow groundwater undergoing sequential anaerobic and aerobic chloroethene biotransformation. *Microbiol. Ecol.*, 60(2), 299-311.

Miller, C.T., Poirier-McNeill, M.M., Mayer, A.S., 1990. Dissolution of trapped nonaqueous phase liquids: Mass transfer characteristics, *Water Resource Research*, 26(11), 2783-2796.

Moran, M.J., Zogorski, J.S., Squilace, P.J., 2007. Chlorinated solvents in groundwater of the United States. *Environ. Sci. Technol.*, 41, 74-81.

Nijenhuis I., Nikolausz M., Köth A., Felföldi T., Weiss H., Drangmeister J., Großmann J., Kästner M., Richnow H.H., 2007. Assessment of the natural attenuation of chlorinated ethenes in an anaerobic contaminated aquifer in

the Bitterfeld/Wolfen area using stable isotope techniques, microcosm studies and molecular biomarkers. *Chemosphere*, 67, 300-311.

Nübel U., GarciaPichel F., Muyzer G., 1997. PCR primers to amplify 16S rRNA genes from cyanobacteria. *Appl. Environ. Microb.*, 63(8), 3327–3332.

Parker J.C. and Park, E., 2004. Modeling field-scale dense nonaqueous phase liquid dissolution kinetics in heterogeneous aquifer, *Water Resource Research*, 40, W05109.

Parker, B.L., 2008, Chapman, S.W., Guilbeault, M.A., 2008. Plume persistence caused by back diffusion from thin clay layers in a sand aquifer following TCE source-zone hydraulic isolation, *J. Contam. Hydrol.*, 102(1-2), 86-104.

Partal, T. and Kahya, E., 2006. Trend analysis in Turkish precipitation data, *Hydrological process*, 151, 2011-2026.

Rao, P.S.C. and Jawitz, J.W., 2003. Comment on “Steady-state mass transfer from single-component dense non-aqueous phase liquids in uniform flow fields” by T.C. Sale and D.B. McWhorter, *Water Resource Research*, 39(3), COM1.

Rao, P.S.C. and Jawitz, J.W., Enfield, C.G., Falta, R., Annabel, M.D., Wood, A.L., 2001. Technology integration for contaminated site remediation: cleanup goals and performance metrics, *Ground Water Quality*. Sheffield, UK, 410-412.

Révész, K.M., Lollar, B.S., Kirshtein, J.D., Tiedeman, C.R., Imbrigiotta, T.E., Goode, D.J., Shapiro, A.M., Voytek, M.A., Lacombe, P.J., Busenberg, E., 2014. Integration of stable carbon isotope, microbial community, dissolved hydrogen gas, and  $2\text{HH}_2\text{O}$  tracer data to assess bioaugmentation for chlorinated ethane degradation in fractured rocks, *J. Contam. Hydrol.*, 156, 62-77.

Rivett, M. O., Chapman, S. W., Allen-King, R. M., Feenstra, S., and Cherry, J. A., 2006. Pump-and-treat remediation of chlorinated solvent contamination at a controlled field-experiment site, *Environ. Sci. Technol.*, 2006, 40, 6770-6781.

Schnarr, M., Truax, C., Farquhar, G., Hood, E., Gonullu, T., Stickney, B., 1998. Laboratory and controlled field experiments using potassium permanganate to remediate trichloroethylene and perchloroethylene

DNAPLs in porous media, *J. Contam. Hydrol.*, 29, 205-224.

Sen, P.K., 1968. Estimates of the regression coefficient based on Kendall's tau, *the Journal of the American Statistical Association*, 63, 1379-1389.

Soga, K., Page, J. W. E., and Illangasekare, T. H., 2004. A review of NAPL source zone remediation efficiency and the mass flux approach, *J. Hazard. Mater.* 110(1-3), 13-27.

Song D.L., Conrad M.E., Sorenson K.S., Alvarez-Cohen L., 2002. Stable carbon isotope fractionation during enhanced in situ bioremediation of trichloroethene. *Environ. Sci. Technol.*, 36(10), 2262-2268.

Stroo, H.F., Unger, M., Ward, C.H., Kavanaugh, M.C., Vogel, C., Leeson, A., Marqusee, J.A., Smith, B.P., 2003. Remediating chlorinated solvent source zones. *Environ. Sci. Technol.*, 37(11), 224A-230A.

Sung Y., Fletcher K.E., Ritalahti K.M., Alkarian R.P., Ramos-Hernandez N., Sanford R.A., Mesbah N.M., Löffler F.E., 2006. *Geobacter lovley* sp.nov.strain SZ, a Novel metal-reducing and tetrachloroethene-dechlorinating bacterium. *Appl. Environ. Microb.*, 72 (4), 2775-2782.

Tabari H., Marofi S., Aeini A., Talaei P.H., Mohammadi K., 2011. Trend analysis of reference evapotranspiration in the western half of Iran, *Agricultural and Forest Meteorology*, 151, 128-136.

Tiehm A., Schmidt K.R., 2011. Sequential anaerobic/aerobic biodegradation of chloroethenes-aspects of field application. *Curr. Opin. Biotech.* 22 (3): 415-421.

Unno T., Jang J.H., Han D.K., Kim J.H., Sadowsky M.J., Kim O.S., Chun J.S., Hur H.G., 2010. Use of barcoded pyrosequencing and shared OTUs to determine sources of fecal bacteria in watersheds. *Environ. Sci. Technol.*, 44(20), 7777-7782.

US EPA, 2003. The DNAPL remediation challenge: Is there a case for source depletion? Expert panel on DNAPL remediation, M.C. Kavanaugh and P.S.C. Rao, Co-Chairs, EPA/600/R-03/143. <http://www.epa.gov/ada/pubs/reports.html>.

van Hylckama V.J.E.T., Janssen D.B., 2001. Formation and detoxification of reactive intermediates in the metabolism of chlorinated ethenes. *J.*

Biotechnol., 85, 81-102.

Wang, C.B. and Zhang, W., 1997. Synthesizing nanoscale iron particles for rapid and complete dechlorination of TCE and PCBs, *Environ. Sci. Technol.*, 31(7), 2154-2156.

Watson J.D., Baker T.A., Bell S.P., Gann A., Levine M., Losick R., 2008. *Molecular biology of the gene*, Sixth ed. Pearson Education Inc. San Francisco.

Wei, Y.-T., Wu, S.-C., Chou, C.-H., Tsai, S.-M. and Lien, H.-L., 2010. Influence of nanoscale zero-valent iron on geochemical properties of groundwater and vinyl chloride degradation: A field case study, *Water. Res.*, 44, 131-140.

Wilkin, R. T., Puls, R.W., Sewell, G.W., 2002. Long-term performance of permeable reactive barriers using Zero-valent iron: geochemical and microbiological effects. *Groundwater*, 41(4), 493-503.

Wilson R.D., Thornton S.F., Mackay D.M., 2004. Challenges in monitoring the natural attenuation of spatially variable plumes. *Biodegradation*, 15(6), 359-369.

Xie, Y., Li, X., Liu, X., Du, X., Li, F., Cao, Y., 2016. Performance evaluation of remediation scenarios for DNAPL contaminated groundwater using analytical models and probabilistic methods, *Procedia Environmental Sciences*, 31, 264-273.

Yang J.H., Lee K.K., Clement T.P., 2011. Impact of seasonal variations in hydrological stresses and spatial variations in geologic conditions on a TCE plume at an industrial complex in Wonju, Korea. *Hydrol. Process.*, 26(3), 317-325.

Yang J.H. and Lee K.K., 2012. Locating plume sources of multiple chlorinated contaminants in groundwater by analyzing seasonal hydrological responses in an industrial complex, Wonju, Korea. *Geosci. J.*, 16(3), 301-311.

Yang, J.-H., Jun, S.-C., Kwon, H.-P., and Lee, K.-K., 2014. Tracing of residual multiple DNAPL sources in the subsurface using  $^{222}\text{Rn}$  as a natural tracer at an industrial complex in Wonju, Korea, *Environ. Earth. Sci.*, 71, 407-417.

Yang, J.-H., Lee, K.-K. and Clement, T. P., 2012b. Impact of seasonal variations in hydrological stresses and spatial variations in geologic conditions on a TCE plume at an industrial complex in wonju, Korea, *Hydrol. Process.*, 26(3), 317-325.

Yu S.Y., Chae G.T., Jeon K.H., Jeong J.S., Park J.G., 2006. Trichloroethylene contamination in fractured bedrock aquifer in Wonju, South Korea. *B. Environ. Contam. Toxi.*, 76(2), 341-348.

Yue, S. and Wang, C.Y., 2002. Discussion: A study of variability of annual river flow of the southern African region, *Hydrological Science Journal*, 47(6), 983-989.

Zhu J. and Fang H., 2016. Temporal dynamics of NAPL source zone strength: relationship between groundwater flux and contaminant mass discharge, *Journal of Hazardous, Toxic, and Radioactive Waste*, [http://dx.doi.org/10.1061/\(ASCE\)HZ.2153-5515.0000322](http://dx.doi.org/10.1061/(ASCE)HZ.2153-5515.0000322).

Zhu, J., Sykes, J.F., 2004. Simple screening models of NAPL dissolution in the subsurface, *J. Contam. Hydrol.*, 72, 245-258.

## 국문 초록

트리클로로에틸렌과 같은 염화유기용제로 오염된 복합적 규모의 지하수계에서 정량적 및 정성적 평가 방법을 통해 정화 전·후의 오염 특성에 대해 평가하였다. 본 연구 지역은 하천이 인접한 산업단지에 위치하고 있다. 연구지역은 트리클로로에틸렌에 의해 장기간 오염이 된 것으로 조사되었으며, 이는 현재까지 연구지역 지하수계에 악영향을 미치고 있다. 오염원 지역에서 누출된 트리클로로에틸렌의 초기 잔류상 질량과 농도에 대한 정확한 정보는 알려진 바가 없다. 이러한 이유로 인해, 오염을 야기하는 오염원들을 특성화 시키는 작업과 오염원 지역에 어떠한 종류의 정화 전략이 적용 되어야 할지에 대한 결정시 어려움이 따르게 된다.

오염원의 일부 저감에 따른 영향을 평가하고 정량화 할 수 있는 해석해를 이용하여 연구지역내 알려지지 않은 초기 잔류상 오염원의 질량과 용해상 농도에 대한 예측을 수행하기 위해 현장 장기 모니터링 자료를 활용하였다. 또한 향후 시간 경과에 따른 잔류상 오염량과 용해상 농도도 예측 가능하였다. 해석해를 통해 초기 잔류상 오염량은 1,000 kg이며, 용해상 농도는 150,000  $\mu\text{g/L}$ 로 예측되었다. 누출된 양 및 농도와 같은 알려지지 않은 오염원 이력을 갖는 오염부지에서 단순한 해석해를 통해 오염원에 대한 정량적 정보 제공이 가능함을 본 연구를 통해 알 수 있었다.

소하천 유역의 불균질한 지하수계에서는 오염된 지하수의 하

천으로 유입은 하천수질 오염을 일으킨다. 따라서 산업단지 하천주변에서 염화유기용매의 운명과 거동에 대해 각각 오염물들의 농도, 수리지화학적, 미생물학적, 탄소 동위원소 데이터들을 이용하여 정성적 평가가 이루어졌다. 연구지역 지하수에 대한 지화학적 분석 결과들은 연구지역 상류부는 호기성 환경이 하류부는 혐기성 환경이 지배적임을 지시하였다. 또한, *cis*-DCE와 VC에 대한 물분율의 증가는 연구지역 하류부에서 감지되었으며, 하천주변에서는 오염원 지역에 비해 TCE의 부화된 탄소 동위원소 값과 *cis*-DCE의 결핍된 탄소 동위원소 값이 관측되었다. 이러한 결과들은 휘발성 유기화합물(VOCs)의 생분해를 지지해준다. 하천 근처 모니터링 관정내 미생물 군집 구조는 16S rRNA gene-based pyrosequencing을 이용하여 생분해와 관련있는 미생물들을 확인하고자 하였다. 이 연구에서 사용된 다양한 접근방법들의 결과들은 오염물들이 하천주변에서 활발한 혐기성 생분해 과정을 거쳐 자연적으로 저감되고 있음을 지시하였다.

주 오염원 지역에서는 TCE 오염원을 제거하고 정화 지정구역으로부터 TCE 오염운의 하류방향으로의 확산을 방지하기 위해서 다양한 정화기술들이 적용되었다. 각각의 정화지정 구역들에서는 TCE 오염운의 용해상 농도가 정화활동의 결과로 인해 주오염원 지역과 주변에서 상당히 감소된 것으로 나타났다. 그러나, 정화 직후에는 하류부의 오염운내 TCE 농도는 정화활동에 영향을 받지 않은 것으로 조사된 반면 이 곳의 농도는 모니터링 기간동안 계절적 함양 변화에 따라 큰 변동 양상을 보여주었다. 따라서, 정화 후 장기간 동안 정화의 영향을 파악하기 위해서 3개의 횡단선을 설정하여 이를 가로지르는

오염 부하량의 변동 모니터링과 TCE 농도 변화에 대해 Sen의 경향성 추정자를 계산하여 통계학적 경향 분석을 수행하였다. 정화이전에는 각각의 횡단선들에서 오염 농도와 부하량은 계절적 함양 변화와 잔류상 오염원에 의해 영향을 받는 것으로 조사되었다. 하지만 정화 후에는 정화의 영향이 주 오염원과 산업단지내의 횡단선에서 명백하게 나타났다으며, 또한 Sen의 경향성 추정자 결과에도 동일하게 나타났다. 오염원 진화의 시간경과에 따른 오염원 진화의 추적을 통해 오염원 주변에서의 TCE 농도 변화가 하류부의 안정한 오염원 보다 상대적으로 큰 변화 폭을 보이는 것으로 조사되었다. 오염원 지역과 하류부 지역에서 오염원들의 TCE 농도에 대한 시간적 경향 차이는 주 오염원 지역에 진행된 집중 정화활동의 결과로 인한 것이라 판단되었다.

본 연구에서는 집중 정화 활동에 대한 효율을 장기간 모니터링 자료와 해석해를 통해 평가하였다, 집중 정화 기간동안 잔류상 오염물의 제거율은 정화직전 오염량 대비 70%가 적합한 값이라 예측되었다. 해석해를 이용한 정량적 평가의 결과들로부터 정화 기간동안 잔류상 오염량의 70% 제거를 통해 효과적인 정화가 수행되었다고 판단되었다. 본 연구에서 언급한 평가 방법들은 오염원지역에서 장기간 정화 수행 및 집중정화활동의 제거 효율을 평가하는데 도움이 될 것이다.

**주요어:** 트리클로로에틸렌, 해석해, 하천 유역, 생저감, 정화 활동, 오염부하량